10-30-2013

Modelling Emergent Patterns of Dynamic Desert Ecosystems

J. Stewart
University of Lincoln, United Kingdom

A. J. Parson
University of Sheffield, United Kingdom

J. Wainwright
Durham University, United Kingdom

G. S. Okin
University of California, Los Angeles

B. T. Bestelmeyer
USDA-ARS, Las Cruces, New Mexico

See next page for additional authors

Recommended Citation

Stewart, J.; Parson, A. J.; Wainwright, J.; Okin, G. S.; Bestelmeyer, B. T.; Frederickson, E. L.; and Schlesinger, W. H., "Modelling Emergent Patterns of Dynamic Desert Ecosystems" (2013). *Agriculture Faculty and Staff Scholarship*. 2.
https://encompass.eku.edu/ag_fsresearch/2

Authors

J. Stewart, A. J. Parson, J. Wainwright, G. S. Okin, B. T. Bestelmeyer, E. L. Frederickson, and W. H. Schlesinger

Modelling Emergent Patterns of Dynamic Desert Ecosystems

J. Stewart[1], A. J. Parsons[2*], J. Wainwright[3], G. S. Okin[4],

B. T. Bestelmeyer[5], E. L. Fredrickson[6], W. H. Schlesinger[7]

(1) School of Engineering, University of Lincoln, UK

(2) Sheffield Centre for International Drylands Research, Department of Geography, University of Sheffield, UK

(3) Department of Geography, Durham University, Science Laboratories, South Road, Durham, UK

(4) Department of Geography, University of California, Los Angeles, USA

(5) USDA-ARS, Las Cruces, New Mexico, USA

(6) Department of Agriculture, Eastern Kentucky University, Richmond, Kentucky, USA

(7) Cary Institute of Ecosystem Studies, Millbrook, New York, USA

* corresponding author:

(a.j.parsons@sheffield.ac.uk / Fax: +44 (0) 114-2797912 / Phone: +44 (0) 114-2227952)

ABSTRACT

In many desert ecosystems vegetation is both patchy and dynamic: vegetated areas are interspersed with patches of bare ground, and both the positioning and the species composition of the vegetated areas exhibit change through time. These characteristics lead to the emergence of multi-scale patterns in vegetation that arise from complex relationships between plants, soils and transport processes. Previous attempts to probe the causes of spatial complexity and predict responses of desert ecosystems tend to be limited in their focus: models of dynamics have been developed with no consideration of the inherent patchiness in the vegetation, or else models have been developed to generate patterns with no consideration of the dynamics. Here we develop a general modelling framework for the analysis of ecosystem change in deserts that is rooted in the concept of connectivity and is derived from a detailed process-based understanding. We explicitly consider spatial interactions among multiple vegetation types and multiple resources, and our model is formulated to predict responses to a variety of endogenous and exogenous disturbances. The model is implemented in the deserts of the American Southwest both to test hypotheses of the causes of the invasion of woody shrubs, and to test its ability to reproduce observed spatial differences in response to drought in the twentieth century. The model's performance leads us to argue that vertical and lateral connectivity are key emergent properties of the ecosystem, which both control its behaviour and provide indicators of its state. If this argument is shown to be compatible with field observations, the model presented here will provide a more certain approach towards preventing further degradation of semi-arid grasslands.

Key words: semi-arid landscape ecology; patchiness; vegetation patterns; positive feedback; spatially explicit model; self-organization

1. Introduction

Desert ecosystems are commonly dynamic and patchy on a range of spatial and temporal scales (Ward, 2008; Wainwright, 2009). Their dynamism is particularly evident in long-term data showing changes in the composition and structure of plant communities (Buffington and Herbel, 1965; Gibbens *et* al, 2005; Turner *et* al, 2003; Osborne and Beerling, 2006; Schlesinger *et al.,* 1990; Archer *et al.,* 1995; Allred, 1996). Their patchiness, in which vegetated areas are interspersed with areas of bare ground, varies with plant growth form. In grasslands, bare and grassy patches alternate over a few decimetres and, on sloping ground, are often associated with a stepped microtopography (Dunkerley and Brown, 1999; Tongway and Ludwig, 2001; Nash *et al.,* 2004; Parsons *et al*., 1997). In shrublands, the spatial scale extends to a few metres and the microtopography may comprise swales (bare patches) and vegetation atop mounds (Barbour, 1969; McPherson *et al.,* 1988; Parsons *et al*., 1996; Rango *et al.,* 2000; Okin and Gillette, 2001). This patchiness in vegetation can lead to the formation of striking, regular patterns such as bands of vegetation alternating with stripes of bare patches (Gillett, 1941), exemplified by 'tiger bush' in Africa (MacFadyen, 1950; Clos-Arceduc, 1956), mulga groves in Australia (Slatyer, 1961) and mogote in Mexico (Cornet *et al.,* 1988). Other geometric and irregular patterns have also been noted such as can be described as spots (Bromley *et al.,* 1997) and labyrinths (Aguiar and Sala, 1999) in the dry zones of the world.

The formation of vegetation patches has typically been explained in two ways. On the one hand, the empirical-conceptual model of Islands of Fertility has been used since its definition by Charley and West (1975), and especially since its development by Schlesinger *et al*. (1990), to explain patches at the scale of individual plants. On the other hand, advection-diffusion models

– usually, but not always (e.g. Lefever *et al.*, 2009) of the Turing-instability type (e.g. Klausmeier, 1999; Couteron and Lejeune, 2001; HilleRisLambers *et al.*, 2001), have been employed to explain patterns at landscape scales.

Both of the existing explanations of patchiness have shortcomings. Both have conceptual limitations, and they produce results that are mutually incompatible and difficult to evaluate independently. The Islands of Fertility approach attempts to consider the system dynamics, but it is poor at addressing the emergence of spatial patterns. Conversely, the advection-diffusion approach is able to simulate emergence of spatial patterns, but often at the expense of an appropriate characterization of the dynamics. The aim of this paper is to advance our understanding of the dynamics of desert ecosystems and the patchiness and patterns that result from these dynamics. Using a conceptual approach with an explicit process basis, a new model is developed that links the dynamics of desert ecosystems with vegetation patchiness that is both quantitative and testable against existing data.

2. Existing approaches – a critique

2.1 The Islands of Fertility Model

The Islands of Fertility model (Charley and West, 1975; Schlesinger *et al.,* 1990) posits that changes in the spatial redistributions of soil resources are caused by the net transport of resources from interspaces to under-canopy areas. The heterogeneous resource distribution in turn affects plant demographic processes to reinforce vegetation patchiness. For example, during rainstorms, patches of vegetation serve as obstructions that slow, trap and accumulate runoff, sediments and nutrients from interpatch areas (Ludwig *et al.,* 2005). This accumulation leads to the increase of patch biomass, which will further accumulate resources (Aguiar and Sala, 1999). Establishment is reported to be particularly successful around the edges of the patch where there is less competition for sunlight (Mauchamp *et al.,* 1993), and where flows of nutrients and water become trapped, such as on the upslope edge of a patch (Montana, 1992). Where individual plants die, wind- and water-induced degradation of the patch are increased, which reduces seed establishment. Propagules are then moved to other locations where they may establish new communities (Goldberg and Turner, 1986).

Over time, changes in concentrations of resources may lead to new vegetation species attaining a competitive advantage within these patchy ecosystems (Osborne and Beerling, 2006). For example, the widely observed encroachment of shrubs into former grasslands (Allred 1996, Schlesinger *et al.,* 1990, Archer *et al.,* 1995) is regarded as a process that, due to different spatial distributions of grasses and shrubs, results in self-reinforcing changes to the spatial redistributions of soil resources (Schlesinger *et al.*, 1996). However, Islands of Fertility cannot explain all the different scales at which patterns appear in desert vegetation (Müller *et al*., 2008). Islands have also been demonstrated to be “leaky” (Wainwright *et al*., 2002; Abrahams *et al*., 2002) and thus linked to ecogeomorphic processes occurring beyond the scale of individual islands. Furthermore, the Islands of Fertility model does not tell us how changes are initiated, simply why they persist. Although the model explains why invading shrubs have a competitive advantage, it does not explain how they were able to invade in the first place, nor why certain types of patterns occur (e.g., stripes) occur under some circumstances. A broader issue with the Islands of Fertility model is that the term itself is tautologous, and hence unsuitable for predictive purposes. If concentrations of resource are present around a shrub, it is an island. If concentrations are absent around a shrub, it is not an island. Because of the qualitative and descriptive nature of the approach (Schlesinger *et al.*, 1990; Ludwig *et al.*, 2005), there is nothing independent of the resource accumulations that would allow this idea to be tested. Although Schlesinger *et al*. (1996) used semivariograms to support the idea of spatial patterns, these patterns are still not independent of the Islands that they are meant to demonstrate.

2.2 Numerical Models

The use of numerical modelling to shed light on dryland vegetation has, so far, been limited in terms of its narrow focus: models of dynamics have either been developed with no consideration of the inherent patchiness or patterns in the vegetation (Thornes and Brandt, 1993 [and discussion in Wainwright and Parsons, 2010]; Peters, 2002a; Koppel and Rietkerk, 2004; Istanbulluoglu and Bras, 2006), or they have been developed to generate patterns with no consideration of the dynamics (Klausmeier, 1999; Couteron and Lejeune, 2001; HilleRisLambers *et al.*, 2001; Rietkerk *et al.*, 2002; van de Koppel and Rietkerk, 2004; Barbier *et al.,* 2006), or they have been parameterized to create a specific ecosystem response (e.g. Dakos *et al*., 2011). Furthermore, if, as seems widely believed, both dynamics, and patterns/patchiness and ecosystem responses are functions of resource (principally water) limitation, then there has been little integration into these models of the temporal and spatial variability of resource availability that are well documented for deserts (Noy-Meir, 1973; Comrie and Broyles, 2002; Wainwright *et al*., 2000).

The most prevalent type of spatial model uses a Turing-like instability to generate regular patterns in desert vegetation. Patterns (Turing structures) originate solely through the coupling of reaction and diffusion processes, and the definition of a Turing structure specifically *excludes* any type of hydro-dynamic (i.e. fluid) motion (Turing, 1952). Despite contravening Turing's definition regarding applicability to hydrodynamic systems, this methodology was applied to vegetation patterns by Klausmeier (1999), whose model was based on the assumption that water cannot infiltrate on bare areas, so it flows downhill into a vegetation stripe where it does infiltrate and support plant growth. The flow of water was assumed to be exhausted before it reaches the downslope side of the stripe where the plants will consequently die off leading to a gradual uphill movement in the vegetation bands (Montana, 1992, but see above). Klausmeier's model involved the solution of two differential equations for water and plant biomass and assumed a uniform evaporation rate and water supply that is a linear function of increasing infiltration with increasing plant biomass. The model was reported to be insensitive to the exact form of functions of growth and infiltration as the resulting patterns are generated entirely by the Turing instability.

The patterns in this type of model result from spontaneous symmetry-breaking phenomena associated with bifurcations of steady states, corresponding to stable stationary solutions to a set of reaction-diffusion equations (Nicolis and Prigogine, 1977; Meinhardt, 1982). In Klausmeier's work, terms for water supply, infiltration and growth represent the contributions of reactive processes while the diffusion terms, such as plant dispersal, bring in the spatial dependence. The reactive processes were set to give realistic values of the intrinsic relative periodicity of the resulting banded patterns. In doing so, however, highly implausible values for input parameters had to be set; for example, water input of up to 750 mm a^{-1} and zero infiltration. Although some banded vegetation is found in areas with up to 750 mm a^{-1}, this is the exceptional (of the order of two to three times higher than the rate in areas where banded vegetation is typically observed), and observed infiltration rates are non-zero (see, for example Abrahams and Parsons, 1991; Casenave and Valentin, 1992), requiring an even more unrealistic rainfall input to match model output.

Klausmeier's approach was extended by HilleRisLambers *et al*. (2001) and Rietkerk *et al*. (2002) so that the water input could be separated into a soil-water component. There are two major problems with the model of HilleRisLambers *et al*. (2001) and Rietkerk *et al*. (2002). First, the key conclusions drawn were that herbivory, plant dispersal, rainfall, drought intolerance and infiltration rate are not the primary factors that are likely to form patterns in vegetation. However, these factors are represented as the reactive processes in the Turing structures. Chandrasekhar (1961) and Klausmeier (1999) had already demonstrated that only the relative periodicity of patterns depends on factors controlling the reactive processes – the resulting patterns themselves are insensitive. Model output showing the formation of patterns in vegetation that are largely not controlled by the levels of water input, plant demographic characteristics and land-management practices is difficult to justify on the basis of our understanding of field processes. Experimental studies have identified these variables as being of significant importance (Coffin and Lauenroth, 1990; Parsons *et al*., 1997, Parsons *et al*., 2006a; Parsons *et al*., 2006b). Field observations have also noted that in some areas, there is an apparent relationship between rainfall and pattern type (e.g. Deblauwe *et al*., 2008). However, this relationship is not universal, and very different patterns can be observed within an area of a few square kilometres, which is too small to be explained by the existence of a precipitation gradient. The second problem is that the authors reported that without positive feedback between vegetation density and water infiltration, pattern formation was not found. However, this linkage is already defined as an essential condition required for Turing instabilities – that the kinetics should include a positive feedback process (Murray, 1989), so the result really states that without one of the essential conditions for Turing instabilities being included, Turing patterns do not form. Although this statement is mathematically true, it does nothing to further the understanding of pattern formation in vegetation.

These more recent models are also applicable to and capable of generating patterns on flat surfaces, and it has subsequently been argued that this result invalidates the class of model that generates patterns only when some degree of pre-patternation is first applied (Couteron and Lejeune, 2001; Barbier *et al*., 2006). However, all reported implementations of Turing-type models require some degree of pre-patterning. For example, Rietkerk *et al*. (2002) perturbed small amounts of plants or water in some areas of the simulation to generate patterns, and even in the original work of Couteron and Lejeune (2001), cells in their simulation were perturbed by a low level of noise. For a Turing-type model such pre-patterning effectively means that the model must produce a pattern. Moreover, according to Couteron and Lejeune (2001), there is no evidence in the literature of patterns appearing in arid or semi-arid environments devoid of a consistent source of anisotropy.

The problems of the Turing-instability models highlight an important consideration that should be made for all numerical modelling techniques – if the underlying mathematical method is designed to generate a pattern, a pattern will be generated. This outcome is reasonable when the mathematics describe a real process. For example, following previous field observations (Thornes, 1990) the model of Thornes and Brandt (1993) was set up to favour shrubs, and therefore showed a continued dominance of shrubs. By contrast, published Turing-type models of vegetation patterning do not rest on field observations, but rely on many parameters that would be difficult or impossible to measure in the field, such as ‘half saturation constant’, or are defined simply to produce the desired result (see comments above about rainfall rates). Moreover, for Turing-type models, the underlying mechanism for symmetry-breaking requires coefficients to become negative under certain conditions – for example in the formulations described here, this would mean that there could be a negative water input for certain spacings of vegetation, which is meaningless in a physical sense. This inherent lack of realism in Turing patterns was reported by Rovinsky (1987), who noted that pattern formation could only occur where values of diffusion coefficients were in contradiction with physical arguments. Castets *et al*. (1990) and later Barbier *et al*. (2006) also observed that no unambiguous experimental observation of Turing patterns had been found. This ambiguity is drawn further into question by the contradictory conclusions drawn from Turing-instability models. For example, HilleRisLambers *et al*. (2001) argued that infiltration is not a primary causal factor in the formation of vegetation patterns, but van de Koppel and Rietkerk (2004) state that patterns do not form unless infiltration rate is linked to biomass. However, this linkage is not easy to define as the relationship between infiltration and biomass is not a straightforward one (Wainwright, 2009).

Other, fundamental problems with applications of the Turing model have been revealed when modelling results are compared to field data. The implementation reported by Couteron and Lejeune (2001) more closely follows the classic description of Turing instabilities applied to chemical reactions where the diffusion term is alternatively expressed as an activator (propagation) and an inhibitory (competition) process. In this case, the essential condition for a Turing pattern is that the inhibitor must diffuse much more quickly than the activator (Castets *et al*., 1990). In ecological terms, this condition would imply that the competition processes must occur over a larger scale than facilitative ones. While this difference in scale of operation may be appropriate for the consideration of a single species (e.g. a shrub canopy that facilitates growth by intercepting rainfall and channelling it to the roots operates over a smaller scale than that of competing root systems of adjacent plants: Abrahams *et al*., 2003; Martinez-Meza and Whitford, 1996; Gibbens and Lenz, 2005; Brisson and Reynolds, 1994), it is not necessarily appropriate when species of different types are competing (e.g. as shrubs invade grassland, the competition effect of canopy interception by the shrub is at the same scale as any facilitation due to shading). Furthermore, the resulting relative periodicity observed by Klausmeier (1999) was noted to be much larger than the range of interactions between plants, and it has been argued that “somehow” local processes are amplified by the spatial instability (Castets *et al*., 1990: 618). When the results of the model were compared to digitised images, Couteron and Lejeune (2001) found that the model yields much lower values for periodicity than were observed in field-site data. In their work, Couteron and Lejeune (2001) used realistic input data and found that the Turing model yields unrealistic intrinsic periods, whereas Klausmeier (1999) had used unrealistic input data to yield plausible intrinsic periods. A further problem arose when convincing field evidence was sought of patterns that are generated by Turing-type models, specifically the hexagonal pattern that corresponds to bare spots appearing in continuous cover of annual grasses. No detectible hexagonal symmetry was found in the digitised images examined by Couteron and Lejeune (2001) nor in the subsequent work of Barbier *et al*. (2006). Many reasons were proposed to explain why this pattern could not be detected, except one – that the model had generated a pattern that does not exist in the real world because it was an inappropriate representation of the real world.

An alternative to Turing-type models is provided by other instability-based approaches characterized by representations of short-range facilitation and long-range competition (e.g. Kéfi *et al*., 2007; Lefever *et al*., 2009). Whilst these alternative models overcome some of the limitations of the Turing-instability approach, they are nonetheless difficult to interpret in terms of physical processes (as discussed above).

2.3 Beyond the limitations of existing approaches

Both the Islands of Fertility model and those based upon instability approaches address patterns in desert vegetation that exist at a specific scale (plant and patch scale). However, there has been a recognition in recent years that there are patterns in desert vegetation that exist at larger scales, such as community and landscape scales (Wainwright *et al*., 2002; Peters *et al*., 2005; Turnbull *et al*., 2008), which are addressed neither by the Islands of Fertility nor by instability-type models. The latter have been further hamstrung by the conceptual limitations of the models – applying models that are inappropriate and based on forcing process representations to fit a model structure rather than modelling the actual processes – and thus the practical limitations of producing meaningful parameterizations. Both approaches are limited by the way in which inherent problems with definition prevent adequate testing.

Modelling studies are nevertheless useful for probing the causes and consequences of the observed dynamic patterns of desert vegetation. Not only may these studies provide a rigorous test of our understanding of ecosystem functioning, they can also provide detailed information that is not readily available from experimental work (for example, due to the timescales involved in measuring changes in plant communities [Parshall *et al.,* 2003] or due to ethical considerations such as large scale experimental modification of vegetation and landscapes). Recent conceptual advances into the understanding of multi-scale processes in drylands have focused on the rôle of process connectivity, drawing on broader concepts of landscape connectivity (Taylor *et al*., 1993; Turner *et al*., 1993; Western *et al*., 2001; Bracken and Croke, 2007; Müller *et al*., 2007; Turnbull *et al*., 2008; Okin *et al*., 2009). Turnbull *et al*. (2008) suggested that spatial patterns emerge as the result of spatial feedbacks between landscape structure and process. As the structure imparted by the vegetation changes, it leads to process feedbacks which lead to further changes in landscape structure. For example, the formation of mounds under shrubs leads to changes in infiltration and flow pathways, which become reinforced by increased erosion rates (Parsons *et al*., 1996). Okin *et al*. (2009) provided a generic overview that suggested that connectivity across a range of processes, such as water and wind transport, animal activity and fire, could be used to understand ongoing degradation in the US Southwest. Based on this overview, it is hypothesized here that a connectivity-based model, when combined with local processes – as derived from empirical work developed from the Islands of Fertility model – will provide a way out of the present impasse, and allow modelling studies to investigate multi-scale pattern formation in desert ecosystems. Specifically, a connectivity-based approach may provide a process-based understanding for the development of a model with advective and diffusive components, that overcomes the limitations discussed above. Furthermore, if such an approach rests upon a theoretical framework with a sound process-based understanding, it can thus be parameterized with data that can be measured and have a clear physical meaning. Testing the ability of such a model to reproduce the spatial and temporal progression of vegetation patterns, will enable it to be used with confidence to generate testable predictions relating to the function of dynamic desert ecosystems in response to a variety of endogenous and exogenous disturbances.

3. Modelling Framework

The ecogeomorphic modelling framework proposed here (figure 1) meets the characteristics outlined above. In this framework, the environment is represented as spatially related locations that may be inhabited by different vegetation types and quantities. Processes operating within the landscape are considered as being either vertical or lateral. Vertical processes act as inputs (e.g. rainfall, or atmospheric deposition of nitrogen) or outputs (e.g. losses of biomass through herbivory), while lateral processes act entirely within the system (e.g. movement of propagules by water). These processes provide locations with resources and propagules (R&P) that are the main drivers of plant growth and recruitment. Resources are defined in the model as abiotic materials that plants need to grow and propagate. Although the model can include any number of resources, emphasis has been placed on water and nitrogen as the principal limitations on growth in deserts (Fitter and Hay, 1985; Whitford, 2002, p14; Wainwright, 2009). Propagules are biotic materials required for reproduction (e.g. seeds, tillers, cladodes).

The lateral processes controlling the movement of R&P can be expressed as a set of vectors. Three vectors are included in the model: water, wind and animals. However, in principle any number could be included. The ability of vectors (in the sense of a geometric entity, having both a direction and magnitude) to redistribute R&P within the landscape is controlled by external factors. These external factors are termed "lateral externalities". For instance, the movement of propagules by wind depends on wind speed and direction (Okin *et al.,* 2001). The movement of material by water depends on raindrop energy, the infiltration-excess runoff, surface topography and the characteristics of the material being moved (Parsons *et al.,* 2004). Animals move material according to foraging strategies. For instance, large grazing mammals can move large amounts of organic carbon and nitrogen in their guts over great distances, while propagules can be moved internally or externally as burrs and cladodes attached to the hide of the animal (Turchin, 2003).

Similarly, the vertical processes that move R&P into and out of the landscape are controlled by external factors, termed "vertical externalities", which include infiltration, leaching, evaporation and wet/dry deposition of nutrients or seeds. Direct disturbance of biomass is controlled by disturbance factors, termed "disturbance externalities", which include, destruction or removal of biomass by fire, disease or herbivory.

The operation of the vectors which control the movement of R&P can be subdivided into two broad process states. These two process states are advection and diffusion. The important advective processes are concentrated overland flow (Wainwright *et al*., 2008a), aeolian transport through large interplant gaps and the movement of, typically, large animals through the landscape. They are a function of lateral externalities such as wind strength, flow hydraulics, or the type and number of large animals. The important diffusive processes are splash, local distribution by small eddies and movements caused by small animals.

For the purpose of the model, connectivity quantifies the extent to which individual cells of the landscape may receive a subsidy as a result of the operation of a specific vector. The effectiveness of vectors to move R&P in the direction of flow depends on the spatial arrangement of what are termed connected pathways (Bartley *et al*., 2006). For wind, connected pathways are quasi-linear, aligned with the direction of the wind and terminated when wind intersects a plant (Okin and Gillette, 2001; Okin *et al*., 2009). For water, gross pathways follow the energy slope and net pathways follow the aspect. For animals, the definition of connected pathways depends on the behaviour of individual species, for example, for large grazing mammals; a connected pathway is defined as contiguous areas with palatable biomass above a threshold amount (Turchin, 2003; Thornes, 2007). In the model, all connected pathways terminate in sinks. For example, a shrub would terminate the wind vector, a vegetation patch would terminate the water vector, and an unvegetated area would terminate the grazing vector. A diagrammatic representation of connected pathways and their terminations is shown in figure 2. The behaviour of the biomass controls the number and arrangement of connected pathways. However, because connectivity is also an emergent property of the model, reflecting the feedbacks between the vectors and vegetation growth and death, it is also an independent measure of the ability of the model to represent the dynamics of desert ecosystems: if the processes in the model operate in a way that is compatible with reality, then connected pathways should be observable in real landscapes, and rates of change should also be equivalent.

Not all distributions of R&P are amenable for movement by vectors. Labile nitrogen beneath canopies, for instance, cannot be moved by infiltration-excess runoff occurring in plant interspaces. The extent to which R&P are amenable to movement by vectors is specified in the model as “availability”. Availability is controlled by the biomass content in each spatial location. For wind and water, which cannot (under non-drought conditions) remove material from under-canopy areas, R&P may only be removed from plant interspaces. Animals, in turn, can forage only where there is a significant amount of palatable forage.

Demographic processes (recruitment, establishment, growth and mortality) control the amount of biomass of individual species (e.g., Coffin and Lauenroth, 1990). The spatial patterning of structurally diverse vegetation controls the strength of vectors acting on the land surface (e.g., Okin and Gillette, 2001). For example an open plant community would allow for a greater number of connected pathways along which wind and water could operate, but some species of plants do not provide palatable forage and so reduce the number of grazer-connected pathways. The latter reduction in connectivity in turn affects the redistribution of R&P, resulting in sinks of resource where plants are more likely to become established and survive. Therefore, this model explicitly considers relationships among the forces that control R&P movement via vertical and lateral externalities and vegetation distribution via connectivity. As a first approximation, it is assumed that soil mechanical properties (including density and hardness) may be neglected and so plant growth is assumed to be equally possible in all locations (Bugmann and Solomon, 1995; Higgens *et al.,* 1996; Starfield, 1996), though, as with the number of vectors, such variables could, in principle, be incorporated into the model.

4. Numerical Implementation of the Model

In order to represent the spatial arrangement and structure of the simulated ecosystem, the area under consideration is divided into a grid of equally spaced nodal points enclosed by square cells of equal size. The number of cells used is specific to the particular implementation. The placement of these points coincides with the physical boundaries of the grid. A general point 'P' and its neighbours are identified using a Moore neighbourhood of the eight neighbouring points (figure 3). In order to limit the effects of numerical boundary conditions, cells are always wrapped (i.e. to form a cylinder) in the direction perpendicular to the vectors using a simple up-and-down procedure (Furukawa *et al.,* 2000). For water the direction of the vector is defined (arbitrarily and in this implementation of the model) as north to south implying a sink of water at the southern edge of the grid. Therefore, the line of action for grazers is south to north (that is, away from the implied water source, e.g. Lange *et al.,* 1984). For both water and grazers, cells are consequently wrapped across the east and west boundaries. Wind is allowed to operate in any direction across the grid, but in the present implementation, the line of action is east to west so the north and south boundaries are wrapped. A periodic boundary condition is applied in the direction aligned with the vector (Leach, 2001) when the grid represents a terrain with no slope.

This condition was also applied to the application of the model described below to demonstrate that numerical boundary conditions did not affect the model results.

The model operates with an annual time step. For each cell the change in resource and propagules (represented through the term Z) in each time step (*t*) is as a result of three actions. These are the actions of vertical processes (Q_V), which add or remove material to the cell, the lateral processes (Q_H), which redistribute material in the grid, and the action of plant species (U), which varies depending on whether resources or propagules are being considered: where abiotic resources are considered, U represents a consumption term and where propagules are considered U represents a production term. The change in each (*i*) abiotic resource and biotic propagule for each cell can be expressed in differential form:

$$\frac{d\,Z_i}{dt} = \frac{d\,Q_{V_i}}{dt} + \frac{d\,Q_{H_i}}{dt} + \frac{d\,U_i}{dt} \qquad (1)$$

The model needs to be general enough to allow a range of physical processes to operate within the grid. However, different physical processes will operate over different spatial and temporal scales. The different spatial scales are accounted for by parameterizing the model according to the size of the cells used in the implementation, but a different procedure must be used for defining the various temporal scales. For example, a summer monsoon-type rainstorm will quickly lead to the generation of overland flow (Parsons *et al.*, 1997), whereas processes allowing this water to infiltrate – particularly to deeper soil layers – may take considerably longer (Hillel, 2004; Wainwright, 2009; Wainwright and Bracken, 2011). In order to calculate the physical responses of such a system, Peters (2002a) used daily totals (for example rainfall rate), which were summed to monthly totals, whereas the more appropriate yearly values for biomass were aggregated over each month. Equation 2 is therefore cast to reflect different temporal scales (represented by θ, ϕ and ψ) summing to the same time scale (t).

$$Z_i = \int_t^{t+1} \left[\left(\frac{d\,Q_{V_i}}{d\theta} \right) \frac{d\,\theta}{dt} + \left(\frac{d\,Q_{H_i}}{d\phi} \right) \frac{d\,\phi}{dt} + \left(\frac{d\,U_i}{d\psi} \right) \frac{d\,\psi}{dt} \right] \qquad (2)$$

The different timescales imply that different processes are applied in a strict order (from fastest to slowest) in the calculation, and each process is enclosed within its own iterative loop. The numerical solution is therefore formulated so that the first calculation procedure adds or removes R&P by vertical processes. Subsequently the R&P are redistributed by lateral processes. Finally the biomass is allowed to respond to these new R&P distributions at the end of the time step (figure 4). All results presented below are for the aggregated effects of these timescales at an annual resolution.

4.1 Vertical Processes

Vertical processes are those that can move R&P into and out of the landscape without intermediate movement across the surface of the grid. To represent different processes, the Q_V term is divided into two parts. The first part ($Q_{V_{external}}$) represents those processes controlled wholly by vertical externalities, and thus operate independently of the biomass in the cell (e.g. precipitation rates); the second part ($Q_{V_{internal}}$) comprises those vertical processes linked to cell biomass (e.g. infiltration rates). For simplicity of implementation, the effects of disturbance externalities are also included within vertical processes and can be internal or external according to whichever disturbance externality is being considered. The term Q_V is therefore a representation of the output of suitable sub-models to describe these phenomena:

$$QV_i = QV_{i,external} + QV_{i,\text{int}\,ernal} \tag{3}$$

By defining a spatial grid of nodal points, the model has the flexibility to include appropriate sub-models for spatial variability that apply to the process in question.

4.2 Lateral Processes

The extent to which R&P are amenable for movement by vectors, is specified by the “availability” (A) term, which is itself a function of biomass in each spatial location. We define a maximum biomass (B_{max}) for each species that can exist in each cell and a linearly decreasing amount of R&P (Greene *et al.* 1994, Morgan 1996) is available to the water and wind vectors as the actual biomass in the cell increases as:

$$A_{i,cell} = \left[Z_i - Z_i \frac{B}{B_{\max}} \right]_{cell} + Q_{up,i} \tag{4}$$

while a linearly increasing amount of R&P is available to grazers as biomass increases:

$$A_{i,cell} = \left[Z_i \frac{B}{B_{\max}} \right]_{cell} + Q_{up,i} \,. \tag{5}$$

For all three vectors, the availability of propagules increases with biomass (equations 4 and 5). The availability term also includes the R&P moved into the cell from its up-vector neighbour ($Q_{up,i}$).

When the connected pathways are terminated, the sum of the resource that has been entrained by the vector along the connected pathway is redistributed from the cell terminating the connected pathway, i.e. R&P movement becomes a diffusive, internally controlled process. The form of this redistribution is modelled by a series of convolution matrices that are specific to each transport vector and each sink (e.g. shrub or grass). It is assumed that upon encountering a cell terminating a connected pathway, and in all subsequent vegetated cells along the line of action of the vector, some proportion of the entrained R&P (α, β, γ, ε and ζ according to the relative position: see equation 6) is redistributed to the eight cells that surround the disconnected cell. First, the R&P moved down-flux is combined with the available R&P of the current cell into a single term, Q_{ADV}, (the sum of all the available R&P). It is considered that part of this R&P remains in the current cell, lateral distributions of R&P from the current cell are symmetrical, but redistributions along the line of the vector can be asymmetrical. These descriptions are summarised in equation set 6, using the water vector as an example. Except for the R&P that is advected to the south cell, the R&P that is redistributed to the neighbour cells is unavailable for further movement by the vectors in the current time step. For the other vectors, the equation set is rotated relative to the appropriate direction of operation of the vector.

NW = $\frac{\varepsilon}{2}Q_{ADV}$	N = βQ_{ADV}	NE = $\frac{\varepsilon}{2}Q_{ADV}$
W = $\frac{\alpha}{2}Q_{ADV}$	Current Cell = $Q_{ADV}(1-\alpha-\beta-\gamma-\varepsilon-\zeta)$	E = $\frac{\alpha}{2}Q_{ADV}$
SW = $\frac{\zeta}{2}Q_{ADV}$	S = γQ_{ADV}	SE = $\frac{\zeta}{2}Q_{ADV}$

(6)

This description links the amount of R&P that is moved to the magnitude of the external controls, in the sense that larger rainfall amounts result in a greater amount of R&P moved via the lateral processes compared with drought years. It should be noted that the length and spatial arrangement of the connected pathways depends upon biomass response, which itself is a function of lateral and vertical processes that occurred during previous time steps.

Only the R&P that is added in the current time step is moved in this way. Propagules are either established as seedlings or fail to establish before subsequent calculation steps, and any resource remaining from previous time steps is considered as unavailable to the lateral processes and moved down through the soil layers by the vertical processes. All resource, whether added and moved in the current time step or accumulated from previous time steps is then available to be used by the biomass for growth and propagation.

The derivation of the convolution matrices is analogous to the discretization of partial differential equations to describe the diffusion of R&P around the current cell, and is based on the finite volume method for computational fluid dynamics (e.g. Versteeg and Malalasekera, 1995). As such, this model can be implemented (via equation 6) analytically, where explicit equations control spatio-temporal dynamics, or numerically, where dynamics are controlled by a combination of analytical equations and neighbourhood-based rules. In the present implementation, these convolution matrices are specified as neighbourhood-based rules that encapsulate the detailed biophysical processes that result in the deposition, and patterns of deposition, of material in the vicinity of plants. This neighbourhood-rule approach allows the transport of material by vectors to be included explicitly without the computational burden of having to model the sub-grid-scale physics explicitly.

4.3 Biomass Response

Any suitable model for vegetation-growth dynamics can be included through the term U (in equations 1 and 2). The present implementation of the model is designed to test the extent to which local redistribution of R&P can lead to emergent patterns of desert vegetation, and so to include a logistic growth equation here (e.g. Thornes and Brandt, 1993) would mask the effects of changing R&P when the biomass content of a cell is near to zero or the carrying capacity (Kot, 2001). Biomass is thus allowed to change linearly in response to new resource levels in the cell.

The change in biomass (B_j) for each species j is calculated using the sum of each resource in the cell (R_{TOT}), which includes the redistributed resource from the current time step plus any resource remaining from previous time steps, which is stored in the lower soil layers. The actual change is biomass is computed from the most limiting of the resources.

$$\Delta B_{j,i} = \left[\frac{R_{tot,i} - B_j M_{i,j}}{E_{i,j}} \right] \quad (7)$$

M is the requirement of each *i* resource to maintain 1 g of perennial material in the plant (used here to describe the resource requirement for maintenance of biomass), and E is the resource needed to yield 1 g of new leafy material (used here to describe the resource requirement for new growth) (Peters, 2002a). This method allows the model to describe vegetation response by process, as multiple species may be parameterized using data that can be measured in the field. As such, multiple actual species are represented, unlike the majority of previous spatial modelling work where generic grass- or shrub-type species have been considered as broad functional types (Thornes and Brandt, 1993; Koppel and Rietkerk, 2004; Istanbulluoglu and Bras, 2006; Klausmeier, 1999; HilleRisLambers *et al.,* 2001; Rietkirk *et al.,* 2002, Couteron and Lejeune, 2001; Barbier *et al.,* 2006).

5. Model Implementation

In order to test the numerical model, it has been implemented with respect to parameters and conditions in the deserts of the south-western USA. Two sets of simulations have been conducted, but only the latter are presented here. In the first, a series of simulations was carried out to explore the behaviour of the model. These simulations are reported in the Appendix.

They showed agreement of the behaviour of our model with observed characteristics of desert vegetation, giving us confidence to use the model test hypotheses of vegetation change in the American Southwest.

The American Southwest is one of the many regions in the world where invasion of woody shrubs into desert grassland has been observed (Schlesinger *et al.*, 1990; Archer *et al.*, 1995; Allred, 1996). Increasing aridity (e.g. Archer, 1995; d'Herbes *et al*., 2001) and overgrazing (e.g. Archer, 1995; Okin *et al.,* 2001; Nash *et al.,* 2004; Westoby *et al.*, 1989; Gibbens and Lenz, 2005) are commonly used explanations for shrub invasions into grasslands. Thus, here we use the model to investigate the viability of these explanations both individually and in combination, and to propose testable hypotheses of why changes in desert ecosystems are initiated. A further advantage of the use of this region for an implementation of the model is that it is relatively data-rich, and thus some information exists that can be used to provide an independent test of the model output.

The specific site chosen for model implementation is the Jornada Basin Long Term Ecological Research site in southern New Mexico (32º37' N, 106º40 W, 1260 m a.s.l.). The Jornada Basin LTER was established with the task of quantifying the processes that have caused dramatic changes of structure and functioning of Chihuahuan desert ecosystems such as have been noted over the past 150 years, and links into pre-existing and continuing datasets collected by the USDA-ARS Jornada Experimental Range field station. An impressive array of data is available for the Jornada Basin, which makes it possible to look for temporal trends, spatial patterns and ecosystem changes over the 20th century (Havstad *et al.,* 2006; Jornada LTER, 2010;

Wainwright, 2005; Yao *et al.,* 2006). Consequently, the region, and particularly the LTER site, is rich in data with which to parameterize our model. The Jornada Basin LTER, experiences severe drought (Palmer Drought Index between -3 and -4) (Nicholson, 1979; 1981) every 20 to 25 years, and extreme drought (Palmer Drought Index of <-4) occurs every 50 to 60 years. Livestock were introduced from Mexico during the early part of the 16th century, but grazing was limited in the Jornada Basin owing to the lack of surface water until the sinking of the first wells in 1867 following the Homestead Act of 1862. Since then it has supported a mainly beef rangeland livestock industry (Gibbens *et al.,* 2005; Havstad *et al.*, 2006). For many arid and semi-arid ecosystems the amount of biomass supported per unit area of primary production is approximately an order of magnitude greater under rangeland livestock production than under natural non-agricultural conditions. For example, in the Jornada the biomass of native consumers is approx 0.03 g m^{-2}, which consume less than 5 g m^{-2} of forage per annum compared to a conservative stocking rate of cattle of 1.7g m^{-2}, which consume 8-14 g m^{-2} per annum on the same grassland (Havstad *et al*., 2006 but see also Pieper *et al.,* 1983).

5.1 Model Parameterization

A realistic test of the conceptual model should be undertaken with reference to specific localities and specific species if insights beyond broad generalizations are to be gained. Such site-specific insights are a prerequisite for informed management interventions (Westoby, 1980). Accordingly, parameterization is based, as far as possible on data obtained from field measurements at the Jornada LTER, or elsewhere in the US Southwest. For the implementation, we use a planar 50 × 50 m grid that is subdivided into cells of 1 m^2 with a downslope gradient of 2° north-south. A summary of the model input conditions is presented in Table 1.

5.1.1 Biomass

The encroachment of grassland by woody shrubs may involve several species, but in this implementation of our model, plant demographic processes were parameterised using two species that are indicative of the grass to shrubland transitions observed in the deserts of the south-western USA (Humphrey and Mehrhoff, 1958; Schlesinger *et al.*, 1990; Peters, 2002a; Peters, 2002b). These two species are *Bouteloua eriopoda* (Torr.) Torr. (black grama) and *Larrea tridentata* (DC.) Coville (creosotebush). The first represents a typical desert grass, which is the dominant species in many hot desert grasslands of the southwest USA (Smith *et al.*, 1996; Nelson, 1934). Black grama typically occurs on rocky or sandy mesas and open ground, with well drained sandy and gravelly soils (Humphrey, 1958) and is particularly abundant in the Chihuahuan desert (Yao *et al.*, 2006; Peters, 2002b).

Black grama often shows an association in upland areas with our second simulated species, creosotebush (Gardener, 1950). Creosotebush is a drought-tolerant, evergreen shrub and a dominant or co-dominant member of many plant communities in the Southwestern deserts (Humphrey, 1958). It usually occurs in open, sparsely populated areas, but also appears as a transitional species in desert grasslands (Humphrey and Mehrhoff, 1958), and is noted to grow on bajadas, gentle slopes, valley floors, sand dunes and in arroyos, typically on calcareous, sandy and alluvial soils that are often underlain by a caliche hardpan (Went and Westergaard, 1949). Creosotebush occurs as far south as north-central Mexico, and as far north as central Nevada

(Ackerman and Bamberg, 1974; Pockman and Sperry, 1997), where average annual rainfall ranges from 100 to 300 mm (Castellanos and Molina, 1990).

5.1.2 Externalities and Vertical Processes

The instrumental record for rainfall at the Jornada begins in 1914, so longer term data for rainfall are only available by reconstructions. Tree-ring data have been used to reconstruct climate data in the US Southwest for the time period extending over the last few hundred years (d'Arigo and Jacoby, 1992), that includes the period of introduced cattle grazing. Data are available from the International Tree Ring Databank for three locations within a 50-km radius of the Jornada Basin, which were used by Wainwright (2005) to reconstruct a common sequence of the Jornada climate (figure 5a) extending from 1659 to 1970. Comparison with the more recent instrumental record (approximately 80 years long) suggests that although the retrodictions can capture extreme events, they tend to underestimate the magnitudes of these events (figure 5b). Cycles were present similar to those in the instrumental record, and drought conditions were retrodicted for the years 1676, 1790, 1721, 1723, 1736, 1872 and 1912. Greater inter-annual variability (in terms of number of rain days, rainfall totals and annual moisture balance) were noted until the late 18th century, whereas the 20th century seems to be particularly anomalous with long wet periods alternating with dry spells. The reconstructed rainfall record provides a regional input in terms of precipitation to our model, and includes disturbances due to drought implicitly.

Cattle-stocking levels over the 20th century for which historical data are available (Havstad *et al.*, 2006) are shown in figure 6. Disturbance due to grazers is modelled explicitly by simulating the removal of a specified quantity of palatable biomass from each vegetated cell, in each year. A summary of the simulated grazing levels is presented in table 2 which reports the minimum and maximum of harvest rates for cattle under three different stocking levels described as conservative, recommended and overgrazed by Havstad *et al.*, 2006. In our simulations, we used the central value of the reported consumption range.

5.1.3 Lateral Processes

In this implementation, three vectors are defined: water, wind and animals. As the action of grazers is being modelled as a disturbance externality, the animal vector in this implementation represents the action of cattle. The model requires rules for the proportion of resources and propagules that can be moved by each vector, and, although all the parameters used in this model could be measured at the field site, as yet much of this information is not available in a form that can be implemented numerically. Consequently, we have inferred the R&P availability and convolution matrices from experimental work which alludes to the mechanisms by which vectors might operate (Parsons *et al.*, 1992; Parsons *et al.*, 1997; Parsons *et al.*, 2004; Parsons *et al.*, 2006a-b; Okin and Gillette, 2001; Okin *et al.*, 2001; Okin *et al.*, 2009), and also from process-based modelling studies (Scoging *et al.*, 1992; Parsons *et al.*, 1997; Wainwright *et al.*, 1999; Wainwright *et al.*, 2002; Wainwright *et al.*, 2008a-c). We specify that, of the resource added to each cell per time step by the vertical processes, water cannot be moved from cell to cell under the action of wind or grazers, and we allocate 45% of the nitrogen to be amenable to movement by water, 45% to be amenable to movement by wind and 10% to be amenable to movement by grazers. These proportions are arbitrary, but based upon the argument that wind and water have equal access to nitrogen in the soil, whereas grazers have access only via vegetation uptake. The redistribution of R&P from vegetated cells is effected according to the species-specific rules defined in table 3a for water-disconnected locations, table 3b for wind-disconnected locations and table 3c for grazer-disconnected locations.

5.1.4 Resources and Propagules

Aside from rainfall and grazing externalities, model parameterization requires information about the abiotic resources necessary to support plant activities. Although the model can be parameterized to accommodate any number of resources, we have focused on two in this implementation: water and nitrogen. The water input to the model is provided through the descriptions of rainfall described previously.

It is, however, difficult to find suitable parameterization data for nitrogen. The analysis of the plant-available nitrogen in the soil is not a particularly useful measure of the total nitrogen available to plants, since nitrogen released by microbes can be rapidly taken up by plants and never appear in the soil pool (Gallardo and Schlesinger, 1992). This issue is noted to be particularly important in semi-arid environments (Clark and Tilman, 2008). The point at which nitrogen becomes limiting to plant growth at the Jornada, under conditions when water is not limiting, must be answered in the short-term, as a longer-term perspective would allow the invasion of non-desert vegetation, with much higher productivity, assuming that such vegetation possesses the necessary adaptations to semi-arid environments. In the short-term, it seems that nitrogen is limiting whenever water (the dominant control in its own right and through its partial control on nitrogen availability) is non-limiting, so the present rate of nitrogen mineralization of up to 5 g m^{-2} a^{-1} (Loreau *et al.*, 2002) would be the lower limit to plant growth in various habitats. The rate of annual nitrogen mineralization has not been measured in much detail since many researchers believe periods of rapid mineralization probably occur during a few wet months, and then no mineralization takes place for the rest of the year. Thus, nitrogen inputs were simulated as a constant values in this work (Baez *et al.*, 2007), but the amount of nitrogen that is used by the plants to support existing biomass, and for new growth was allowed to vary linearly with rainfall (Burke *et al.,* 1990; Peters, 2006a; Wainwright, 2009).

After a resource has been added by vertical processes, and moved by the lateral processes, it is then used to support plant growth. Descriptions of resource use by the biomass (table 4) are based on data given in Peters (2002a), Maneta *et al.* (2008) and Wainwright (2009).

The consumption of resource by the biomass is calculated using the sum of each resource in the cell, which includes the resource from the current time step plus any resource remaining from previous time steps, which are stored in the middle and deep soil layers. Three soil layers are simulated:

- The top layer, from depths of 0 to 100 mm. This layer contains resource added in the current time step, and subsequently redistributed by the vectors. The depth was selected to coincide with measured wetting-front depths (Martinez-Meza and Whitford, 1996; Wainwright *et al.*, 2008b-c; Parsons *et al.*, 1997).
- The middle layer, from depths of 100 to 350 mm. This layer corresponds to the maximum observed depth for root-channelized water in creosotebush (Martinez-Meza and Whitford, 1996; Scott *et al.,* 2008) and encloses the point of maximum root density for both creosotebush and black grama (Martinez-Meza and Whitford, 1996; Sun *et al.*, 1998; Gibbens and Lenz, 2001; Peters, 2002a).

- The deep layer, from depths of 350 to 1500 mm. This layer corresponds to the maximum observed depth of creosotebush roots (Peters, 2002a; Gibbens and Lenz, 2005).

Black grama is an intensive exploiter of water and derives the majority of its moisture through dense root networks in shallow soil layers that enable it to exhibit rapid growth and water absorption following rainfall. Black grama tolerates short droughts, and recovers rapidly from stress when water is available (Burgess, 1995). These factors are reflected in the higher proportion of roots in our simulated top layer, which allows grass to access the resources that are added in each time step ahead of creosotebush. During conditions with adequate water input, the top and middle layers will receive a greater quantity of water, and this will favour the grass (Walter, 1971; Thornes, 1990). Creosotebush has a greater proportion of roots in the middle and particularly the deep layers where unused resource from previous time steps is stored. During times of resource stress, creosotebush can access this store ahead of black grama, reflecting the greater drought tolerance of shrubs (Walter, 1971; Herbel *et al.*, 1972; Casper and Jackson, 1997). These arguments represent competition processes between the species (Thornes, 1990).

The proportion of resource in each layer that can be used by each species is a function of root biomass (table 5, figure 7). The above-ground biomass is converted to below-ground biomass using the relationship proposed by Peters (2002a) wherein black grama root biomass is estimated to be 1.44 times greater than the above-ground biomass, and the root biomass of creosotebush is estimated to be equal to the above-ground biomass. In order to distribute root biomass among the layers, we follow the method described by Peters (2002a) which was itself based on the analyses of root distributions of a large number of grassland species in the US by Sun *et al*.

(1998). The method assumes that root biomass increases linearly to a species-specific depth, then decreases allometrically to the maximum depth. Parameterization data were all obtained from Peters (2002a).

If creosotebush is the dominant species in the cell, then a proportion of the top layer resource, (equal to the proportion of creosotebush biomass in the cell), is directly channelled into the middle and deep layers (Martinez-Meza and Whitford, 1996; Abrahams *et al.,* 2003). The movement of resource through the soil layers acts as a facilitation term. Once established, creosotebush is thought to improve sites for the annual plants that grow beneath its canopy by trapping sediment, organic matter and propagules, and by increasing water infiltration and storage (Bainbridge and Virginia, 1990). Although this description of channelization should strictly apply only to water, nitrogen is also handled in the same way in the model implementation to reflect the ability of a plant with access to deep water to use more of other nutrients (Martinez-Meza and Whitford, 1996), and it is reasonable to assume that the water contains significant amounts of dissolved nitrogen (Schlesinger *et al.*, 1990; Schlesinger and Peterjohn, 1991; Grimm and Railsback, 2005; Brazier *et al.*, 2007; Michaelides *et al.*, 2012; Turnbull *et al.*, 2010).

In each cell, if there is insufficient resource at a particular time step to satisfy maintenance requirements, the biomass is reduced. When the outcome is a loss of biomass, and this loss is due to insufficient water, the model allows all water to be used but no other resources are consumed (Hooper and Johnson, 1999). When the loss of biomass is due to a deficit of nitrogen, the model allows the biomass to consume all resources in sufficient amounts to maintain (as far as possible) existing biomass. Under conditions of biomass loss, no propagules are generated. These rules reflect some of the observed adaptations of desert vegetation to survive extremes of climate (Walter, 1971; McClaran and Van Devender, 1995).

Descriptions of propagule movement are also inferred from literature. Although black grama provides excellent forage, populations are damaged by grazing as these plants rely heavily on stoloniferous regeneration (Gosz and Gosz, 1996; Canfield, 1948). Whilst these means of reproduction are effective under arid conditions, they do not promote extensive migration. Consequently, black grama is slow to colonize adjacent areas (Brown and Gersmehl, 1985). This effect is compounded by the low viability of its rarely produced seeds (Nielson, 1986). The effect of droughts and grazing are to decrease tuft area, which allows for greater wind erosion of the upper loose soil litter layer required for stolon rooting. Creosotebush is a stable member of desert plant communities owing to its primarily vegetative method of reproduction via cloning (Romney *et al.*, 1989; Cody, 1986). Germination of seeds is rare, and the rate is reported to be less than 20% outside of the optimal summer rainfall of between 75 and 150 mm (Ackerman and Bamberg, 1974). The seeds are primarily adapted for tumbling, as they are too heavy for lofting and the trichomes are not stiff enough to penetrate animal skin therefore not adapted to animal dispersal (Chew and Chew, 1970).

In the model, we simplify these complex conditions of propagule production and movement by allowing propagules to be generated whenever a positive growth rate is recorded. For our purposes, propagules are a species-specific proportion of the new growth of each plant, and a proportion of these propagules is available to the vectors for redistribution within the environment. A small proportion of this annual new growth is allowed to move under the action of the vectors in the next time step, and will become established in new cells only if resource levels in these new locations are sufficient to support an increase in biomass. The majority of the propagules for each species will move to adjacent cells by diffusion to represent the predominantly asexual method of reproduction utilised by desert plants. If some propagules are moved to a connected cell, they are then dispersed along connected pathways by the vectors (Barbour, 1969; Miller and Donart, 1979).

For both species, water availability is the primary controlling factor in terms of propagule dispersal (Aguiar and Sala, 1999). This control is modelled by having the majority of propagules following the line of action of the water vector (i.e.downslope). These parameter values can be changed to account for the different germination probabilities of individual species, but for the simulations presented here, the values are fixed (table 6). Species with seeds easily transported by the wind could be similarly moved in the model along the wind direction.

5.2 Descriptions of the simulations

The simulations have been carried out to test hypotheses of the different rôles of precipitation and grazing in explaining woody shrub invasion and of the causes of spatial variability in response to drought. Conflicting results exist in the literature evaluating the effects of temporal variability in precipitation on vegetation. It is suggested that one cause of this conflict may be the consequence of the representation of the rainfall pattern in a model. To assess the extent to which this is the case, four simulations have been undertaken in order to explore different levels of complexity in the representation of rainfall on the resultant vegetation patterns and their interactions with grazing pressure. Simulations were characterized by (a) stochastic rainfall with no temporal autocorrelation; (b) rainfall reconstructed from the tree-ring record for the period 1659-1970; (c) as (b) but with variable grazing levels. For simulation (a) the stochastic rainfall is generated from the mean and standard deviation of the reconstructed rainfall of simulations (b) and (c). Finally, in simulation (d) we use the model in conjunction with the 80-year instrumented rainfall-data record to examine reported differences in response to the same climatic conditions.

5.3 Initial conditions

All simulations were initialized from the same randomly generated landscape (Table 1) which included a random distribution of black grama biomass and a uniform distribution of shrub biomass (to represent a seedbank). An initial biomass of 60 g m^{-2} was specified for black grama. This initial value was then perturbed by a low level of white noise (a random signal with a flat power spectral density, in this case, by generating a pseudorandom matrix of numbers lying between 0 and 1 with an average value of 0.5). This procedure follows the method of Couteron and Lejeune (2001). This method of perturbation of the biomass yields an initially random distribution of grass in each cell and the same initial random distribution was used as a starting point in all of the simulations presented here. The initial biomass of the shrubs was specified as 10g m^{-2} in all cells, to represent a seed bank. The randomly generated map of biomass is depicted in figure 8. The initial resource level in the mid and deep layers was set to 25g/m^2 for water and 0.25g/m^2 for nitrogen. Resource levels of the top layer were provided by the input of water and nitrogen in each time step.

In all of the following simulations, all three vectors (water, wind and grazers) operate to move R&P through the landscape. The effect of herbivory by grazers is included only in simulations c and d.

5.4 Presentation of results

We present the results of the simulations in two formats. In the first, we present three graphs showing a) the average change in grass and shrub biomass in the cells along a transect along the centre line of the grid; b) the average change in water and nitrogen in mid and deep soil layers for the same cells; and c) changes in connectivity for these cells. In the second format we display maps of grass and shrub biomass in each cell at selected times during the simulations.

6. Results

Simulation a – Stochastic rainfall

Results from Istanbullouglu and Bras (2006) have suggested that increased variability in rainfall and lower rainfall levels are mechanisms that on their own, and in combination with each other, will decrease the average grass biomass cover. This suggestion may be linked to the observation of Thornes and Brandt (1993), that more frequent woody plant encroachment and desertification are more likely to occur when the grass is in a degraded condition. Williams and Albertson (2006) argued similarly that some account must be taken of rainfall structure in models of dryland vegetation in order to understand the changes in a more meaningful way, (although they did not pursue this argument in their paper). For our first examination of the effects of rainfall representation on shrub invasion, we have reproduced Williams and Albertson’s model, which controls the statistical structure of annual rainfall by generating a synthetic rainfall time (t) series (P) that is represented by the equation

$$P_t = \langle P \rangle + U_t + A_p \sin\left(\frac{2\pi t}{T_p}\right) \qquad (7)$$

where U_t is an uncorrelated, log-normally distributed random variable with variance $\gamma\sigma^2_p$ where γ is a parameter lying between 0 and 1 that controls the partitioning of the total variance (σ^2_p) between uncorrelated (white) noise and correlated (sinusoidal) components (shown in figure 9a). A_p is the sinusoidal amplitude (mm) and T_p is the period (years). The mean annual rainfall $<P>$ is the long term average calculated from the tree-ring rainfall record as 228 mm a^{-1} and the interannual variability of rainfall is represented by the coefficient of variance of rainfall [CV(P)], which is calculated as 49.0 %. The synthetic rainfall fluctuates in values between years and has no periodicity within the rainfall structure (figure 9b). The simulation was run for the same length of time as the length of the reconstructed rainfall record.

The response of biomass in our model correspondingly shows wild fluctuations in values. Depending on the features of the synthetic rainfall series, either of the two species is equally likely to become the dominant biomass in the grid without any bias towards the grass or the shrub. In the realization of the stochastic model shown in figure 10a, the grass and shrub continually alternate as the dominant species, and neither species shows any evidence of spatial reorganization.

When the grass is the dominant species in a cell, little available resource migrates to the deeper soil layers (figure 10b). However, when the shrub is the dominant species, a large amount of water resource is channelled to the deep layers. Transitions between one dominant species and another are accompanied by a change in connectivity (figure 10c). When a drought occurs, the biomass of both grass and shrubs is reduced, and when rainfall subsequently increases the grass and the shrubs both increase their biomass. The principal difference between the two plant species during recovery is growth rate. As the grass has a higher growth rate, it can recover slightly more quickly than the shrubs and suppress shrub invasion. In this sense, the variability in the rainfall itself inhibits shrub invasion, and confirms that the periodicity in rainfall is an important control on vegetation response.

Simulation b – Reconstructed rainfall

For this simulation the actual 312-year rainfall series that was reconstructed from tree-ring data was used. Results of same centre-line averages as in Figure 10 are presented in figure 11. The initial decline of grass biomass is caused by initiating the calculation with uniform resources in the mid and deep soil layers. Over the first 25 years of the simulation, the biomass adjusts to these arbitrary resource levels, and so these first few data points are excluded from further analysis. Figure 11a shows that after this initial period, although the average value of grass fluctuates, the shrubs are unable to become established.

It is noteworthy is that even after the most extreme drought (that of the 1950s), the grass population is able to recover and the shrub population continues to be suppressed. It is not unreasonable to expect that the same recovery of grass should be observed if droughts of a similar magnitude occurred at earlier points in the simulation (c.f. McClaren and Van Devender, 1995), assuming that the reconstructed data underestimate the magnitude of earlier droughts (see section 5.1.2).

The middle layer water resource fluctuates markedly (figure 11b). As the average grass biomass increases, water levels decrease and *vice versa*. In spite of the accumulation of the water in this layer, the shrubs are not able to invade, which, assuming our model is faithfully reflecting the impacts of rainfall variability, suggests that some other mechanism apart from drought must be important in shrub-invasion processes.

Connectivity (figure 11c) also fluctuates during the simulation. The average connectivity values show that whereas the magnitude of change in the grass population reflects the magnitude of change in the rainfall record, the response of the grass population tends to lag slightly behind changes in the rainfall (typically by two years). The lag is partly due to the unused resource being moved down through soil layers, and partly due to the structure of the rainfall in the sense that multiple wet years will increase patch biomass, which delays the effect of subsequent dry years on population decline (and *vice versa*). Although this delay may in part be an artefact of the calculation scheme, it is not inconsistent with the observations of the actual behaviour of the system as evaluated by Reynolds *et al*. (1999). The maximum number of connected cells also changes, related to a change in the spatial organization of the grass patterns. Therefore, the implication is that the temporal structure of rainfall plays a significant role in the spatial organization of vegetation, as well as its dynamic response.

In order to examine the changing spatial distributions of the biomass, maps of the distributions of grasses and shrubs are shown in figure 12. The biomass of grass decreases during times of water scarcity in a consistent and predictable way. During dry years, grass is first lost from cells containing the lowest biomass. These cells connect to the wind and water vectors and resource ‘flows’ into the next vegetated (i.e. disconnected) cell. This flow has the effect of concentrating resource into distinct spatial locations and allowing a higher biomass of grass to survive than would otherwise be possible were the resources more homogenously distributed (Humphrey, 1958; Buffington and Herbel, 1965; Allred, 1996; Couteron and Lejeune, 2001; Barbier *et al.,* 2006). At first, the vegetation loss occurs only in the lowest biomass cells. During prolonged periods of water stress, vegetation is lost from the downslope edge of the vegetation patch, because the water input provided by the vector is exhausted before it reaches this edge and consequently a ‘banded’ pattern is formed (e.g. noted in years 1783 to 1883). As noted in the Appendix, this banded pattern that is widely reported in the literature on desert vegetation. Over time, these bands become more fragmented. When the water input is increased, grass recovery initiates from all surviving grass cells. The relationship between the number of connected cells and the width of the grass band is a function of both the resource input and the biomass of the band.

Meanwhile, the shrub biomass declines (as suggested by Goldberg and Turner, 1986) and by the time grass reaches its quasi-average value the initial shrub biomass has been reduced to an average value of almost zero. Where shrubs are able to survive, they do so only on the edge of a grass patch which has accumulated excess resources, and in effect, the grass patch acts as a nurse plant to the new creosotebush (McAuliffe, 1988). This quasi-static equilibrium level for the grass controls the resource and propagule movement, by which it is meant that the pattern of resource movement in this simulation is predominantly lateral, locally limited, and observed in the top layers on the same spatial scale as the individual grass plants (Müller *et al.*, 2008). This result is consistent with evidence that the dominant species redistributes resource to suit its own colonization strategy, which has been noted by Westoby *et al*. (1989).

The grass never quite reaches a stable equilibrium, irrespective of the duration of the simulation. Model runs of 1000 years were also carried out using both repetitions of the stochastic rainfall record and repeated cycles of the tree-ring record. In these model runs the grass population did not get any closer to reaching a steady equilibrium, which allows the idea that equilibrium is asymptotically reached, given an infinitely long time, to be rejected.

Simulation c – Reconstructed rainfall and variable grazing levels

Simulations 2a and 2b indicated that the temporal structure of the rainfall is a causal factor leading to the generation of patchy vegetation, but the results also suggest that historical climatic conditions appear to be insufficient to cause the invasion of shrubs into grasslands. The introduction of grazers to the Jornada has often been cited as a reason behind woody plant encroachment (e.g. Archer, 1995) and so in this simulation, the variable rainfall input is combined with three different grazing intensities. These grazing levels are modelled as a disturbance externality by allowing some of the grass in each cell (as a percentage of the maximum cell biomass) to be removed. This percentage corresponds to the mid-point of three grazing intensities reported for the Jornada (table 2).

Figure 13a(i) show that with a conservative grazing intensity, the average biomass, resources and connectivity are little changed compared with simulation b (mean average grass and shrub biomass 30.6 g m^{-2} and 0.4 g m^{-2}, and 27.5 g m^{-2} and 0.6 g m^{-2}, respectively) where the effects of herbivory were not simulated (although the grazing vector did operate to move R&P in simulation b). Although average grass biomass levels (figure 13b(i)) are reduced in the simulation with “recommended” (Havstad *et al.*, 2006) compared with the “conservative” grazing intensities, there is little difference in the average shrub levels (mean average grass and shrub biomass 27.5 g m^{-2} and 0.6 g m^{-2}, and 27.8 g m^{-2} and 0.6 g m^{-2}, respectively). The connectivity values (figure 13(iii)) show that under recommended grazing levels, the effects of droughts become more pronounced with a greater number of cells connecting to the wind and water vectors, and the average connectivity suggests different spatial patterns in the vegetation occurs in response to the elevated grazing levels(maximum continuous connected cells 38 and 38, respectively, and average connected cells 4.6 and 5.6, respectively). The “overgrazed” simulation (figure 13c) produces conditions that result in a dramatically reduced grass biomass and a much high higher average shrub biomass (18.7 g m^{-2} and 10.6 g m^{-2}, respectively). The effect of the increased shrubs is also seen in the average resource levels (figure 13c(ii)) where greater levels of water resources are able to penetrate the deep soil layers (different spatial scale arguments). By the time that the drought of the 1950s occurs, the biomass of the shrubs exceeds that of the grass (Schlesinger and Pilmanis, 1998). In spite of this change, the connectivity values (figure 13c(iii)) imply a very static pattern in the spatial pattern of biomass.

In order to interpret the patterns of connectivity in the overgrazed case (figure 13c(iii)), the spatial patterns of biomass for the overgrazed case are shown in figure 14. It can be seen that the typical banded pattern is established early in the simulation. The resources that are moved by the vectors should be able to sustain a high level of grass in the disconnected cells (as in simulation b); however, the grazers remove some of this biomass. What would have been adequate resource becomes an excess resource on these grass patches, and the shrubs are able to colonise these areas of resource excess. Once the shrubs have become established in the locations shown in figure 14, the model identifies them as the dominant species, which has two consequences. First, the diffusion descriptions (table 3) pertaining to shrubs are used in place of the diffusion descriptions for grass. Secondly the shrubs are allowed to channel some of the water input to their cells directly to the middle and deep soil layers. At this point, the resource redistribution changes from a predominantly lateral process (where resources move to adjacent cells in the top soil layer) to a more vertical process where the shrubs are able to channel a higher proportion of water resources directly into deeper layers. During times of resource scarcity, these shrub patches contract and shrub biomass is reduced, but they are to some extent buffered from the effects of water shortage by the deep-water store (Thornes and Brandt, 1993). Thus the shrub community is quite stable, and therefore the spatial distribution of biomass and connectivity values also become more static. In the earlier simulations, the grass community was able to adapt to resource scarcity by expanding and contracting in patches as a function of connectivity. In the present case, the shrub population interrupts this connectivity and the grass patches become increasingly fragmented. At the end of the simulation, most of the grass survives only at the edge of the shrub patch (as observed in the field by McAuliffe, 1988).

Simulation d – Instrumented rainfall data and a conservative grazing level

Reynolds *et al.* (1999) and Yao *et al.* (2006), reported that different sites within the Jornada Basin have responded differently to the same climatic conditions: some stands of perennial grass became extinct before the drought of the 1950s, some during the drought, some immediately afterwards, and some not at all. Yao *et al.* (2006) used long-term cover data over a period from 1915 to 2001 to identify this spatial variation in grass cover in the Jornada and, in the absence of a consistent causal factor, hypothesised that local transport processes for resources and propagules between patches must be somehow be important. In this simulation we use 80 years of instrumented rainfall data to generate simulated grass responses in order to explore the model's ability to test Yao *et al*'s hypothesized explanation. Unlike previous simulations, the initial conditions for this simulation (in terms of middle and deep soil layer resources and biomass distribution) are taken from the results obtained at year 1915 of the previous simulation using the reconstructed rainfall series in order to avoid, or at least minimise the effects of adjusting to initial resource redistribution. Yao *et al.* (2006) reported a low (conservative) grazing level applied on their quadrats over the period from 1915 to 2001 which was calculated from averaged monthly stocking data that also accounted for changes in fence positions. We therefore apply the same conservative grazing level following the management strategies evolved by the Research Station over this period (Havstad *et al.*, 2006).

The centre-line averaged results are presented in figure 15, where it can be seen that the grass biomass follows (but lags behind) the rainfall pattern (figure 5a). The average shrub biomass is low, but remains above zero due to the grazing disturbance. The wetter years following the 1950s drought allow an accumulation of middle and deep-layer soil resources, and a trend for average connectivity values to increase is also evident. An increase in connectivity may indicate that the spatial distribution tends towards a more open plant community (Okin *et al.,* 2001), or that there is an increase in spatial organisation of the plant community.

The spatial distributions of the grass and shrubs are plotted in figure 16. The increasingly fragmented pattern in the grass distribution becomes apparent during the dry years of the 1920s and 1930s, as a result of the persistence of shrubs (compare maps for 1925 and 1935). The recovery process of both species is particularly well illustrated in the results for 1965, 1975 and 1985. During the drought of the 1950s, the shrubs persist as isolated spots, whereas the grass survives as short horizontal bands (orientated across the slope). As the grass recovers, these bands extend laterally, and then coalesce to form longer and more continuous bands, while the shrubs recover to form isolated communities that are orientated in the direction of the driving flux (shown also in figure 14). This pattern is caused by the shrubs' requiring longer connected pathways than the grass (the length of this pathway is again a function biomass and resource input) and because R&P diffusion around the shrub is vertical (through the soil layers) as well as lateral.

The contraction and recovery of biomass is also shown by plots of biomass and resource concentration (figure 17) that are plotted for the centre-line. In 1925, cells with high grass biomass are interspersed with cells with low biomass. Shrubs exist on the edges of these grass peaks, and water resources are concentrated onto the grass patches. Following the drought and subsequent recovery during the 1930s, the number of grass cells is reduced, and in some places, the shrubs have recovered to higher biomass levels than those observed for the grass. This recovery happens where the vectors move excess resource to a patch, which then loses some biomass by drought or disturbance.

During the severe drought of the 1950s, most of the biomass is lost except in the locations that contained the highest biomass prior to the drought, and recovery initiates from these cells during the 1960s. From this point on, the surviving biomass exists at higher concentrations, but in fewer cells. Resources are concentrated in patches, which are interesting in a number of ways. First, the concentrations are at levels that greatly exceed the resource input to the grid. Secondly, they exceed the resource requirement of the grass. Thirdly, they also exceed the level that can be consumed, even under the maximum growth rate for the grass (table 4). The concentration of resources into patches supports a higher biomass than the same resource could support, were the grass more homogenously distributed (as suggested by Aguiar and Sala, 1999; Barbier *et al.*, 2006). It can be noted that the biomass on the up-gradient edge of the band is higher than at any point earlier in the simulation on a more uniform grid (as observed by Ludwig *et al.*, 2005).

Inspection of the resource transects show that for similar (and fairly static) banding patterns, the distribution of subsurface resources can be very different from each other. On the transect (figure 18), the shrubs are ultimately suppressed by the grass, but elsewhere in the grid, some shrubs cells are able to survive. Two conditions are met by the surviving shrub cells. First, they are those that contained a high pre-drought biomass. Secondly, these shrub cells are located on the edge of a surviving grass band (McAuliffe, 1988). This pattern occurs because the grass bands are able to concentrate resources to an extent that exceeds their maintenance and maximum growth-rate requirements. The shrubs can capitalise on this excess resource, but elsewhere, any surviving shrubs that do not lie on the resource bands die off, even where the initial pre-drought shrub density was high (Schlesinger *et al.*, 1990). Whether or not shrubs will survive after the drought (during times when resource inputs are increased and grass populations recover) is a little more complicated. Even with a sufficiently long connected path, shrub cells will not persist in locations where resource movement is controlled by the grass, i.e. predominantly lateral. In order to persist the shrubs also require sufficient vertical input of resources that can be channelled to the deeper soil layers (a process documented in the literature, e.g. Martinez_Meza and Whitford, 1996; and included in the model). This result points towards the importance of different pathways of resources movement occurring within the shrub populations – specifically a vertical connection between water input and deep layer soil resources (which could be considered as a type of connectivity).

In figure 18, the experimental data of Yao *et al.* (2006) are compared to simulated data from cells selected manually from the transect of figure 17 that show a similar response to Yao *et al*'s data. The selected simulated responses show markedly similar trends, although the specific values are different. This difference most probably arises because the experimental data measured the area covered by a plant in each quadrat to evaluate basal cover, whereas the model computes biomass.

In the first example (figure 18a), where grass is lost during the early 1920s, the biomass of this cell was lower than in neighbouring cells, and so biomass was shed from this cell very quickly. A number of upslope cells subsequently became connected, and the biomass increased slightly as a result of the extra resource input, before becoming extinct in 1924. After grass was lost from this cell, the number of upslope connected cells continued to increase. Without any nearby surviving patches to exchange resource and propagules with, this cell remained empty for the remainder of the simulation (figure 17).

The second example (figure 18b) shows the biomass response of a cell where grass was lost during the drought of the 1950s. Initially, this cell was towards the downslope edge of a grass patch. Grass persisted for a time on this patch while upslope cells were connected to the vectors. A consequence of this increased connectivity was that new growth appears to have occurred on the upslope edge of this cell and biomass was progressively lost on the downslope edge of this band during periods of climatic stress. During the drought of the 1950s, there was insufficient resource added by precipitation to sustain the biomass in this cell and the additional resource that was delivered to the patch by the vectors was consumed by upslope biomass before it could reach the cell. Consequently, grass in this location was lost. It is worth noting that towards the end of the simulation, the grass in this cell is able to recover most likely because this simulation does not account for concomitant soil degradation, which almost certainly occurs. This recovery is not observed in the data of Yao *et al*. (2006).

The third example (figure 18c) shows a cell where grass was lost immediately following the 1950s drought. This cell is located immediately upslope of the cell in the second example, and the processes applying in the two locations are the same. The difference is that this cell is located further towards the centre of the grass patch and survives for longer. After the drought, the upslope biomass was able to increase quickly in response to higher rainfall inputs and higher water input by the vectors. This rapid growth inhibits the recovery of this cell and ultimately grass is lost in this location, immediately following the drought. Elsewhere in the grid, an upslope shrub cell has the same effect, in that it interrupts the connectivity to the grass cell.

The final example (figure 18d) shows a cell where grass has survived throughout the duration of the simulation. This cell exists near the upslope edge of a grass patch (*cf.* Montana, 1992) and as such it has received high water inputs from upslope connected cells, even during the droughts, and its connectivity was not interrupted following the drought.

Yao *et al.* (2006) reported data from 98 1-m^2 quadrats in the Jornada, and reported that black grama became locally extinct on 21% of these plots prior to the 1950s drought, 39% during the drought, and 30% after the drought, and the grass persisted throughout the time of study in the remaining 10% of quadrats that were examined. Simulation d generated biomass data in 1-m^2 cells, using a parameterization consistent with the location of the data of Yao *et al*.. In simulation d, black grama became locally extinct in 26% of the cells prior to the 1950s drought, 38% during the drought, 20% after the drought, and black grama persisted in 16% of the cells. The simulated and measured results show remarkably good agreement with each other, with the largest differences occurring after the 1950s drought where simulation d overpredicts the number of cells where grass survives. This overprediction may be because there is no mechanism within the model that would allow for a spatial location to be degraded by hillslope processes during a disturbance and therefore inhibit biomass recovery (Montana, 1992; Abrahams *et al.*, 1995).

7. Discussion

In the early part of this paper, we have argued that, though modelling can provide unique insights into understanding the dynamics of the patchiness of desert vegetation, such insights are valuable only if models yield testable predictions and if the models are firmly grounded in, and compatible with, empirical data. That is not to say that empirical data are uncontestable. All data are collected within a conceptual framework, and it may be that modelling will yield results that lead us to challenge that conceptual framework. Even so, such a challenge is only valid where the model makes explicit reference to that conceptual framework. Against that argument, we have developed a numerical model for the dynamics of desert ecosystems within the conceptual framework of connectivity, and we have parameterized the model for implementation in a specific desert setting where the available data set for parameterization is particularly rich. In this section, we discuss the model output in terms of its ability to generate testable hypotheses.

Four testable hypotheses emerge from our modelling of shrub invasion of grasslands. First, our results show that, contrary to Thornes and Brandt (1993), rainfall variability does not enhance shrub invasion. Instead, because the annual re-growth rate of grass rate is higher than that of shrubs it recovers faster and is thus able to suppress shrub invasion by re-establishing its control on resource redistribution. This result suggests the hypothesis that the propensity of a grassland for shrub invasion is a function of the relative growth rate of the two. It should be noted, however, as a caveat to this hypothesis there may be extremes of drought beyond those tested here under which such a control breaks down.

Secondly, Yao *et al* (2006) hypothesized that control by transport processes on local resource and propagule distribution may somehow explain the spatial variation in grass survival within the Jornada Basin. Our analysis suggests that the timing of grass loss depends on both initial cell biomass and connectivity properties. Low biomass density patches will always become extinct first during times of resource shortage. During prolonged periods of drought, biomass on the downslope edge of a patch is the most vulnerable, particularly if a shrub exists nearby, because the shrub will channel some of the resource input to deeper layers and so a longer connected pathway or a greater resource input is required to supply the grass cell than would be required if the shrub were not located nearby. Cells that lose biomass tend to have low numbers of upslope connected cells. Patches that survive drought conditions are those that are located near the upslope edge of the patch, where there is a high degree of connectivity in up-vector cells. These results lead us to suggest the hypothesis that changes in the values of connectivity for grassland indicate conditions where it would be particularly vulnerable to a disturbance externality.

Thirdly, our results lead us to hypothesize that when the grass species becomes established and forms a stable community, it is able to control the resource and propagule movement within the landscape to suit its own survival strategy. In the case of pure stands of grass, this hypothesis means that the resource distributions coincide with the scale of grass plants, and underlying resources in deeper layers are at a minimum (Müller *et al.*, 2008). When conditions change to allow deeper layer resources to accumulate, shrub invasion into a grass stand can occur. This hypothesis therefore predicts a vertical resource gradient should occur beneath shrub communities, whereas the resource gradient surrounding grass patches should be predominantly lateral. These predictions are supported at least qualitatively by the results of Schlesinger *et al.*

(1996). The simulations also suggest that a vertical resource profile could be an independent means by which the islands of fertility model can be tested. Furthermore, it has been argued that under conditions (that are usually driven by a strong externality) where the dominant grass species has collapsed, permanent changes in soil condition (such as caused by erosion, as noted by Westoby *et al*., 1989; Abrahams *et al*., 1995; Li *et al.,* 2007) would become much more important and are likely to inhibit future vegetation establishment in eroded areas (Wainwright *et al.,* 2000; Okin *et al*., 2006; Li *et al*., 2009). Mauchamp *et al.,* (1993) theorised that stripes are controlled by different recruitment histories, and that on a landscape scale it is the successive die-back and regrowth that controls stripes. Because our model only allows these different recruitment processes to occur in response to resource inputs, and because we are, nevertheless, able to generate plausible results, it leads to the hypothesis that resources rather than changes in soil conditions *per* se that are the primary controlling factors.

Fourthly, the distinct differences in our modelling results between diffusion-advection and advection-only simulations (see Appendix) lead us to hypothesize that the balance of these two sets of processes and the nature of diffusion play a large part in controlling vegetation behaviour. It would be possible to test this hypothesis by conducting field experiments in which the ability of vectors to move resources and propagules in these ways was examined.

That our model is able to generate specific testable hypotheses is due to the specific parameterization that we have been able to provide for the data-rich Jornada Basin. However, the relationship between the utility of a model and the available data for parameterization is not a simple one. Where such data do not exist, a model may be used to identify specific data needs for testing of hypotheses. Sensitivity of model output to particular parameters can drive empirical research just as much as the results of empirical research can lead a model to produce testable hypotheses. For example, key parameters in understanding the process of shrub invasion and the potential for its reversal are the rates of establishment and mortality for creosotebush. Current estimates for these parameters are derived from other modelling studies (Peters, 2002a), suggesting that further empirical work is needed to constrain the potential values of parameters to which the model is highly sensitive.

8. Conclusions

In this paper, a modelling framework that explicitly considers spatial interactions among multiple vegetation types and multiple resources has been applied to the analysis of ecosystem change in deserts. The model is designed to explore causes of spatial complexity as well as predict specific responses to a variety of endogenous and exogenous disturbances. This contribution differs from previous work in that it rests on a sound process-based understanding and data that has both a clear physical meaning and can be measured in the field. Both abiotic and biotic processes have been considered in greater detail than previous modelling studies, while maintaining a level of parsimony that means that parameter uncertainty is unlikely to drown out the effects of the processes under investigation.

A general modelling framework has been developed, and specific implementation of this model was employed to evaluate the framework against data that has been obtained from field studies. In doing so, it is noted that even with the simplifications made, the model was able to closely match measured conditions at the field site, in terms of species response and the generation of plausible patterns of vegetation loss. On this basis, the general framework can be considered to have captured the key processes within the ecosystem and may make a useful contribution towards understanding desert vegetation more straightforwardly.

Rather than developing predictions of vegetation change under hypothetical future scenarios, historical data have been used to retrodict grassland responses to climatic conditions. In doing so, it was possible to compare the model results to current conditions, which comparison provides a robust test of both the model and our understanding of how desert ecosystems operate. Moreover, the approach has led to the generation of a number of testable predictions that can be compared to other field data.

The results suggest that the desert grasslands have been stable under historic conditions for three reasons. First, the structure of the rainfall itself inhibits shrub invasion; secondly, the faster growth rate tends to allow grass to outcompete with shrubs for available resources; and thirdly, the banding patterns themselves are much more stable structures in semi-arid ecosystems than a homogenous distribution of grass. During droughts, the resource that is input to connected cells will flow onto the bands where it is supports the patch biomass, and the length of the connected cells and the length of grass bands are related. The resource distribution across patches remains predominantly lateral, with little (or no) resource accumulated beneath the bands. The shrubs (in this simulation) are only able to invade grass stands when a disturbance causes a grass plant to be removed from a location where resource has accumulated, but the persistence of the shrub is also a function of two types of connectivity. First, the length of the connected pathways to the shrub must be longer than the connected pathways to the grass plant, and secondly, shrubs will only survive in locations where they are able to develop a pronounced vertical distribution of resources beneath them. This difference would suggest that lateral accumulations of resource around a shrub indicate that recent climate conditions have caused a great degree of R&P movement along newly emerged connected pathways, but the absence of that accumulation points towards vector operation along more stable connected pathways. The results point to the introduction of cattle grazing, and specifically overgrazing, as the cause of the historical shrub invasion.

The agreement of the model results with experimental studies indicates that this method has merit and is worth pursuing further. It is acknowledged that the implementation presented here far from perfect in two significant respects. First, we have, for instance, used a number of linear relationships which would not be appropriate in a more general implementation, and many of the surrogate data used here (with respect to the relationships between vectors and resource movement) ought to be parameterised more fully. In particular, experimental data aiming to quantify the redistribution of laterally-transported resources at the end of a connected pathway (i.e. Equation (6)) is deserving of attention. The lack of detail supported by field research in these factors means that while we can see that the connected pathways must be longer to enable shrubs to survive than for grass plants, we are not able to quantify them with any confidence. Secondly, some of our model results are unrealistic. For example, the accumulation of nitrogen in the mid and deep soil layers is unrealistic. As was pointed out in the model parameterization (5.1.4), there is a dearth of suitable data for this parameterization. Our results suggest that this dearth of data is a significant limitation on our current understanding. The application of the model to a very specific implementation was worthwhile in order to establish that the general framework produces plausible results, and to inform future experimental work that may obtain data in the form required to establish the causal factors that lead to ecosystem changes. On the basis of this work, vertical and lateral connectivity are key emergent properties of the system which both control its behaviour and provide indicators of its state. If these predictions are shown to be compatible with actual conditions, the model presented here will provide a more certain approach towards preventing further semi-arid grassland degradation.

ACKNOWLEDGEMENTS

This research was supported by the University of Sheffield and LTER Grant DEB-0618210.

REFERENCES

Abrahams, A. D., Parsons, A. J., 1991. Relation between infiltration and stone cover on a semiarid hillslope, southern Arizona., J. Hydrol., 122, 49–59.

Abrahams, A.D., Parsons, A.J., Wainwright, J., 1995. Effects of vegetation change on interrill runoff and erosion, Walnut Gulch, southern Arizona. Geomorph. 13(1-4), 37-48.

Abrahams, A.D., Parsons, A.J., Wainwright, J., 2003. Disposition of rainwater under creosotebush. Hydrol. Proc. 17, 2555-2566.

Ackerman, T.L., Bamberg, S.A., 1974. Phenological studies in the Mojave Desert at Rock Valley. In: H. Lieth (Editor), Ecological studies; Analysis and synthesis Springer-Verlag, New York, pp. 215-226.

Aguiar, M.R., Sala, O.E., 1999. Patch structure, dynamics and implications for the functioning of arid ecosystems. Trends in Ecology and Evolution. 14, 273-277.

Allred, K.W., 1996. New Mexico's Natural Heritage: Biological diversity in the land of enchantment. New Mexico Acad. Sci. Albuquerque, pp 168-231

Archer, S., Schimel, D.S., Holland, E.A., 1995. Mechanisms of shrubland expansion: land use, climate or CO_2. Climatic Change. 29, 91-99.

Baez, S., Fargione, J., Moore, D.I., Collins, S.L., Gosz, J.R., 2007. Atmospheric nitrogen deposition in the northern Chihuahuan desert: Temporal trends and potential consequences. J. Arid Environ. 68, 640-651.

Bainbridge, D.A., Virginia, R.A., 1990. Restoration in the Sonoran Desert of California. Restoration and Management Notes, 8, 3-14.

Barbier, N., Couteron, P., Lejoly, J., Deblauwe, V., Lejeune, O., 2006. Self-organized vegetation patterning as a fingerprint of climate and human impact on semi-arid ecosystems. J. Ecology. 94, 537-547.

Barbour, M.G., 1969. Age and space distribution of the desert shrub Larrea divaricata. Ecology. 50, 679-685.

Bartley, R., Roth, C.H., Ludwig, J.A., McJannet, D., Leidloff, A.C., Corfield, J., Hawdon, A., Abbot, B., 2006. Runoff and erosion from Australia¹s tropical semi-arid rangelands: Influences of ground cover for differing space and time scales. Hydrological Processes 20: 3317-3333

Bracken LJ, Croke J. 2007. The concept of hydrological connectivity and its contribution to understanding runoff-dominated geomorphic systems. Hydrological Processes 21, 1749–1763

Brazier, R.E., Parsons, A.J., Wainwright, J., Powell, D.M., Schlesinger, W.H., 2007. Upscaling understanding of nitrogen dynamics associated with overland flow in a semi-arid environment. Biogeochemistry, 82, 265-278.

Brisson, J. and Reynolds, J.F. 1994 'The effect of neighbors on root distribution in a creosotebush (*Larrea tridentata*) population', Ecology **75**, 1693–1702.

Bromley, J., Brouwer, J., Barker, A.P., Gaze, S.R., Valentin, C., 1997. The role of surface water distribution in an area of patterned vegetation in a semi-arid environment, south west Niger. J. Hyd. 198, 1-29.

Brown, D.E., 1982. Semi-desert grassland. In: Brown, David E., ed. Biotic communities of the American Southwest--United States and Mexico. Desert Plants. 4(1-4), 123-131.

Brown, D.W., Gersmehl, P.J., 1985. Migration models for grasses in the American midcontinent. Annals Association Am. Geographers, 75, 383-394.

Buffington, L.C., Herbel, C.H., 1965. Vegetational changes on a semi-desert grassland range from 1858 to 1963. Ecol. Monogr. 35, 139-164.

Bugmann, H.K.M., Solomon, A.M., 1995. The use of a European forest model in North America: a study of ecosystem response to climate gradients. J. Biogeog. 22, 477-484.

Burgess, T.L., 1995. Desert grassland, mixed shrub savanna, shrub steppe or semidesert scrub? The dilema of coexisting forms. In: M.P. McClaran and T.R. Van Devender (eds.), The desert grassland. The University of Arizona Press, Tuscon, pp. 31-67.

Burke, I.C., Schimwl, D.S., Yonker, C.M., Parton, W.J., Joyce, L.A., and Lauenroth, W.K., 1990. Regional modelling of grassland biogeochemistry using GIS. Landscape Ecology. 4, 45-54.

Campbell, R.S., 1931. Plant succession and grazing capacity on clay soils in southern New Mexico. J. Agri. Res. 43(12), 1027-1051.

Canfield, R.H., 1948. Perennial grass composition as an indicator of condition of Southwestern mixed grass ranges. Ecology, 29, 190-204.

Casenave, A., Valentin, C., 1992. A runoff capability classification-system based on surface-features criteria in semiarid areas of West Africa. J. Hydrol. 130, 231–249.

Casper, B.B., Jackson, R.B., 1997. Plant competition below ground. Ann. Rev. Ecological Systems 28, 545-570.

Castellanos, A.E., Molina, F.E., 1990. Differential survivorship and establishment in Simmondsia chinensis (jojoba). J. Arid Environ. 19, 65-76.

Chandrasekhar, S. (Editor) 1961. Hydrodynamic and Hydromagnetic Stability. Springer-Verlag, Berlin.

Charley, J.L., West, N.E., 1975. Plant-induced soil chemical patterns in some shrub-dominated semi-desert ecosystems of Utah. J. Ecology.

Chew, R., Chew, A.E., 1970. Energy relationships of the mammals of a desert shrub (*Larrea tridentata*) community. Ecol. Monogr. 40, 1-21.

Clark, C.M., Tilman, D., 2008. Loss of plant species after chronic low-level nitrogen deposition to prairie grasslands. Nature. 451, 712-715.

Clos-Arceduc, M., 1956. Etude sur photographies aeriennes d'une formation vegetale sahelienne:la brousse tigree. Buletin de L'IFAN Serie A 18,678-684.

Cody, M.L., 1986. Spacing patterns in the Mojave Desert plant communities: near neighbour analysis. J. Arid Environ. 11, 199-217.

Coffin, D.P., Lauenroth, W.K., 1990. A gap dynamics simulation model of succession in the shortgrass steppe. Ecol. Model. 49, 229-266.

Comrie, A.C., Broyles, B. 2002. Variability and spatial modelling of fine-scale precipitation data for the Sonoran Desert of south-west Arizona. J. Arid Environ 50, 573-592

Cornet, A., Delahoume, J.P., Montana, C. (Editors), 1988. Dynamics of striped vegetation patterns and water balance in the Chihuahuan Desert. SBP Academic Publishing, The Hague, pp 221-231

Couteron, P., Lejeune, O., 2001. Periodic spotted patterns in semi-arid vegetation explained by a propagation-inhibition model. J. Ecology. 89, 616-628.

Dakos, V., Kéfi, S., Rietkerk, M., van Nes, E.M., Scheffer, M. 2011. Slowing down in spatially patterned ecosystems at the brink of collapse. The American Naturalist, 177, E153-E166.

d'Arigo, R.D., Jacoby, G.C., 1992. A tree-ring reconstruction of New Mexico winter precipitation and its relation to El Nino/Southern Oscillation events. In: H.F. Diaz and V. Markgraf (eds.), El Nino. historical and Paleoclimatic Aspects of the Southern Oscillation. Cambridge University Press, Cambridge, pp. 7-28.

Deblauwe, V., Barbier N., Couteron P., Lejeune O., Bogaert J., 2008. The global biogeography of semi-arid periodic vegetation patterns. Global Ecology and Biogeography 1**7**, 715–723.

d'Herbes, J.M., Valentin, C., Tongway, D.J. (eds.), 2001. Banded vegetation patterning in arid and semiarid environments; ecological processes and consequences for management. Springer, Hiedelberg, 1-19 pp.

D'Odorico, P., Laio, F., Ridolfi, L., 2006. Patterns as indicators of productivity enhancement by facilitation and competition in dryland vegetation. Journal of Geophysical Research 111, G03010.

Dunkerley, D.L., Brown, K.J., 1999. Banded vegetation near Broken Hill, Australia: significance of surface roughness and soil physical properties. Catena. 37(1-2), 75-88.

Furukawa, K., Imai, K., Kurashige, M., 2000. Simulated effect of box size and wall on porosity of random packings of spherical particles. Acta Mechanica .140, 219-231.

Gallardo, A., Schlesinger, W.H., 1992. Carbon and nitrogen limitations of soil microbial biomass in desert ecosystems. Biogeochemistry, 18, 1-17.

Gardener, J.L., 1950. The effects of thirty years of protection from grazing in desert grasslands Ecology, 31, 44-50.

Gibbens, R.P., McNeely, R.P., Havstad, K.M., Beck, R.F., Nolen, B., 2005. Vegetation changes in the Jornada Basin from 1858 to 1998. J. Arid. Environ. 61, 651-668.

Gibbens, R.P., Lenz, J.M., 2001. Root system of some Chihuahuan Desert plants. J. Arid Environ. 49, 221-263.

Gillett, J., 1941. The plant formations of western British Somaliland and the Harar province of Abyssinia. Kew Bull. 2, 37-75.

Goldberg, D.E., Turner, R.M., 1986. Vegetation change and plant demography in permanent plots in the Sonoran desert. Ecology. 67, 695-712.

Gosz, R.J., Gosz, J.R., 1996. Species interactions on the biome transition zone in New Mexico: response of blue grama (*Bouteloua gracilis*) and black grama (*Bouteloua eripoda*) to fire and herbivory. J. Arid Environ. 34, 101-114.

Greene, R. S. B., Kinnell P. I. A., Wood J. T., (1994) Role of plant cover and stock trampling on runoff and soil erosion from semi-arid wooded rangelands. Aust. J. Soil. Res. 32, 954-973.

Greig-Smith, P., 1979. Pattern in vegetation. J. Ecology. 67, 755-779.

Grimm, V., Railsback, S.F., 2005. Individual-Based Modelling and Ecology. Princeton University Press, Princeton.

Havstad, K.M., Huenneke, L.F., Schlesinger, W.H. (eds.), 2006. Structure and Function of a Chihuahuan Desert Ecosystem: The Jornada Basin Long-Term Ecological Research Site. Oxford University Press, New York.

Herbel, C.H., Ares, F.N., Wright, R.A., 1972. Drought effects on a semidesert grassland range. Ecology, 53, 1084-1093.

Higgins, S.I., Richardson, D.M., Cowling, R.M., 1996. Modelling invasive plant spread: the role of plant-environment interactions and model structure. Ecology. 77, 2043-2054.

Hillel, D., 2004. Introduction to Soil Physics. Elsevier.

HilleRisLambers, R., Rietkerk, M., van den Bosch, F., Prins, H.H.T., de Croon, H., 2001. Vegetation Pattern formation in semi-arid grazing systems. Ecology. 82, 50-61.

Hooper, D.U., Johnson, L., 1999. Nitrogen limitation in dryland ecosystems: Responses to geographical and temporal variation in precipitation. Biogeochemistry, 46, 247-293.

Humphrey, R.R., 1958. The desert grassland: a history of vegetational change and an analysis of causes. Botanical Rev. 24, 164-193.

Humphrey, R.R., Mehrhoff, L.A., 1958. Vegetation changes on a southern Arizona grassland range. Ecology. 39, 720-726.

Istanbulluoglu, E. and Bras, R.L., 2006. On the dynamics of soil moisture, vegetation, and erosion: Implications of climate variability and change. Water Resour. Res. 42.

Jornada LTER 2010 Jornada Basin Long Term Ecological Research. http://jornada-www.nmsu.edu/ [last accessed 21st July 2010]

Kéfi, S., Rietkerk, M., van Baalen, M., and Loreau, M. 2007. Local facilitation, bistability and transitions in arid ecosystems. Theoretical Population Biology 71:367–379.

Klausmeier, C.A., 1999. Regular and Irregular Patterns in Semiarid Vegetation. Science 284, 1826-1828.

Kot, M., 2001. Elements of Mathematical Ecology. Cambridge University Press.

Lange, R.T., Nicholson, A.D., Nicholson, D.A., 1984. Vegetation management of chenopod rangelands in South Australia. Aust. Rangeland J. 6, 46-54.

Leach, A.R., 2001. Molecular Modelling: Principals and Applications. Prentice Hall.

Lefever R., Barbier, N., Couteron, P., and Lejeune, O., 2009. Deeply gapped vegetation patterns: on crown/root allometry, criticality and desertification. Journal of Theoretical Biology 261, 194–209.

Loreau, M., Naeem, S., Inchausti, P., 2002. Biodiversity and ecosystem functioning: synthesis and perspectives Oxford University Press.

Li, J., Okin, G. S., Hartman, L. J., Epstein, H. E., 2007. Quantitative assessment of wind erosion and soil nutrient loss in desert grasslands of southern New Mexico, USA. Biogeochemistry 85, 317-332.

Ludwig, J.A., Wilcox, B.P., Breshears, D.D., Tongway, D.J., Imeson, A.C., 2005. Vegetation patches and Runoff-Erosion as Interacting Ecohydrological Processes in Semiarid Landscapes. Ecology. 86, 288-297.

MacFadyan, W.A., 1950. Vegetation patterns in the semi-desert plains of British Somaliland. Geographical Journal 116, 199–210.

Maneta, M.P., Schnabel, S., Wallender, W.W., Panday, S., Jetten, V., 2008. Calibration of an evapotranspiration model to simulate soil water dynamics in a semiarid rangeland. Hydrological Proc., 22.

Michaelides, K., Lister, D., Wainwright, J., Parsons, A.J., 2012. Linking runoff and erosion dynamics to nutrient fluxes in a degrading dryland landscape. Journal of Geophysical Research – Biogeosciences 117, G00N15, doi:10.1029/2012JG002071.

Martinez-Meza, E., Whitford, W.G., 1996. Stemflow, throughfall and channelization of stemflow by roots in three Chihuahuan desert shrubs. J. Arid Environ. 32, 271-287.

Mauchamp, A., Montana, C., Lepart, J., Rambal, S., 1993. Ecotone dependent recruitment of a desert shrub, Flourensia cernua, in vegetation stripes. Oikos. 68, 107-116.

May, R.M., 1977. Thresholds and breakpoints in ecosystems with a multiplicity of stable states. Nature. 269, 477.

McAuliffe, J.R., 1988. Markovian dynamics of simple and complex desert plant communities. The Am. Naturalist, 131, 459-490.

McClaran, M. P., Van Devender, T. R., 1995. The Desert Grassland. Tuscon University of Arizona Press

McPherson, G.R., Wright, H.A., Wester, D.B., 1988. Patterns of shrub invasion in semi-arid Texas grasslands. Am. Midland Naturalist. 120, 391-397.

Meinhardt, H., 1982. Models of Biological Patterns Formation. Academic, New York.

Miller, R.F., Donart, G.B., 1979. Response of *Bouteloua eriopoda* (Torr.) Torr. and *Sporobolus flexuosus* (Thurb.) Rhbd to season of defoliation. J. Range Manage. 32, 449-452.

Monger, H.C., Bestelmeyer, B.T. 2006. The soil-geomorphic template and biotic change in arid and semi-arid ecosystems. J. Arid Environ. 65, 207-218.

Montana, C., 1992. The colonization of bare areas in two phase mosaics of an arid ecosystem. J. Ecology. 80, 315-327.

Morgan R.P.C (1996) Soil erosion and conservation, second edition, Harlow: Longman.

Müller, E.N., Wainwright, J., Parsons. A.J., 2007. The impact of connectivity on the modelling of water fluxes in semi-arid shrubland environments. Water Resources Research 43: doi 10-1029/2006WR005006.

Müller, E.N., Wainwright, J., Parsons, A.J., 2008. Spatial variability of soil and nutrient parameters within grasslands and shrublands of a semi-arid environment, Jornada Basin, New Mexico. Ecohydrology. 1, 3-12.

Murray, J.D., 1989. Mathematical Biology. Springer-Verlag, Berlin.

Nash, M.S., Jackson, E., Whitford, W.G., 2004. Effects of intense, short-duration grazing on micro-topography in a Chihuahuan Desert grassland. J. Arid Environ. 56(3), 383-393.

Neilson, R.P. (1986). High-resolution climatic analysis and Southwest biogeography. Science. 232, 27-34.

Nelson, E.W., 1934. The influence of precipitation and grazing upon black grama grass range, US Department of Agriculture, Washington, DC.

Nicholson, S.E., 1979. Revised Rainfall series for the West African Subtropics. Monthly Weather Rev. 107, 620-623.

Nicholson, S.E., 1981. Rainfall and atmospheric circulation during drought periods and wetter years in West Africa. Monthly Weather Rev. 109, 2191-2208.

Noy-Meir, I., 1973. Desert Ecosystems: Environment and Producers. Ann. Rev. Ecology. 4, 25-51

Okin, G.S., Gillette, D.A., 2001. Distribution of vegetation in wind-dominated landscapes: Implications for wind erosion modelling and landscape processes. J. Geophys. Res. 106, 9673-9683.

Okin, G.S., Murray, B., Schlesinger, W.H., 2001. Degradation of sandy arid shrubland environments: observations, process modelling and management implications. J. Arid Environ. 47,123-144.

Okin, G. S., Herrick, J. E., Gillette, D. A., 2006. Multiscale controls on and consequences of aeolian processes in landscape change in arid and semiarid environments. Journal of Arid Environments 65, 253-275.

Okin, G.S., D'Odorico, P.D., Archer, S., 2009. Impact of feedbacks on Chihuahuan desert grasslands: transience and metastability driven by grass recruitment. Global Change Biology.

Okin, G.S., Parsons, A.J., Wainwright, J., Herrick, J.E., Bestelmeyer, B.T., Peters, D.P.C., Fredrickson, E.L., 2009. Do changes in connectivity explain desertification?. BioScience 59, 237–244.

Osborne, C.P. and Beerling, D.J., 2006. Nature's green revolution: the remarkable evolutionary rise of C_4 plants. Phil. Trans. Royal Soc. London B Bio. Sci. 361, 173-194.

Parshall, T., Foster, D.R., Faison, E., MacDonald, D. and Hansen, B.C.S., 2003. Long-term history of vegetation and fire in pitch pine-oak forests on Cape Cod, Massachusetts. Ecology. 84, 736-748.

Parsons, A.J., Abrahams, A.D., Simanton, J.R., 1992. Microtopography and soil-surface materials on semi-arid piedmont hillslopes, southern Arizona. J. Arid Environ. 22, 107-115.

Parsons, A.J., Abrahams, A.D., Wainwright, J., 1996. Responses of interrill runoff and erosion rates to vegetation change in southern Arizona. Geomorph. 14, 311-317.

Parsons, A.J., Wainwright, J., Abrahams, A.D., Simanton, J.R., 1997. Distributed dynamic modelling of interrill overland flow. Hydrol. Proc. 11, 1833-1859.

Parsons, A.J., Wainwright, J., Powell, D.M., Kaduk, J., Brazier, R., 2004. A conceptual model for determining soil erosion by water. Earth Surf. Process. Landforms. 29, 1293-1302.

Parsons, A.J., Brazier, R.E., Wainwright, J., Powell, D., 2006a. Scale relations in hillslope runoff and erosion. Earth Surf. Process. Landforms. 31, 1384-1393.

Parsons, A.J., Abrahams, A.D., Luk, S.H., 2006b. Size characteristics of sediment in interrill overland flow on a semiarid hillslope, Southern Arizona. Earth Surf. Process. Landforms. 16, 143-152.

Parton, W.J., 1978. Dynamics of C, N, P and S in grassland soils: a model. Biogeochemistry 5, 109-131.

Paulsen, H.A. Jr., Ares, F.N., 1962. Grazing values and management of black grama and tobosa grasslands and associated shrub ranges of the Southwest. Tech. Bull. No. 1270. Washington, DC: U.S. Department of Agriculture, Forest Service, pp 56

Peters, D.P.C., 2002a. Plant species dominance at a grassland-shrubland ecotone: an individual-based gap dynamics model of herbaceous and woody species. Ecol. Model. 152, 5-32.

Peters, D.P.C., 2002b. Recruitment potential of two perennial grasses with different growth forms at a semiarid-arid transition zone. Am. J. Botany. 89(10), 1616-1623.

Peters, D.P.C., Gosz, J.R., Pockman, W.T., Small, E.E., Parmenter, R., Collins, S.L., Polley, E., Johnson, H.B., Derner, J D., 2002. Soil- and plant-water dynamics in a C3/C4 grassland exposed to a subambient to superambient CO_2 gradient. Global Change Biology. 8, 1118–1129.

Peters, D.P.C., Bestelmeyer, B.T., Herrick, J.E., Fredrickson, E., Monger, H.C., Havstad, K.M., 2006a. Disentangling complex landscapes: new insights to forecasting arid and semiarid system dynamics. Bioscience. 56, 491-501.

Peters, D.P.C., Gosz, J.R., Pockman, W.T., Small, E.E., Parmenter, R., Collins, S.L., Muldavin, E., 2006b. Integrating patch and boundary dynamics to understand and predict biotic transistions at multiple scales. Landscape Ecology. 21, 19-23.

Pockman, W.T., Sperry, J.S., 1997. Freezing-induced xylem cavitation and the northern limit of *Larrea tridentata*. Oecologia. 109,19-27.

Rango, A., Chopping, M., Ritchie, J., Havstad, K., Kustas, W., Schmugge, T., 2000. Morphological Characteristics of Shrub Coppice Dunes in Desert Grasslands of Southern New Mexico derived from Scanning LIDAR Remote Sensing of Environ. 74, 26-44.

Reynolds, J.F., Virginia, R.A., Kemp, P.R., de Soyza, A.G., Tremmel, D.C., 1999. Impact of drought on desert shrubs: Effects of seasonality and degree of resource island development. Ecol. Monogr. 69, 69-106.

Rietkerk, M., Boerlijsr, M.C., van Langevelde, F., HilleRisLambers, R., Van de Koppel, J., Kumar, L., de Roos, A.M., 2002. Self-organization of vegetation in arid ecosystems. Am. Naturalist, 160, 524-530.

Rietkerk, M.F., Van der Koppel, J., 1997. Alternate stable states and threshold effects in semi-arid grazing systems. Oikos 79, 69-76.

Romney, E.M., Wallace, A., Hunter, B., 1989. Pulse establishment of woody shrubs of denuded Mojave Desert land. In: W. A, E.D. McArthur and M.R. Haferkamp (eds), Symposium on shrub ecophysiology and biotechnology. US Department of Agriculture, forest service, Intermountain Research station, Logan, UT, pp. 54-57.

Rovinsky, J.B., 1987. Twinkling Patterns and Diffusion-Induced Chaos in a Model of the Belousov-Zhabotinsky Chemical Medium. J. Phys. Chem. 91.

Seghieri, J., Galle, S., Rajot, J.L., Ehrmann, M., 1997. Relationships between soil moisture and growth of herbaceous plants in a natural vegetation mosaic in Niger. J. Arid Environ. 36,87-102

Schlesinger, W.H., Peterjohn, W.T., 1991. Processes controlling ammonia volatilization from Chihuahuan desert soils. Soil Biology and Biochemistry 23, 637-642.

Schlesinger, W.H., Reynolds, J.F., Cunningham, G.L., Huenneke, L.F., Jarrell, W.M., Virginia, R.A., Whitford, W.G., 1990. Biological feedbacks in global desertification. Science 247,1043-1048.

Schlesinger, W.H., Raikes, J.A., Hartley, A.E., Cross, A.F., 1996. On the spatial pattern of soil nutrients in desert ecosystems. Ecology 77,364-374.

Scoging, H. 1992. Modelling overland-flow hydrology for dynamic hydraulics. In Overland Flow Hydraulics and Erosion Mechanics. A. J. Parsons and A. D. Abrahams (eds). London, UCL Press Limited.

Scott, R.L., Cable, W.L., Hultine, K.R., 2008. The ecohydrological significance of hydraulic redistribution in a semiarid savanna. Water Resour. Res. 44

Smith, G., Holechek, J.L., Cardenas, M., 1996. Wildlife numbers on excellent and good condition Chihuahuan Desert rangelands: an observation. J. Range Manage. 49, 489-493.

Slatyer, R.O., 1961. Methodology of a water balance study conducted on a desert woodland (*Acacia anuera F. Muell*) community in central Australia. UNESCO Arid Zone Res. 16,15-26.

Starfield, A.M., 1996. Model of transient changes in arctic and boreal vegetation in response to climate and land use change. Ecological Applications 6,842-864.

Sun, G., Coffin, D.P., Lauenroth, W.K., 1998. Comparison of root distributions of species of North American grasslands using GIS. J. Vegetation Science. 8, 587-596.

Taylor, P.D., Fahrig, L., Henein, K., Merriam, G., 1993. Connectivity is a vital element of landscape structure. Oikos 68, 571–573.

Thornes, J.B., 1990. The interaction of erosional and vegetational dynamics in land degradation: spatial outcomes. In JB Thornes (ed.) Vegetation and Erosion, John Wiley and Sons, Chichester, pp 41–53

Thornes, J. B., 2007. Modelling Soil Erosion by Grazing: Recent Developments and New Approaches. Geographical Research 45: 13-26

Thornes, J.B., Brandt, J. 1993. Erosion-Vegetation competition in a stochastic environment undergoing climatic change. In AC Millington and KJ Pye, (eds.) Environmental Change in the Drylands: Biogeographical and Geomorphological Responses, John Wiley and Sons, Chichester, pp 306–320

Tongway, D.J., Ludwig, J.A. (Editors), 2001. Theories on the origins, maintenance, dynamics and functioning of banded landscapes. Springer, Heidelberg.

Turchin, P., 2003. Complex Population Dynamics. Princeton University Press, Princeton.

Turing, A.M., 1952. The chemical basis of morphogenesis. Phil. Trans. Royal Soc. London B Bio. Sci. 237,37-72.

Turnbull, L., Wainwright, J. Brazier, R.E., 2008. A conceptual framework for understanding semi-arid land degradation: ecohydrological interactions across multiple-space and time scales. Ecohydrology 1, 23–34.

Turnbull, L., Wainwright, J., Brazier, R.E., 2010. Nitrogen and phosphorus dynamics during runoff events over a transition from grassland to shrubland in the south-western United States. Hydrological Processes 24, 393–414. DOI: 10.1002/hyp.7806

Turner, M.G., Romme, W.H., Gardner, R.H., O'Neill, R.V., Kratz, T.K., 1993. A revised concept of landscape equilibrium: disturbance and stability on scaled landscapes. Landscape Ecology 8, 213–227.

van de Koppel, J., Rietkerk, M., 2004. Spatial interactions and resilience in arid ecosystems. Am. Naturalist 163,113-121.

Versteeg, H.K., Malalasekera, W., 1995. An Introduction to Computational Fluid Dynamics: The Finite Volume Method. Prentice Hall, London.

Wainwright, J., 2009. Desert ecogeomorphology, in AJ Parsons and AD Abrahams (eds) *Geomorphology of Desert Environments*, 2nd edition, Springer, Berlin.

Wainwright, J., Bracken, L.J., 2011. Overland flow and runoff generation, in DSG Thomas (ed.) *Arid Zone Geomorphology*, 3rd ed., 235–268, John Wiley and Sons, Chichester.

Wainwright, J. and Parsons, A.J. 2010 Thornes, J.B. 1985: The ecology of erosion. Geography 70, 222-35. *Progress in Physical Geography,* 34, 399-408.

Wainwright, J., Parsons, A.J., Abrahams, A.D., 1999. Field and computer simulation experiments on the formation of desert pavement. Earth Surf. Process. Landforms. 24, 1025-1037.

Wainwright, J., Parsons, A.J., Abrahams, A.D., 2000. Plot-scale studies of vegetation, overland flow and erosion interactions: case studies from Arizona and New Mexico. Hydrol. Proc. 14,2921–2943.

Wainwright, J., Parsons, A.J., Schlesinger, W.H., Abrahams, A.D., 2002. Hydrology–vegetation interactions in areas of discontinuous flow on a semi-arid bajada, southern New Mexico. J. Arid Environments 51, 319-330.

Wainwright, J., Parsons, A.J., 2002. The effect of temporal variations in rainfall on scale dependency in runoff coefficients. Water Resour. Res. 38(12), 1271.

Wainwright, J., 2005. Climate and Climatological Variations in the Jornada Experimental Range and Neighbouring Areas of the US Southwest. Adv. Environ. Monitor. Model. 1,39-110.

Wainwright, J.W., Parsons, A.J., Müller, E.N., Brazier, R.E., Powell, D.M., Fenti, B., 2008a. A Transport-Distance Approach to Scaling Erosion Rates: 1. Background and Model Development. Earth Surf. Process. Landforms. 33, 813–826.

Wainwright, J.W., Parsons, A.J., Müller, E.N., Brazier, R.E., Powell, D.M., Fenti, B. 2008b. A Transport-Distance Approach to Scaling Erosion Rates: 2. Sensitivity and Evaluation of MAHLERAN. Earth Surf. Process. Landforms. 33, 962–984.

Wainwright, J.W., Parsons, A.J., Müller, E.N., Brazier, R.E., Powell, D.M., Fenti, B., 2008c. A Transport-Distance Approach to Scaling Erosion Rates: 3. Evaluating Scaling Characteristics of MAHLERAN. Earth Surf. Process. Landforms. 33, 1113–1128.

Wainwright, J. 2009. Desert ecogeomorphology. In AJ Parsons and AD Abrahams (eds) Geomorphology of Desert Environments, Springer, Berlin

Walter, H., 1971. *Ecology of Tropical and Subtropical Vegetation*. Oliver and Boyd, Edinburgh.

Ward, D 2008 *The Biology of Deserts*. Oxford University Press, Oxford.

Went, F.W., Westergaard, M., 1949. Ecology of desert plants. III. Development of plants in the Death Valley National Monument, California. Ecology. 30, 26-38.

Western AW, Bloschl G, and Grayson RB. 2001. Towards capturing hydrologically significant connectivity in spatial patterns. *Water Resources Research* **37**, 83–97.

Westoby, M., 1980. Elements of a theory of vegetation dynamics in arid rangelands. Israel J. Botany 28,169-194

Westoby, M., Walker, B., Noy-Meir, I., 1989. Opportunistic management for rangelands not at equilibrium. J. Range Manage. 42(4),266-274

White, L.P., 1997. Vegetation stripes on sheet wash surfaces. J. Ecology 59, 615-622

Whitford, W.G., 2002. *Ecology of Desert Systems*, San Diego, Academic Press, 343pp.

Williams, C.A., Albertson, J.D., 2006. Dynamical effects of the statistical structure of annual rainfall on dryland vegetation. Global Change Biology. 12, 777-792.

Yao, J., Peters, D.P.C., Havstad, K.M., Gibbens, R.P., Herrick, J.E., 2006. Multi-scale factors and long-term responses of Chihuahuan Desert grasses to drought. Landscape Ecology 21,1217-1231.

ECOLOGICAL ARCHIVES MATERIAL

Appendix: Exploration of Model Behaviour

1663

Table 1 Summary of input conditions used in model simulations

Length of rainfall record used in simulations	312 years, 80 years, or 80-year average	
Size of grid	50 x 50 m	
Gradient of slope	2 degrees	
Nitrogen input	0.65g m^{-2}	
Water input to each cell	Constant, long term average	= 228 mm yr^{-1}
	Stochastic, average	= 243 mm yr^{-1}
	Instrumented, average	= 243 mm yr^{-1}

Table 2 Ranges of biomass consumption under three different grazing strategies (Havstad *et al.*, 2006)

	Consumption of palatable biomass in g m^{-2} yr^{-1} and converted to a percentage of biomass consumed as applied in the model		
Range	Conservative	Recommended	Overstocked
Lowest quoted value	8 g/m^{-2} yr^{-1} (2.5%)	7 g/m^{-2} yr^{-1} (2.2%)	30 g/m^{-2} yr^{-1} (9.4%)
Highest quoted value	14 g/m^{-2} yr^{-1} (4.4%)	21 g/m^{-2} yr^{-1} (6.6%)	60 g/m^{-2} yr^{-1} (18.8%)

		UP SLOPE (NORTH)		
EAST	0.0	0.1	0.0	WEST
	0.1	0.5	0.1	
	0.05	0.1	0.05	
		DOWN SLOPE (SOUTH)		
		Percentage of resource moved out from a cell containing black grama by the water vector		

		UP SLOPE (NORTH)		
EAST	0.0	0.2	0.0	WEST
	0.05	0.5	0.05	
	0.05	0.1	0.05	
		DOWN SLOPE (SOUTH)		
		Percentage of resource moved out from a cell containing creosotebush by the water vector		

		UP SLOPE		
EAST	0.0	0.05	0.0	WEST
	0.15	0.5	0.15	
	0.05	0.05	0.05	
		DOWN SLOPE		
		Percentage of nitrogen moved out from a cell containing black grama by the wind vector		

		UP SLOPE		
EAST	0.0	0.05	0.0	WEST
	0.05	0.45	0.05	
	0.05	0.3	0.05	
		DOWN SLOPE		
		Percentage of nitrogen moved out from a cell containing creosotebush by the wind vector		

		UP SLOPE (SOUTH)		
EAST	0.1	0.1	0.1	WEST
	0.1	0.2	0.1	
	0.1	0.1	0.1	
		DOWN SLOPE (NORTH)		
		Percentage of nitrogen moved out from a cell containing black grama by the grazing vector		

		UP SLOPE (SOUTH)		
EAST	0.0625	0.0625	0.0625	WEST
	0.0625	0.5	0.0625	
	0.0625	0.0625	0.0625	
		DOWN SLOPE (NORTH)		
		Percentage of nitrogen moved out from a cell containing creosotebush by the grazing		

	vector

Table 4 Summary of species demographic data

Demograpic data	**Grass**	**Shrub**	**Data source**
Maximum annual growth rate (%)			Peters, (2002a)
Maximum biomass in 1-m^2 cell (g)	319	222	Maneta *et al* (2008)
Water Efficiency (g water per g of biomass)	3.5	2.48	Peters, (2002a)
Nitrogen use efficiency (g nitrogen per g of biomass)	0.6206	0.2767	Peters, (2002a)
Water maintenance requirement (g water per g of biomass)	0.7	0.496	Peters, (2002a)
Nitrogen maintenance requirement (g nitrogen per g of biomass)	0.125	0.055	Wainwright (2009)
Failure rate of species (% of species in cell)	5	5	
Mortality rate of species (% of species in cell)	10	10	

Table 5 Percentage of roots of the grass and shrub species that are distributed between the three soil layers

	Bouteloua eriopoda	***Larrea tridentate***
Top Layer	13.3%	6.7%
Middle Layer	50.4%	32.0%
Deep Layer	36.3%	61.3%

Table 6 Percentage of propagules for each species that is amenable to movement by the vectors

	Vector		
Propagules	Water	Wind	Grazer
Black grama	75%	20%	5%
Creosotebush	85%	10%	5%

LIST OF FIGURES

Figure 1	Conceptual framework for modelling dynamic relationships bewteen elements of desert ecosystems.
Figure 2	The mechanisms for resource and propagule redistribution based on cell connectivity. If a cell is disconnected (i.e. receives no input of resources and propagules from up-vector cells), or is at the end of a connected pathway, available resources and propagules entering that cell are redistributed according to rules given in Table 3. If the cell lies on a connected pathway, available resources and propagules are moved down-vector.
Figure 3	Simulation grid showing an arbitrary cell and its Moore neighbourhood. Labelling of the neighbours denotes their direction with respect to the grid.
Figure 4	Schematic diagram of model execution in which QV is input from vertical processes; QH is redistribution by lateral processes; R is resources; P is propagules; and θ, φ and ψ are three temporal scales.
Figure 5	a) Rainfall data reconstructed from tree ring data at the Jornada Headquarters from 1659 to 1969. Measured values from the

instrumental record are plotted from 1915 to 1995 for comparison (Wainwright, 2005). NB g m^{-2} a^{-1} are equivalent to mm a^{-1}

b) Comparison of reconstructed with real rainfall data over common years at the Jornada Headquarters (Wainwright, 2005).

Figure 6 Stocking levels of cattle (represented by animal unit equivalents) in the Jornada basin from 1915 to 2001. An animal unit is a mature, non lactating 1100 lbs beef cow consuming 26 lbs of forage per day.

Figure 7 Schematic diagram to show distribution of roots in relation to the three soil layers in the model.

Figure 8 The randomly generated initial conditions for the model runs.

Figure 9 a) Lognormal probability distribution (P) shown by the dotted line to approximate observed rainfall (shown by the solid line) at the Jornada LTER

b) Example of the resulting stochastic rainfall model.

Figure 10 Averages of a) biomass of grass and shrubs; b) water and nitrogen levels in the mid and deep soil layers; c) connectivity with respect to the water vector for the 50 cells along the centre line of the grid for each year of the

312-year stochastic rainfall simulation. Note that because the rainfall record is a stochastically generated one individual model realizations may differ substantially. However, all that we have run show no long-term spatial reorganisation of the vegetation.

Figure 11 Averages of a) biomass of grass and shrubs; b) water and nitrogen levels in the mid and deep soil layers; c) connectivity with respect to the water vector for the 50 cells along the centre line of the grid for each year of the 312-year reconstructed-rainfall series simulation.

Figure 12 Maps depicting the spatial distribution of grass and shrub biomass in years 1683, 1783, 1883, 1958 and 1970 for the reconstructed-rainfall series simulation.

Figure 13 Averages of i) biomass of grass and shrubs; ii) water and nitrogen levels in the mid and deep soil layers; iii) connectivity with respect to the water vector for the 50 cells along the centre line of the grid for each year of the 312-year reconstructed-rainfall series simulation, for a) a conservative grazing level, b) the recommended grazing level, and c) and the overgrazed case.

Figure 14 Maps depicting the spatial distribution of grass and shrub biomass in years 1683, 1783, 1883, 1958 and 1970 for the overgrazed -grazing simulation.

Figure 15	Averages of a) biomass of grass and shrubs; b) water and nitrogen levels in the mid and deep soil layers; c) connectivity with respect to the water vector for the 50 cells along the centre line of the grid for each year using the instrumented rainfall record and a conservative grazing level.
Figure 16	Maps depicting the spatial distribution of grass and shrub biomass at 10-year intervals for the simulation using the instrumented rainfall record and a conservative grazing level.
Figure 17	Biomass and resource distribution along the centre line of the grid at 10-year intervals for the simulation using the instrumented rainfall record and a conservative grazing level. For ease of representation, modelled biomass and resource density are scaled (normalised) the maximum potential biomass given in Peters (2002a).
Figure 18	Selected comparisons of individual cells taken from the centre line of the grid compared with experimental-plot data from Yao *et al* (2006). For ease of representation, modelled biomass is presented as a proportion (normalised biomass) of the maximum potential biomass given in Peters (2002a).


VECTORS
• Wind
• Water
• Animals
lead to
movement of
RESOURCES AND PROPAGULES
control growth of
EXTERNALITIES
• Climate
• Landscape Position
• Regional Inputs/Outputs
• Disturbance
BIOMASS
• By Species
has patchy
distribution with
CONNECTIVITY
allows action of


Connected Cell
Disconnected Cell
Line of vector action
Redistribution of resources and propagules

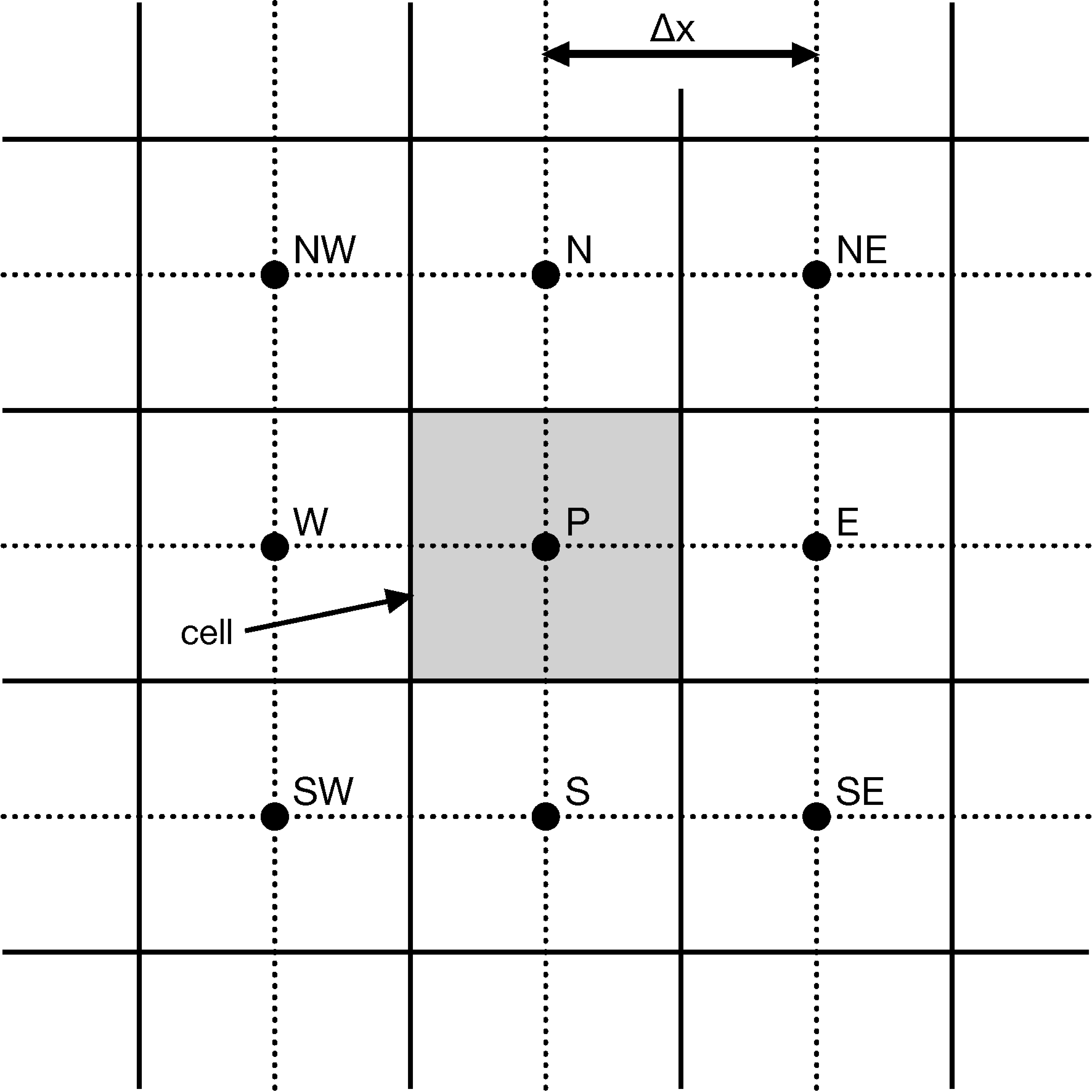
Δx
NW
N
NE
W
P
E
cell
SW
S
SE


START
Define field size; species specific data; number of species, vectors and resources; simulation time
Time = end ?
Y
N
Each cell
Add QV values for R and P to each cell
dθ = dφ ?
Y
N
Each cell
Assign a proportion of QV to each vector
Redistribute available resources as QH
dθ = dψ ?
N
Y
Each cell
Change of biomass due to new resource in cell
Calculate growth rate in proportion to most limiting resource
dψ = dt ?
N
Y
END


(a)
Observed annual rainfall at JER HQ
Predicted from Tree-ring data
ave- 1 sd
Annual rainfall (mm)
0
50
100
150
200
250
300
350
400
450
500
1650
1700
1750
1800
1850
1900
1950
Year
(b)
RMS - 82.5mm
NRMSE - 36.5%
1:1
Predicted rainfall at JER HQ (mm)
0
50
100
150
200
250
300
350
400
450
500
0
100
200
300
400
500
Observed rainfall at JER HQ (mm)

Numbers of Cattle (Animal Unit Equivalent)
45000
40000
35000
30000
25000
20000
15000
10000
5000
0
1910
1920
1930
1940
1950
1960
1970
1980
1990
2000
2010
Year

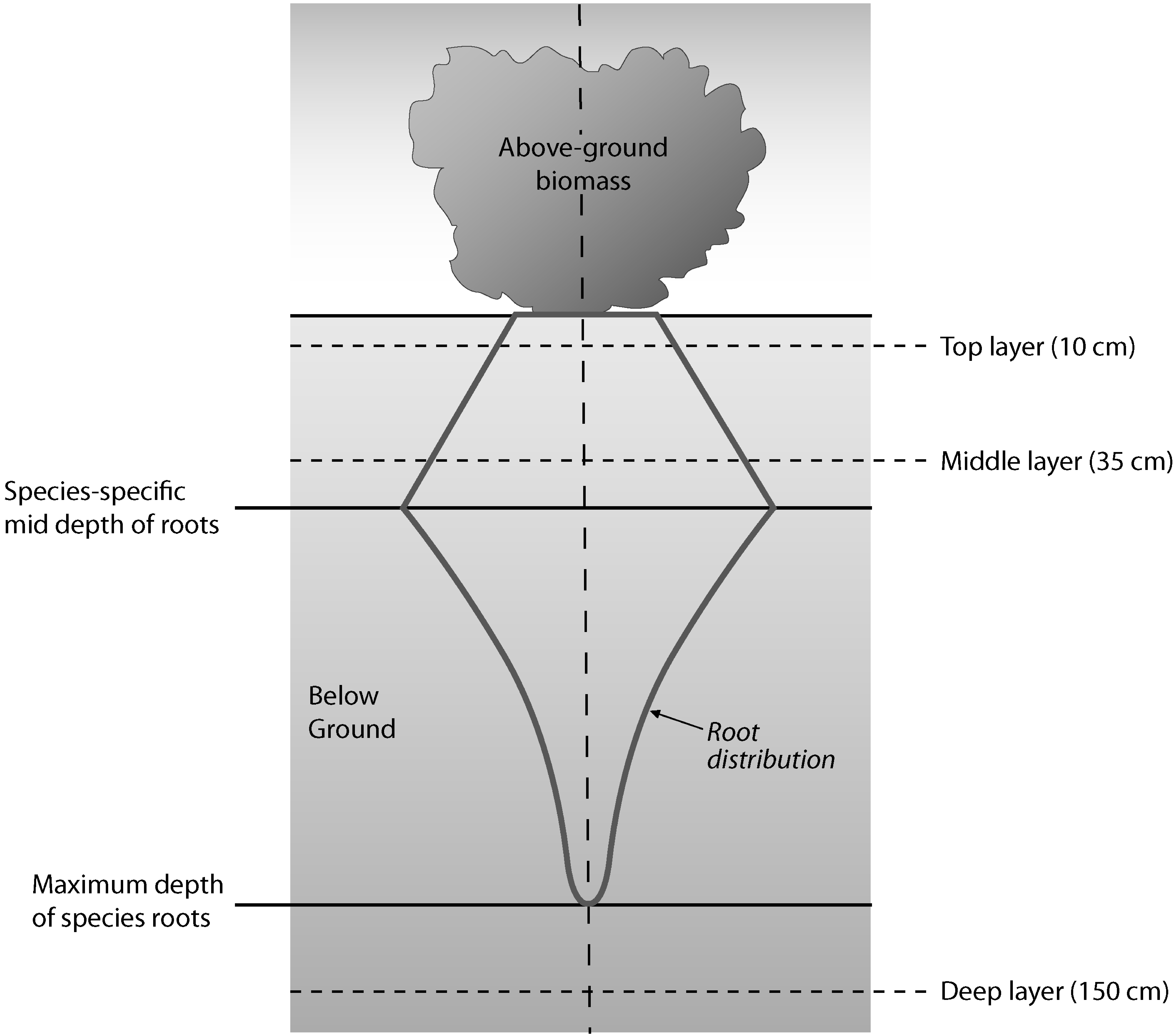
Above-ground biomass
Top layer (10 cm)
Middle layer (35 cm)
Species-specific mid depth of roots
Below Ground
Root distribution
Maximum depth of species roots
Deep layer (150 cm)

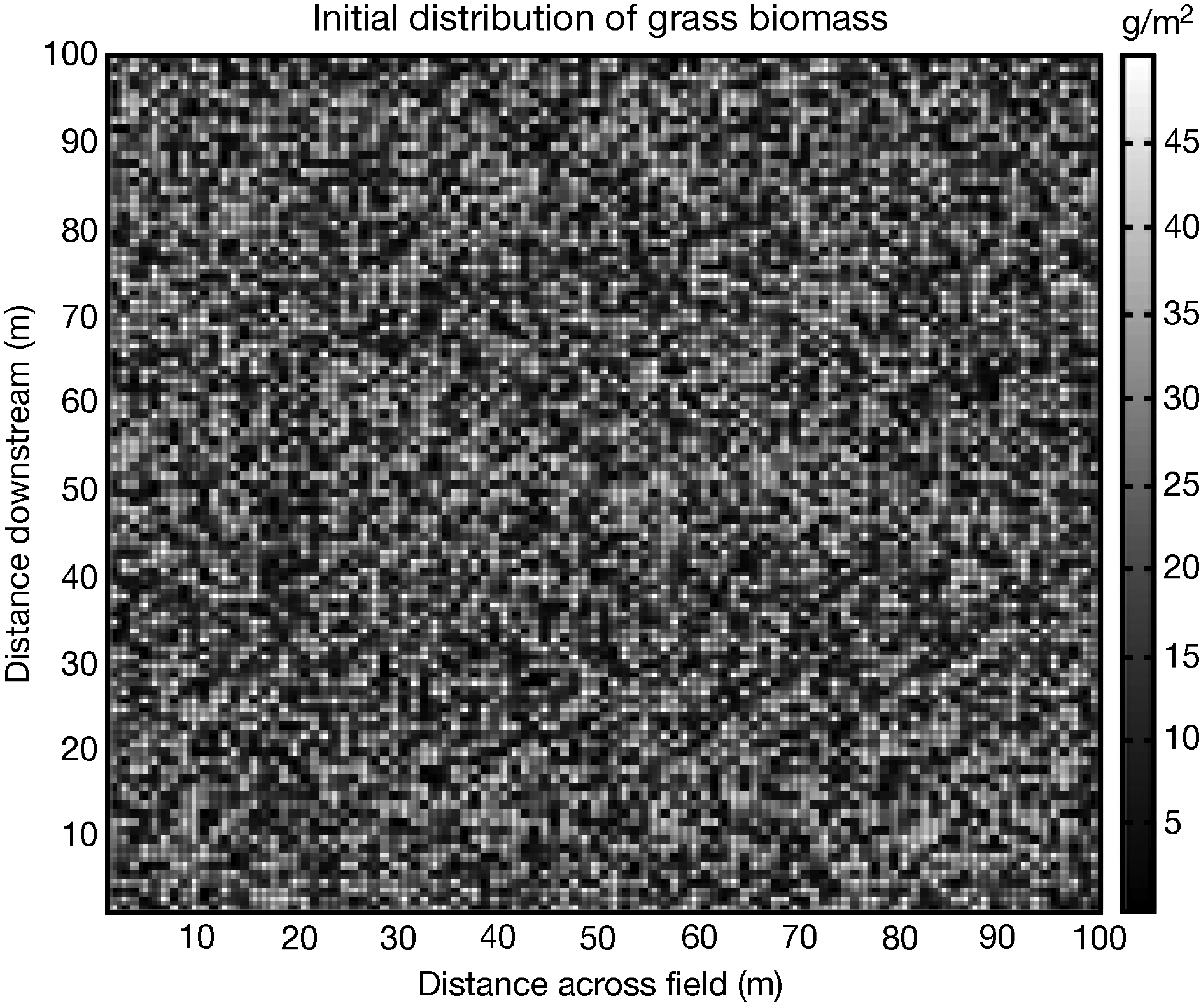
Initial distribution of grass biomass
g/m²
45
40
35
30
25
20
15
10
5
Distance downstream (m)
100
90
80
70
60
50
40
30
20
10
10
20
30
40
50
60
70
80
90
100
Distance across field (m)


(a)
log
data
$p(P)x10^3$
4.0
3.5
3.0
2.5
2.0
1.5
1.0
0.5
0.0
0
100
200
300
400
500
600
P (mm)
(b)
Rainfall (P) (mm yr^{-1})
500
450
400
350
300
250
200
150
100
50
0
0
50
100
150
200
250
300
350
Year


(a)
Species biomass
Average species biomass (g m^{-2})
0
5
10
15
20
25
30
35
40
45
50
grass
shrub
1700
1750
1800
1850
1900
1950
Time (years)
(b)
Average lower soil layer resources in field
Average resources (g m^{-2})
0
50
100
150
200
250
300
350
400
450
500
mid water
mid nitrogen
deep water
deep nitrogen
1650
1700
1750
1800
1850
1900
1950
2000
Time (years)
(c)
Connectivity measures in column transect 25
cells
0
10
20
30
40
50
60
70
80
90
100
max. continues connected cells
average connected cells
1650
1700
1750
1800
1850
1900
1950
2000
Time (years)

(a)

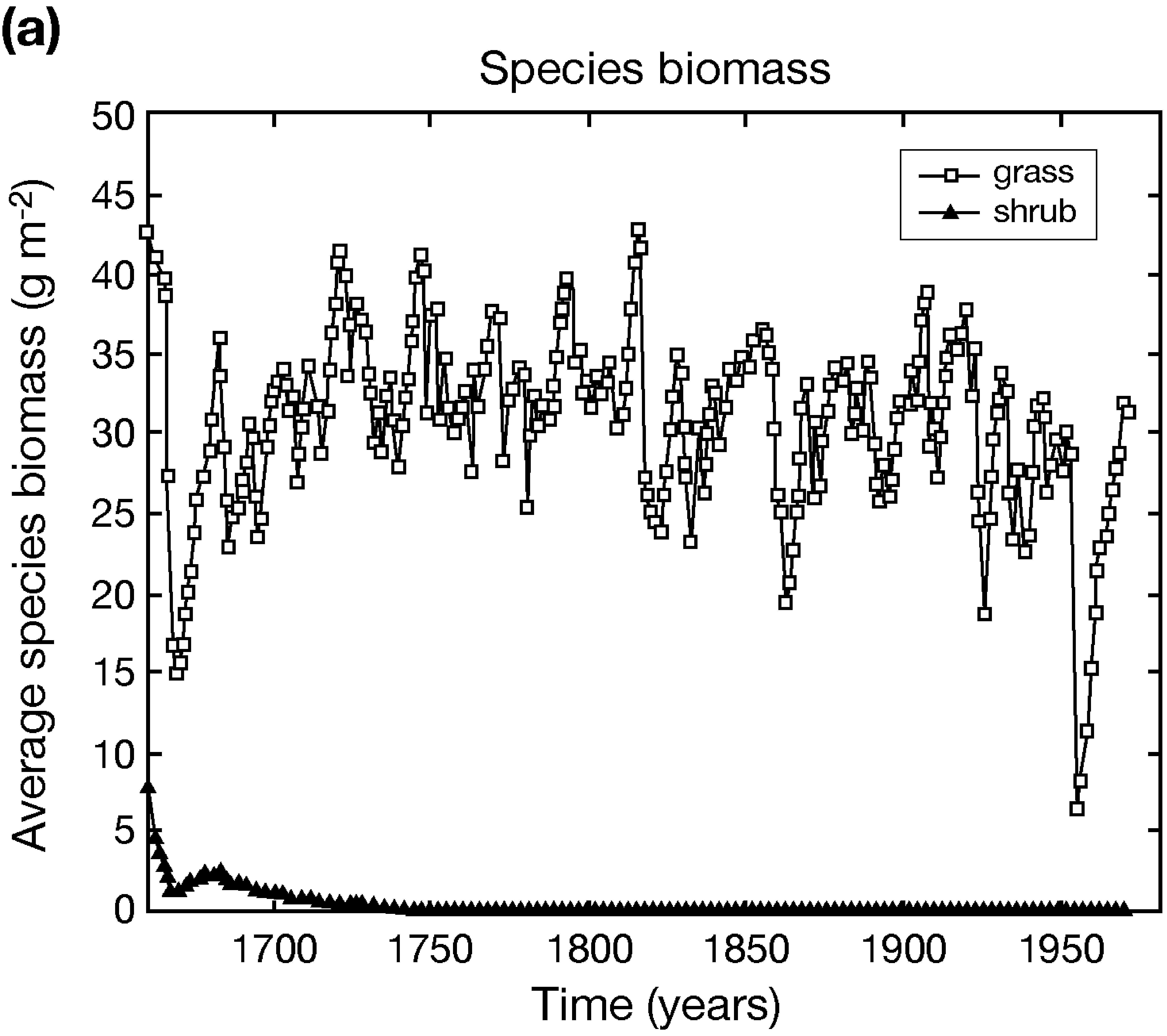

Species biomass

(b)

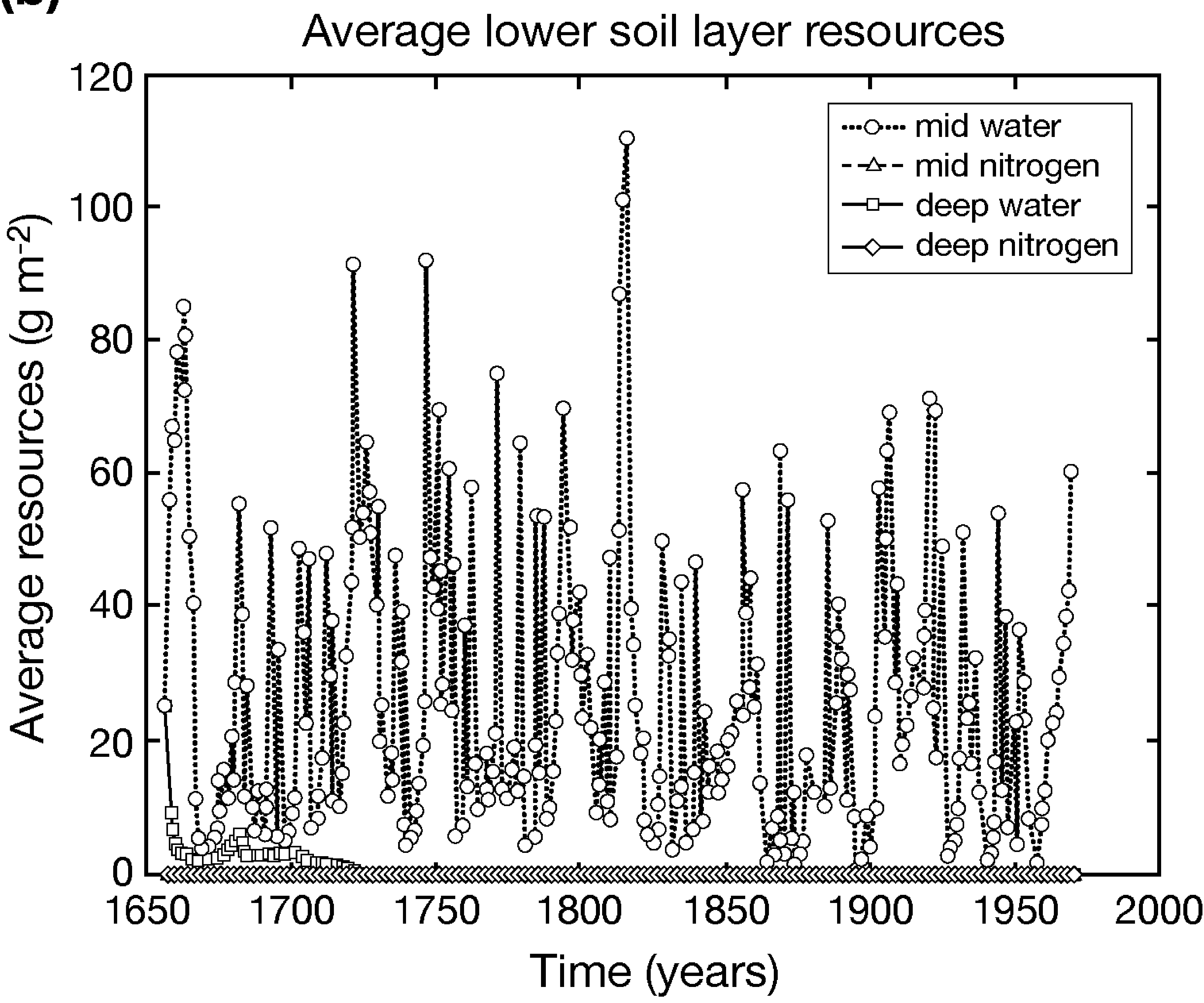

Average lower soil layer resources

(c)

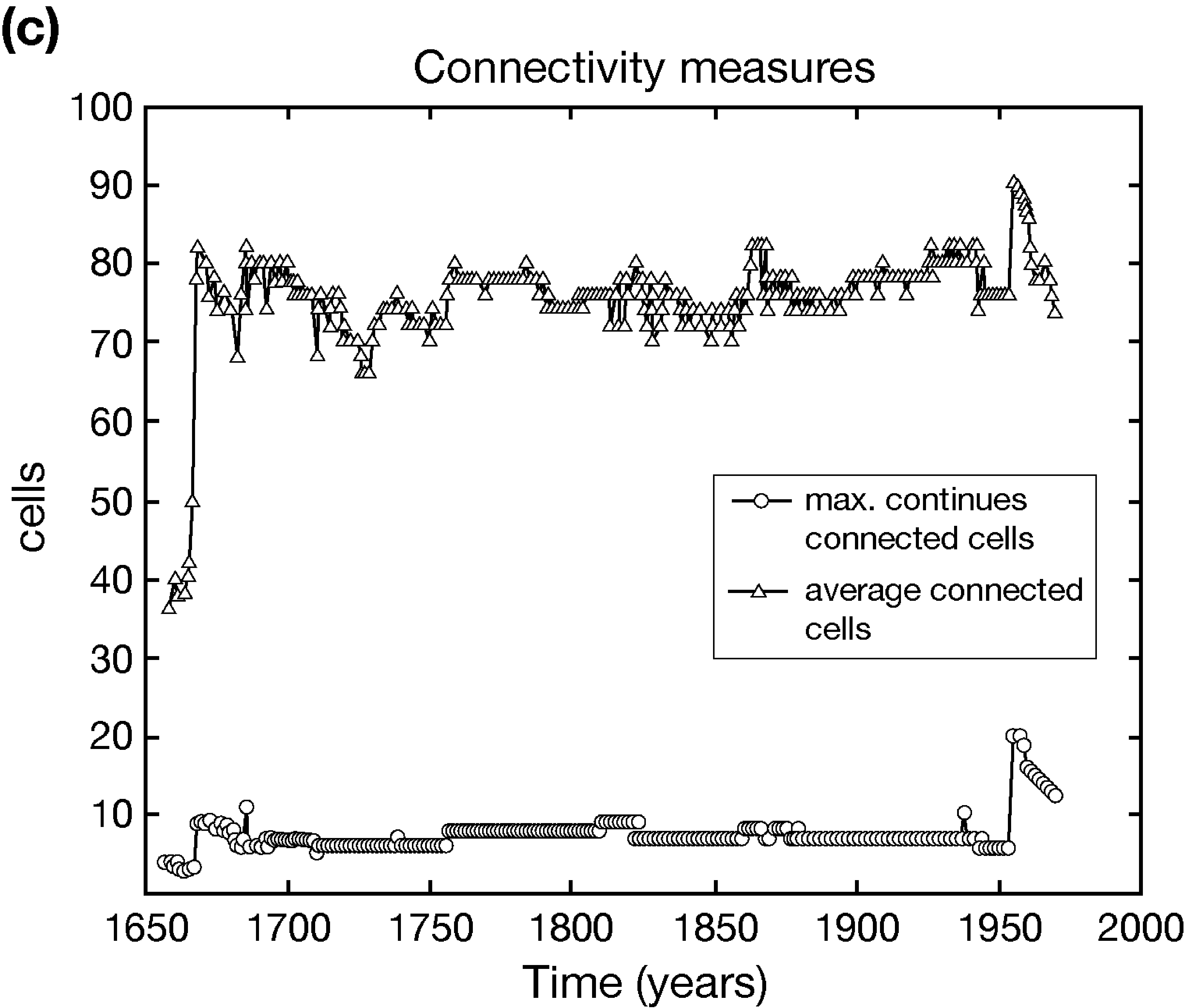

Connectivity measures


Year
map of grass biomass
map of shrub biomass
1683
1783
1883
1958
1970
Distance downslope (m)
Distance across slope (m)
0 5 10 15 20 25 30 35 40 45 50
(g m^{-2})
0 50 100 150 200 250
0 20 40 60 80 100 120 140 160
0 50 100 150 200
0 5 10 15 20 25 30 35 40 45
(g m^{-2}) x 10^{-3}
0.0 0.2 0.4 0.6 0.8 1.0 1.2 1.4 1.6
0 1 2 3 4 5 6 7 8 9 10
0.0 0.1 0.2 0.3 0.4 0.5

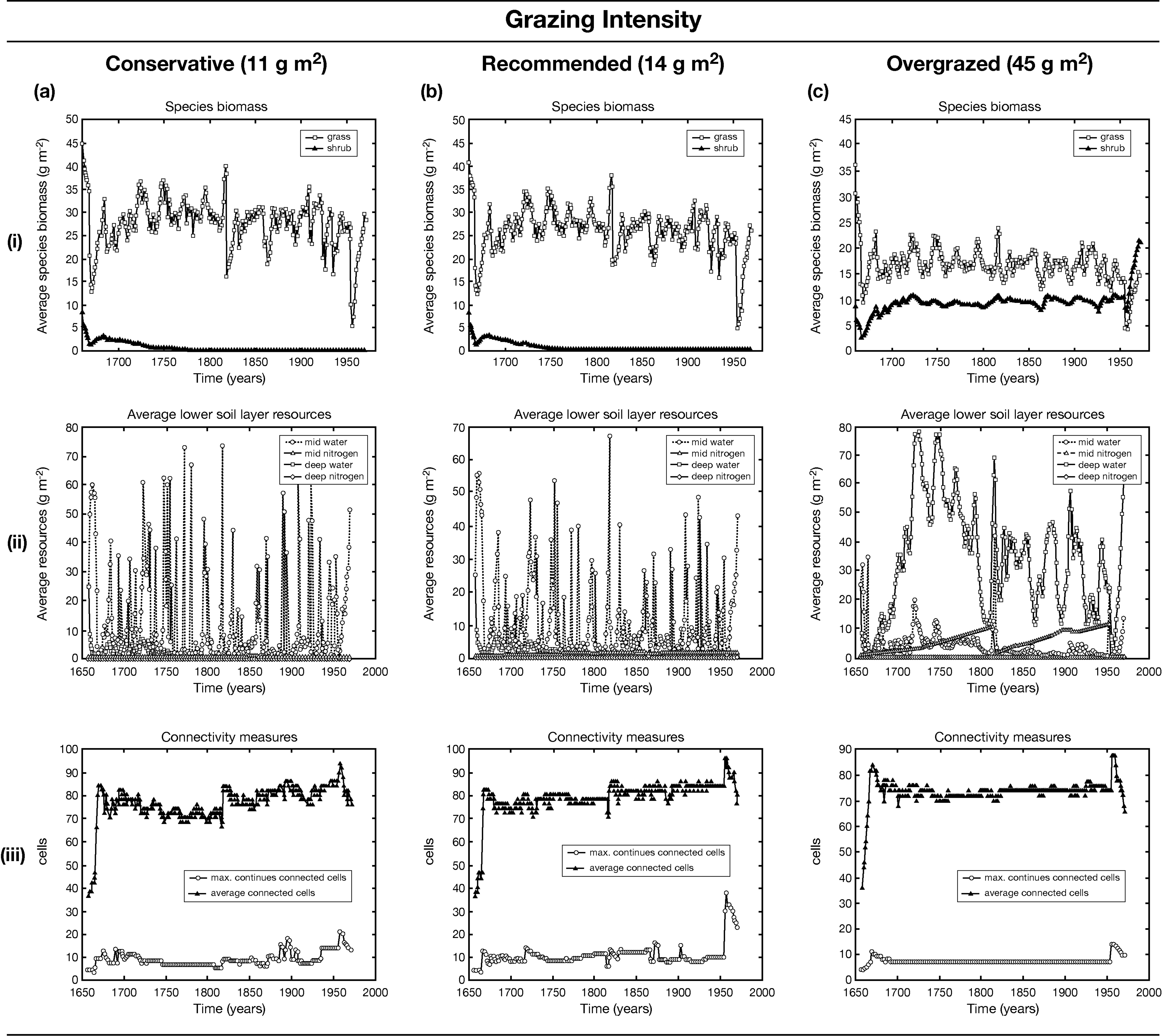
Grazing Intensity
Conservative (11 g m^2)
Recommended (14 g m^2)
Overgrazed (45 g m^2)
(a)
(b)
(c)
(i)
(ii)
(iii)
Species biomass
Average species biomass (g m^{-2})
grass
shrub
Time (years)
Average lower soil layer resources
Average resources (g m^{-2})
mid water
mid nitrogen
deep water
deep nitrogen
Connectivity measures
cells
max. continues connected cells
average connected cells
0
5
10
15
20
25
30
35
40
45
50
50
60
70
80
90
100
1650
1700
1750
1800
1850
1900
1950
2000

Year	map of grass biomass	map of shrub biomass
1683	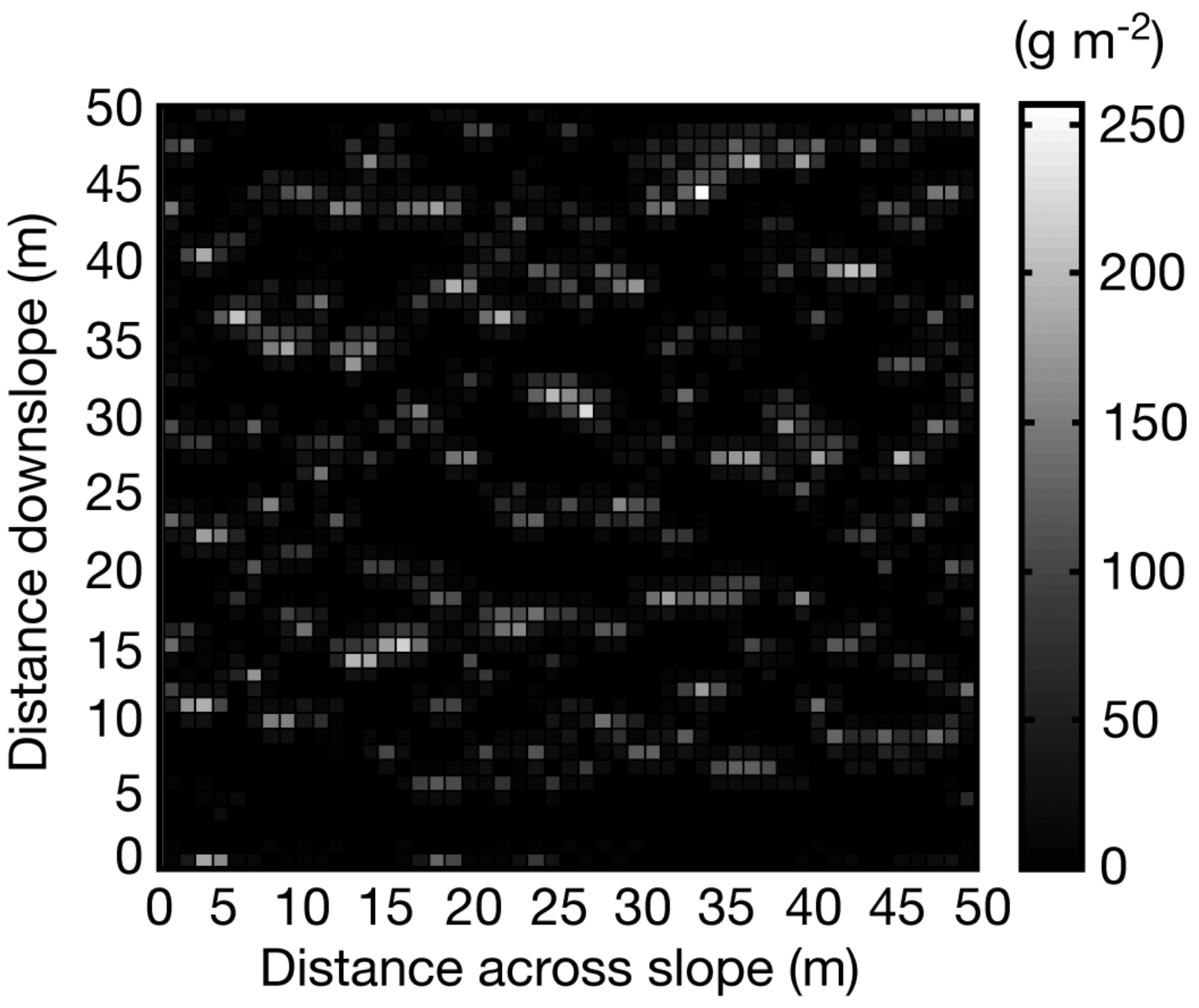	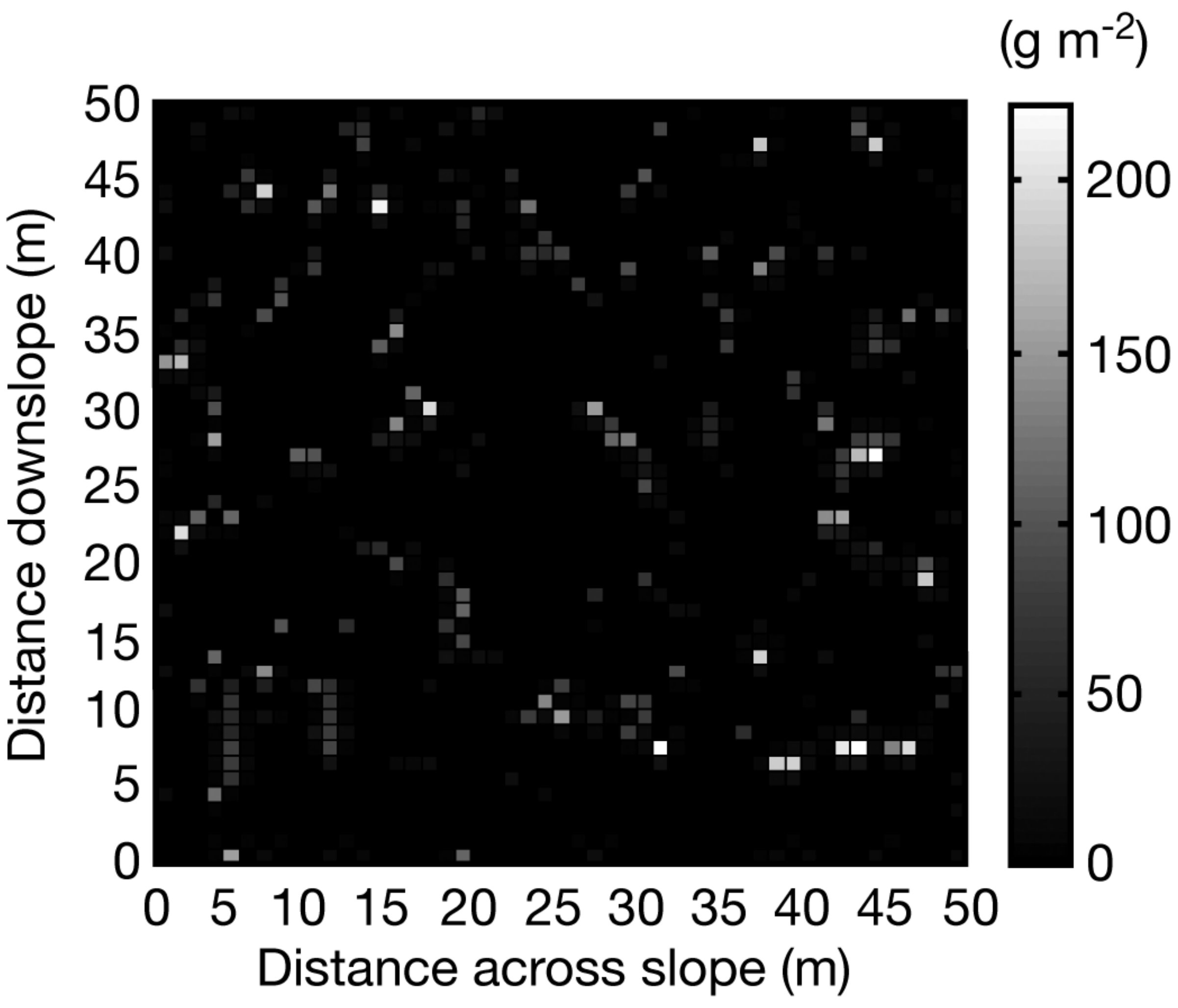
1783	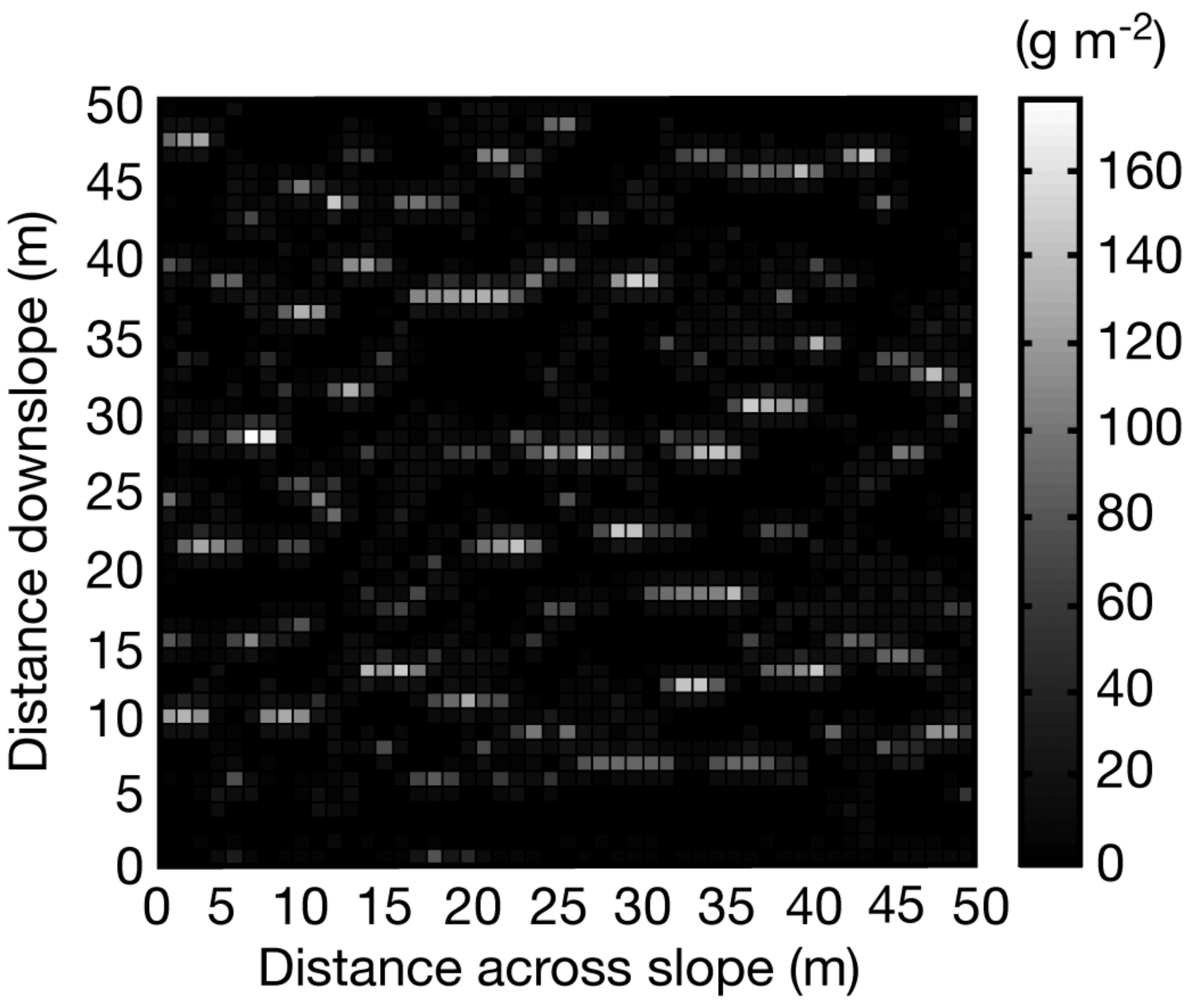	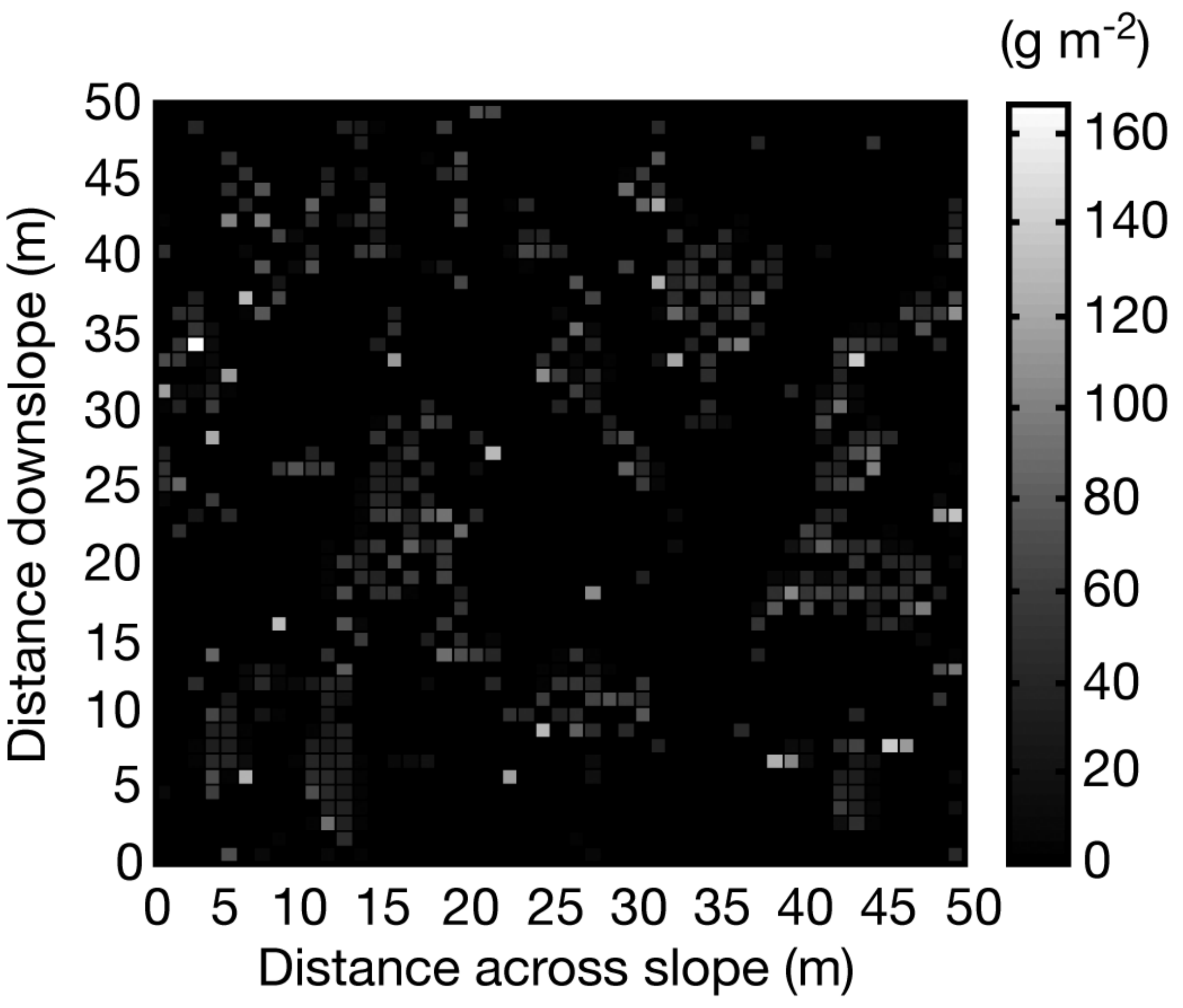
1883	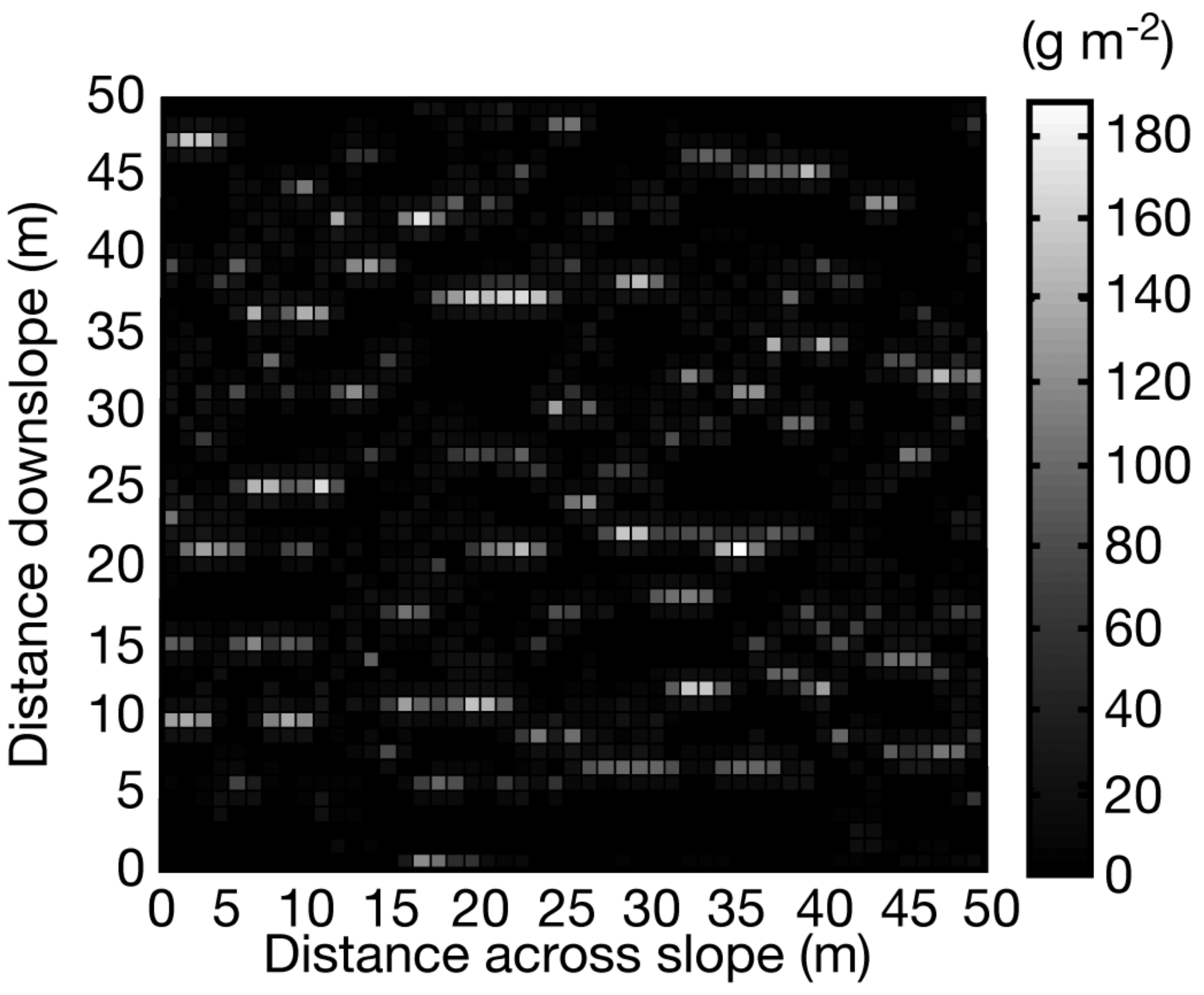	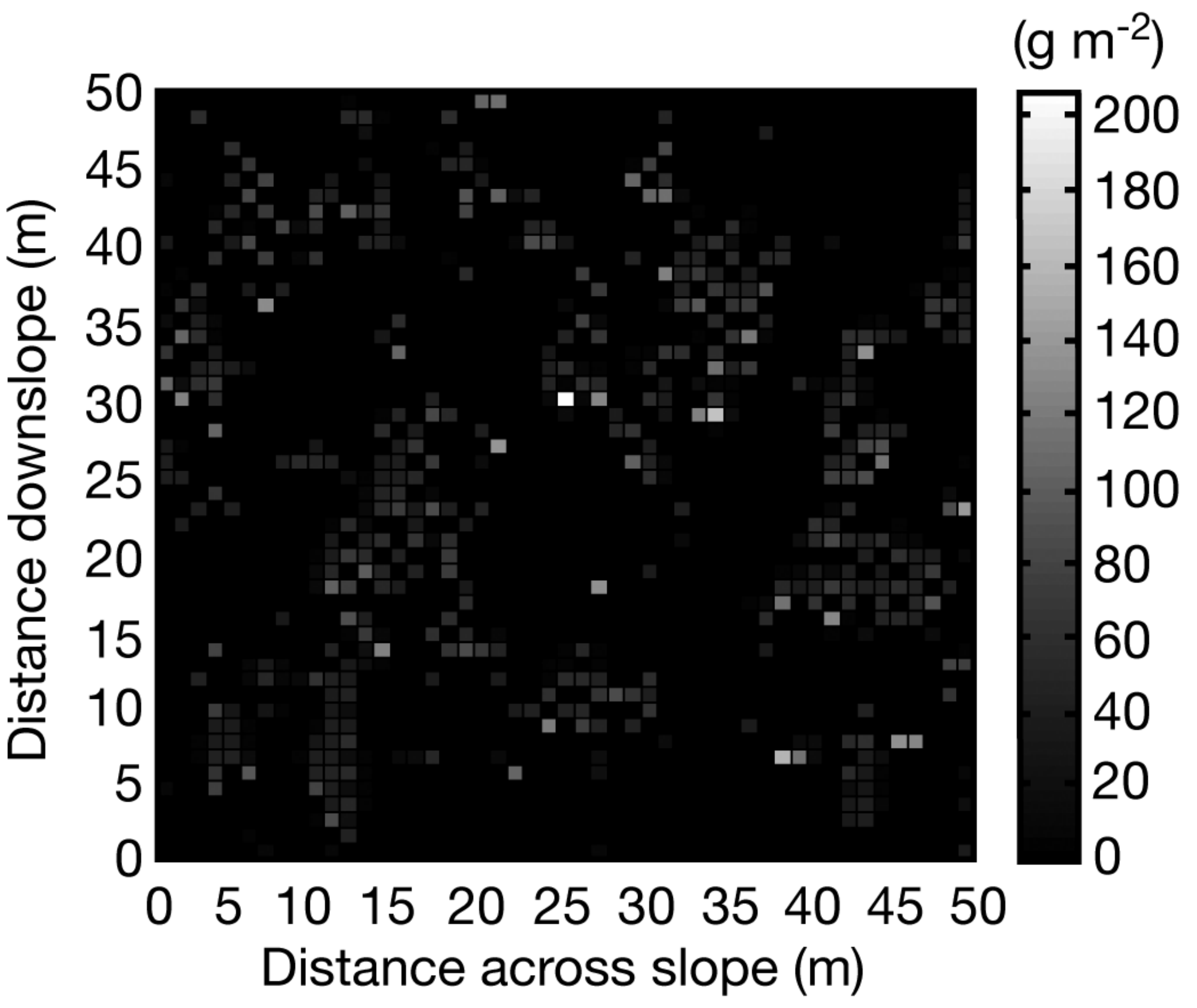
1958	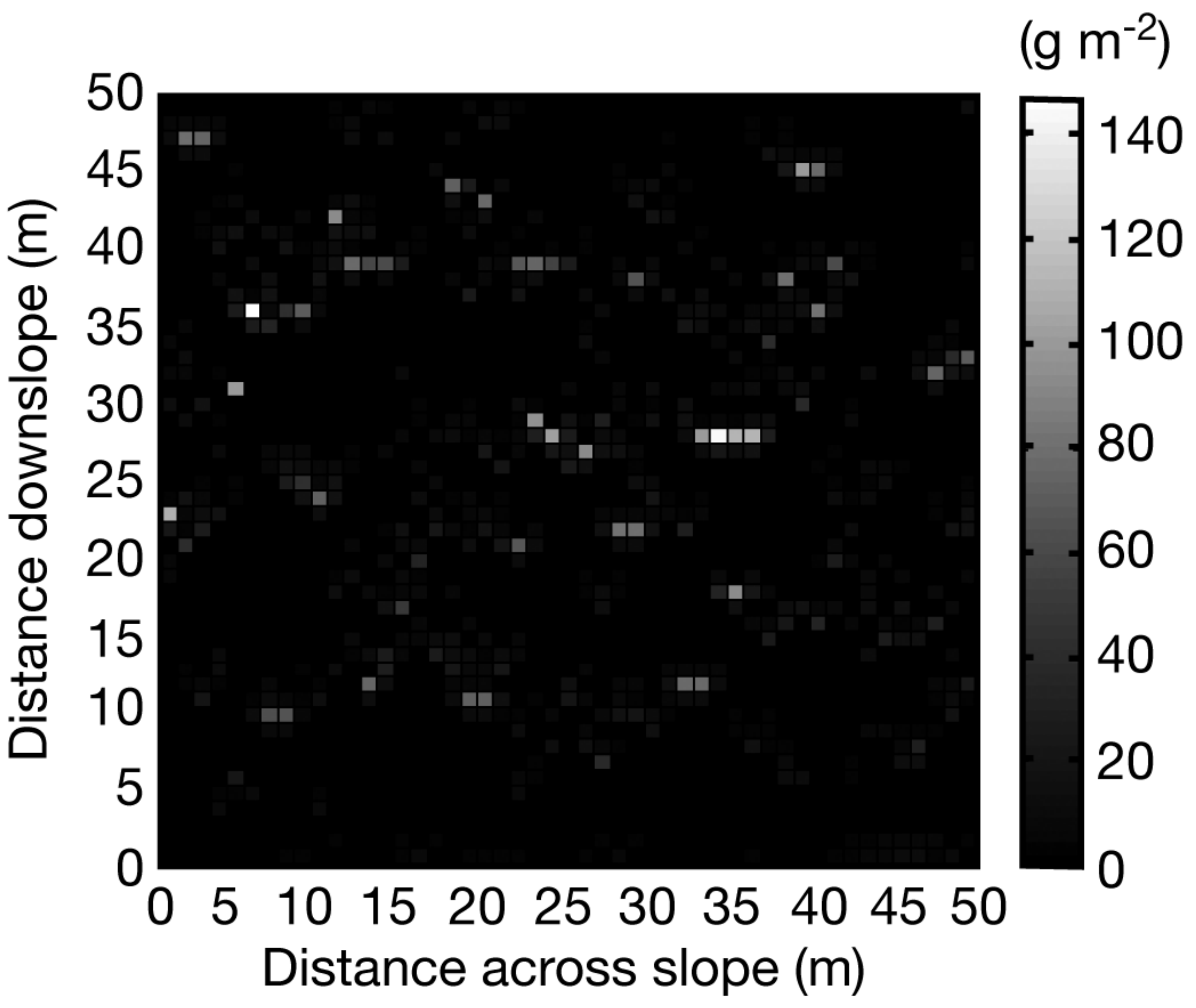	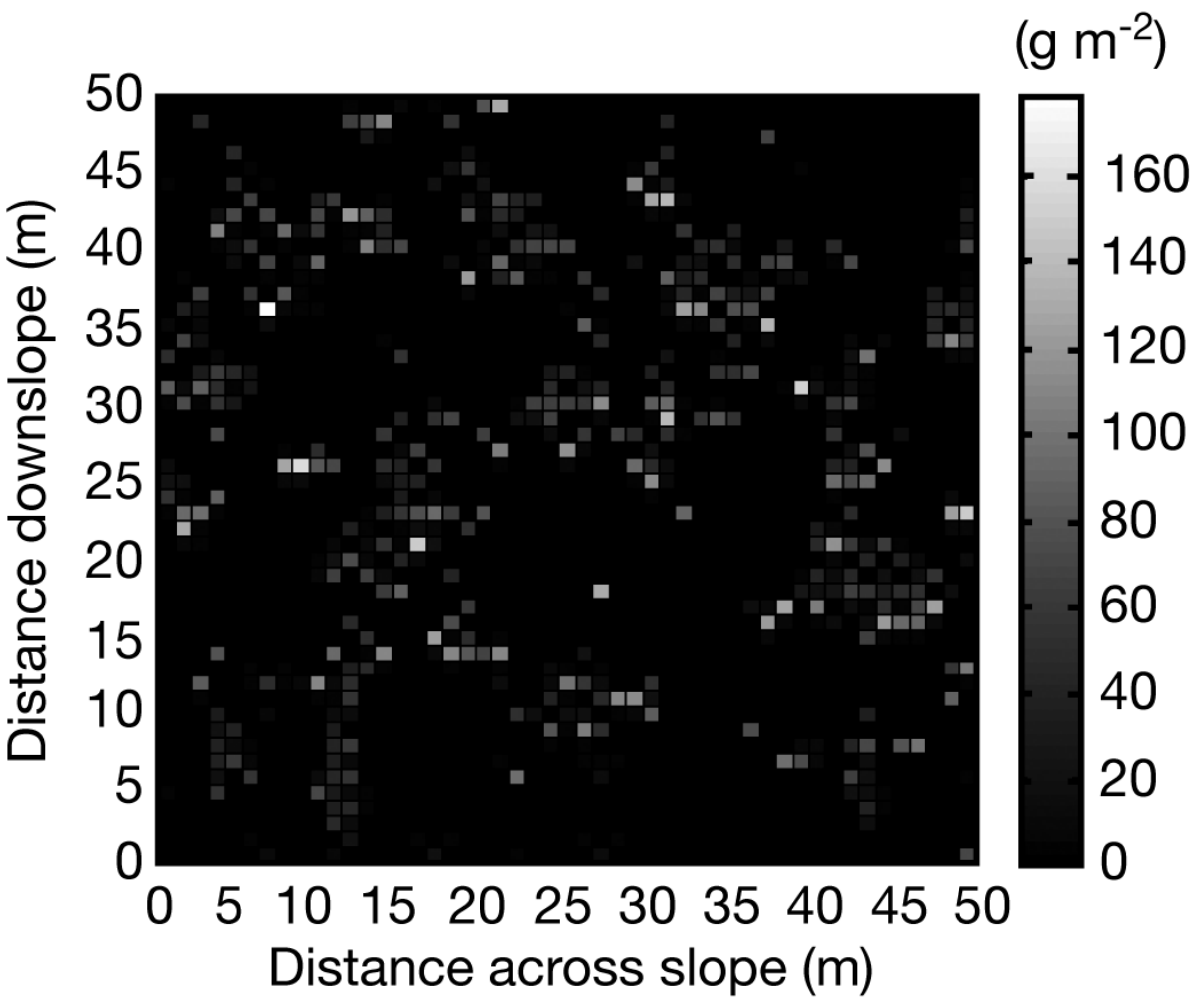
1970	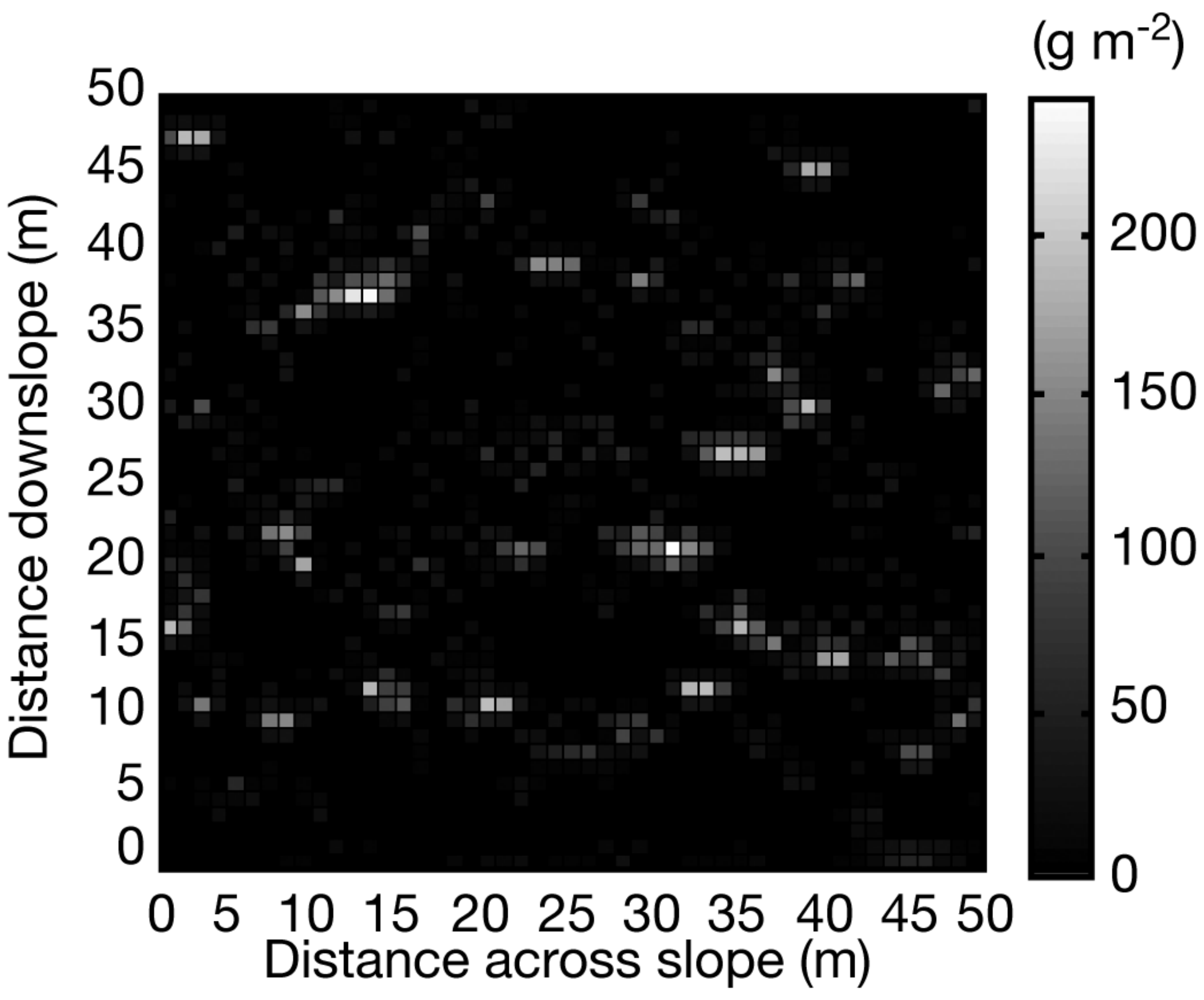	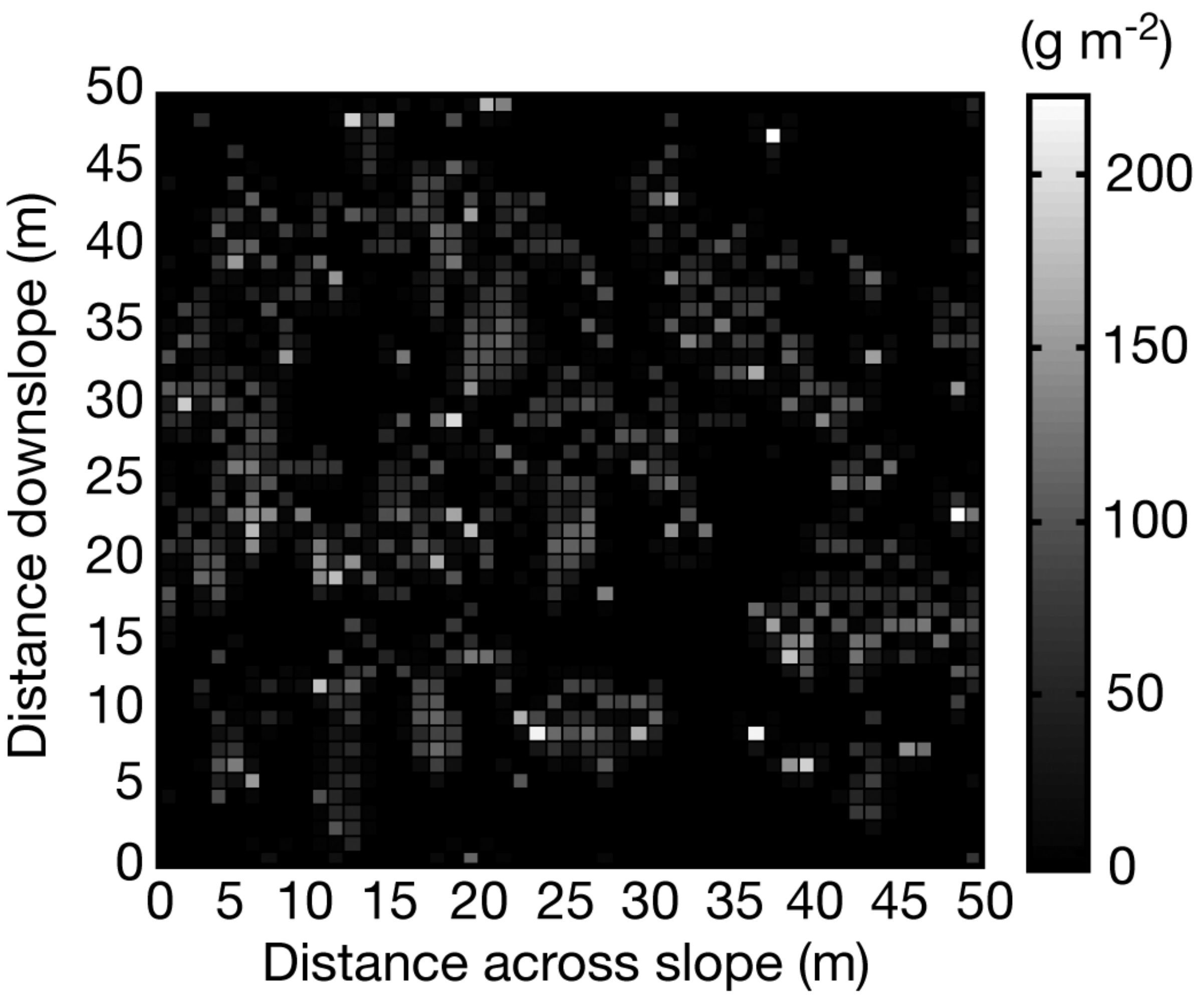


(a)
Species biomass
Average species biomass (g m-2)
50
45
40
35
30
25
20
15
10
5
0
grass
shrub
1910
1920
1930
1940
1950
1960
1970
1980
1990
2000
Time (years)
(b)
Average lower soil layer resources
Average resources (g m-2)
90
80
70
60
50
40
30
20
10
0
mid water
mid nitrogen
deep water
deep nitrogen
1910
1920
1930
1940
1950
1960
1970
1980
1990
2000
Time (years)
(c)
Connectivity measures
cells
100
90
80
70
60
50
40
30
20
10
max. continues connected cells
average connected cells
1910
1920
1930
1940
1950
1960
1970
1980
1990
2000
Time (years)

Year **map of grass biomass** **map of shrub biomass**

1925

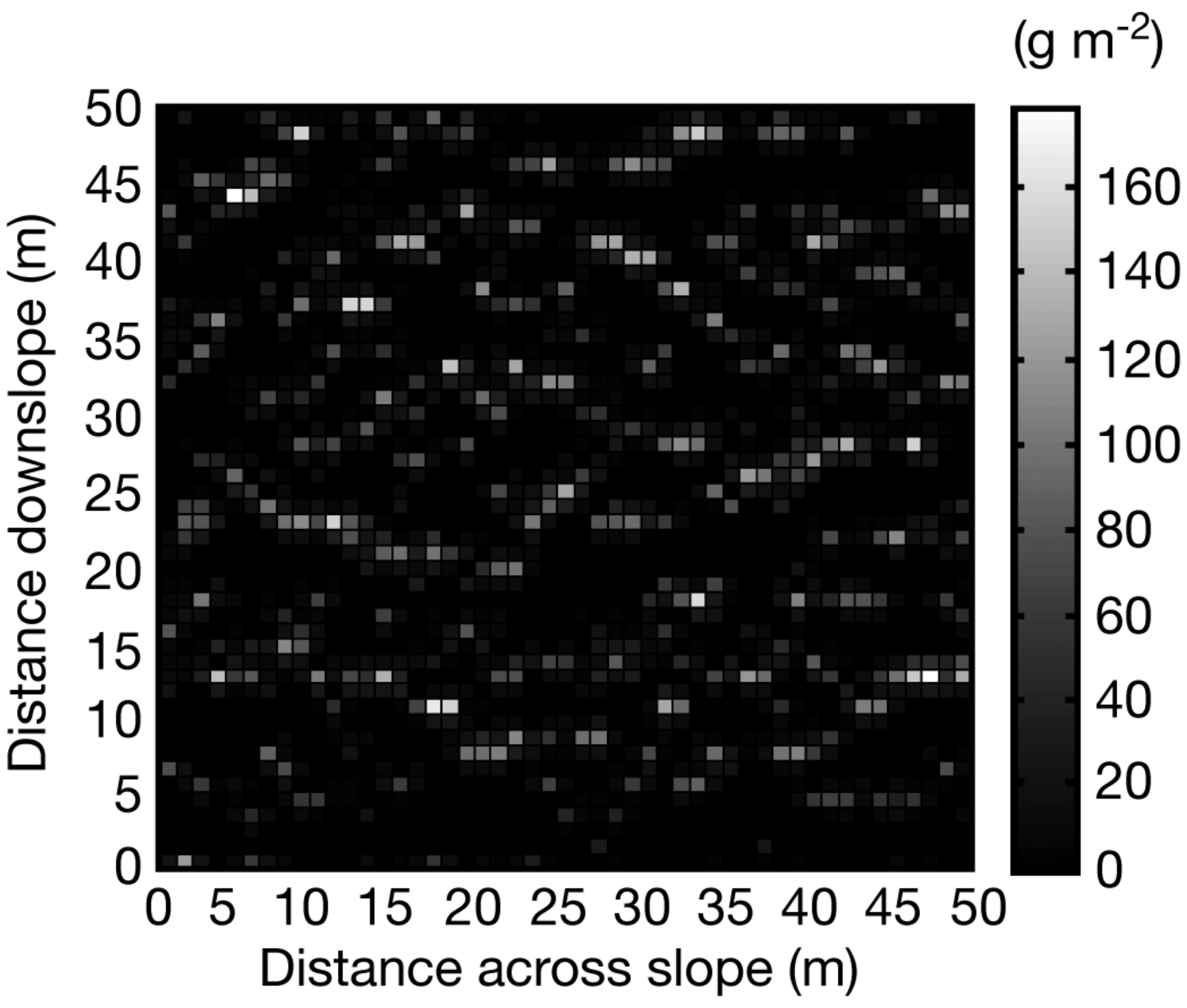

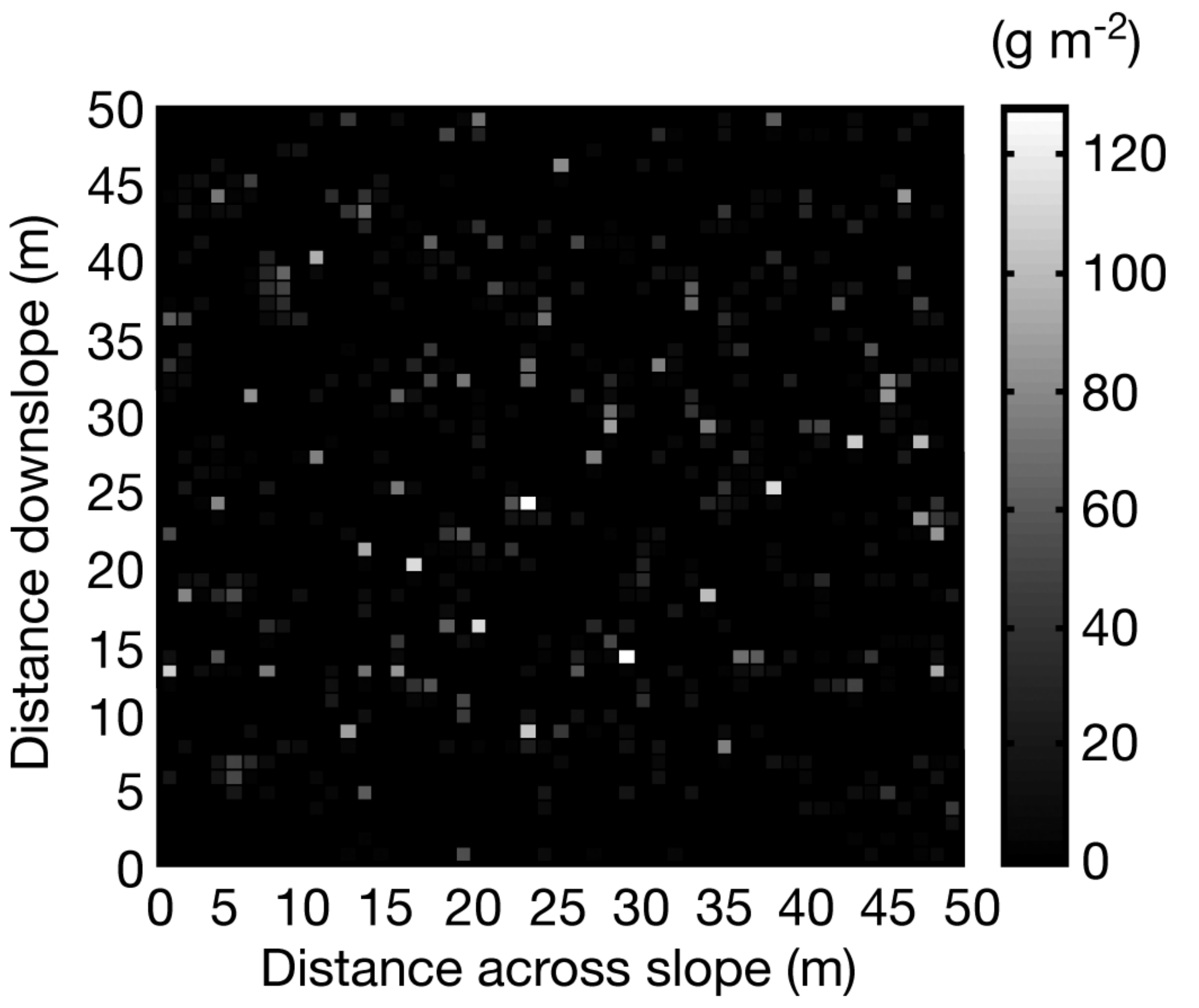

1935

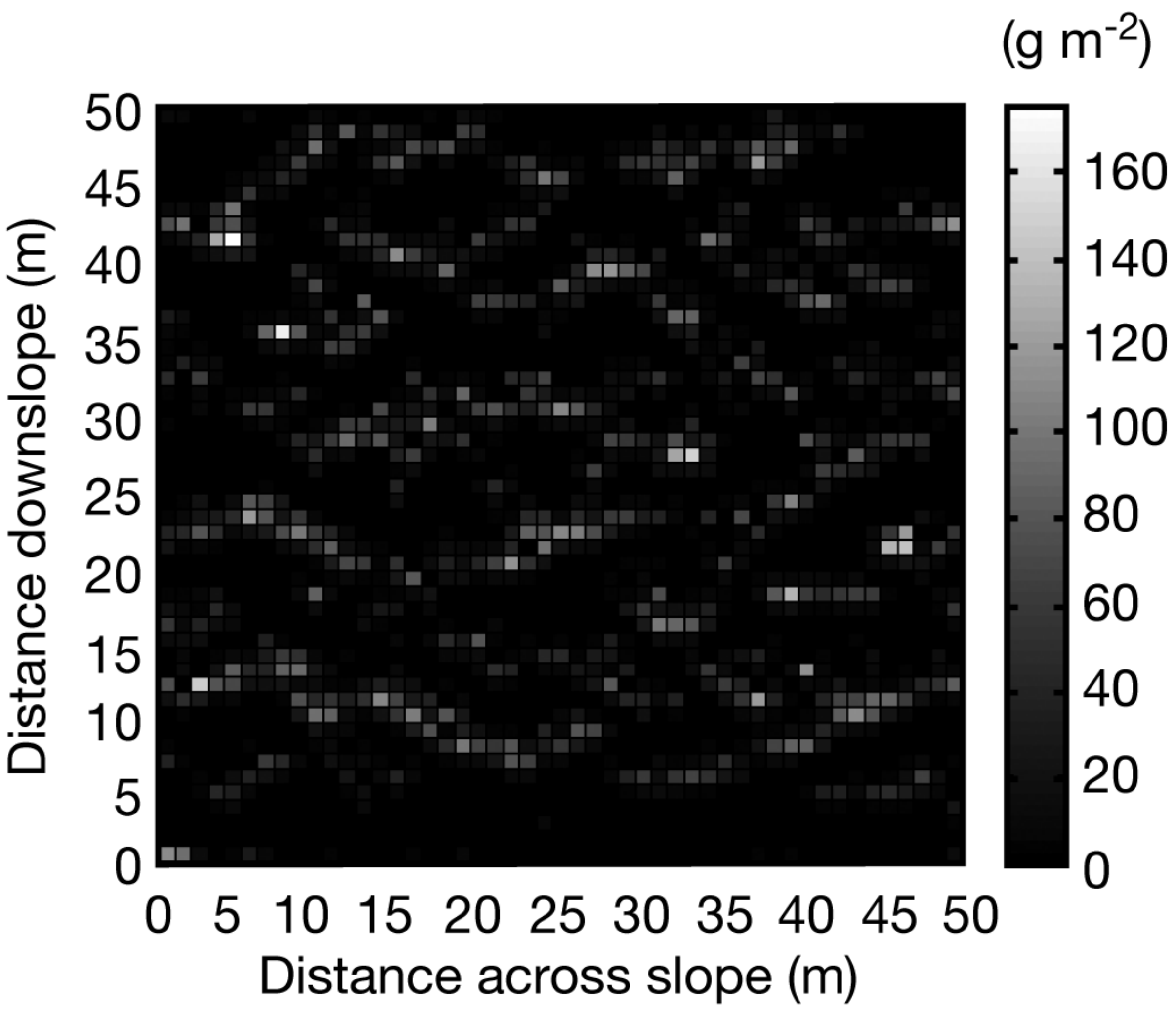

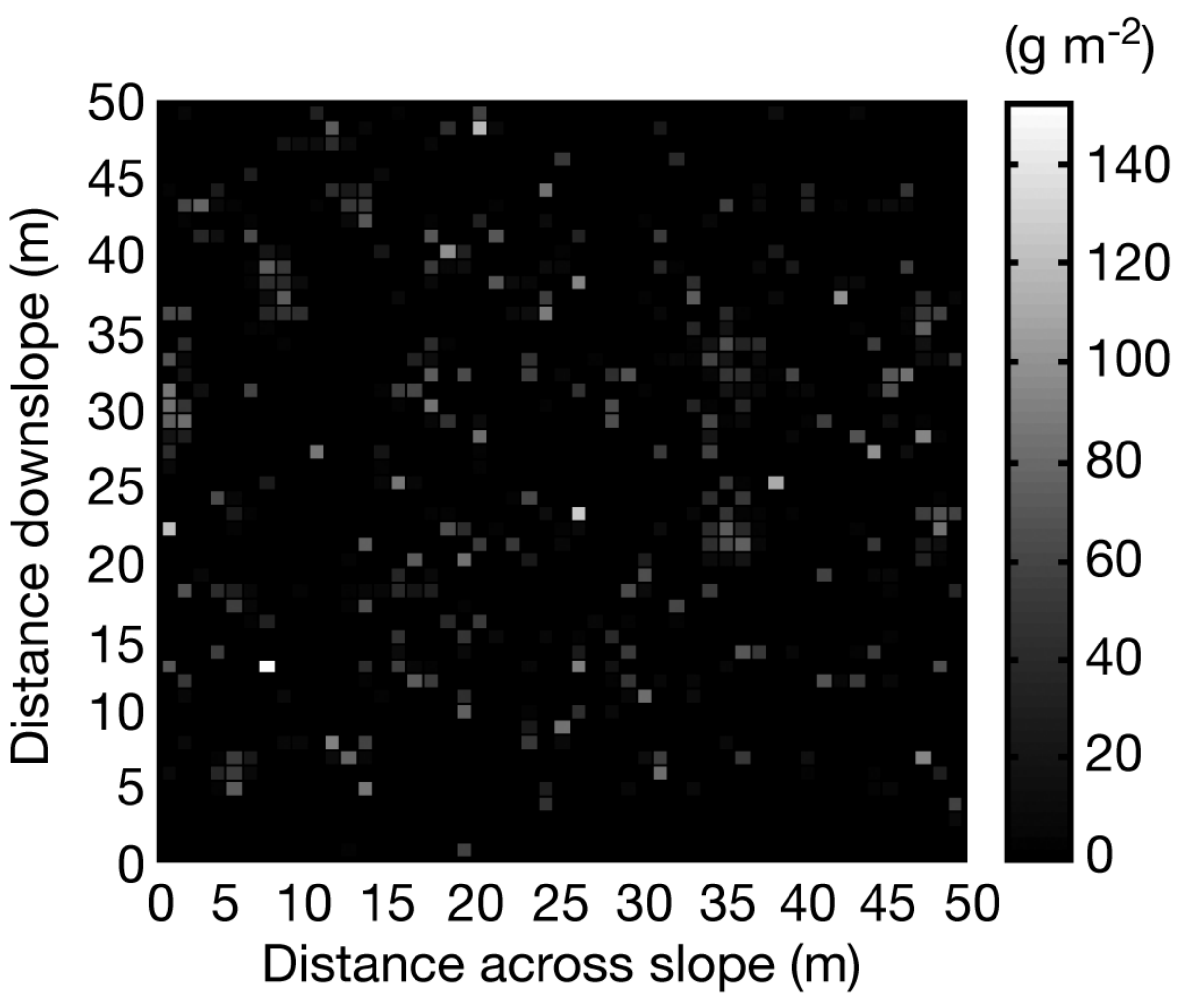

1945

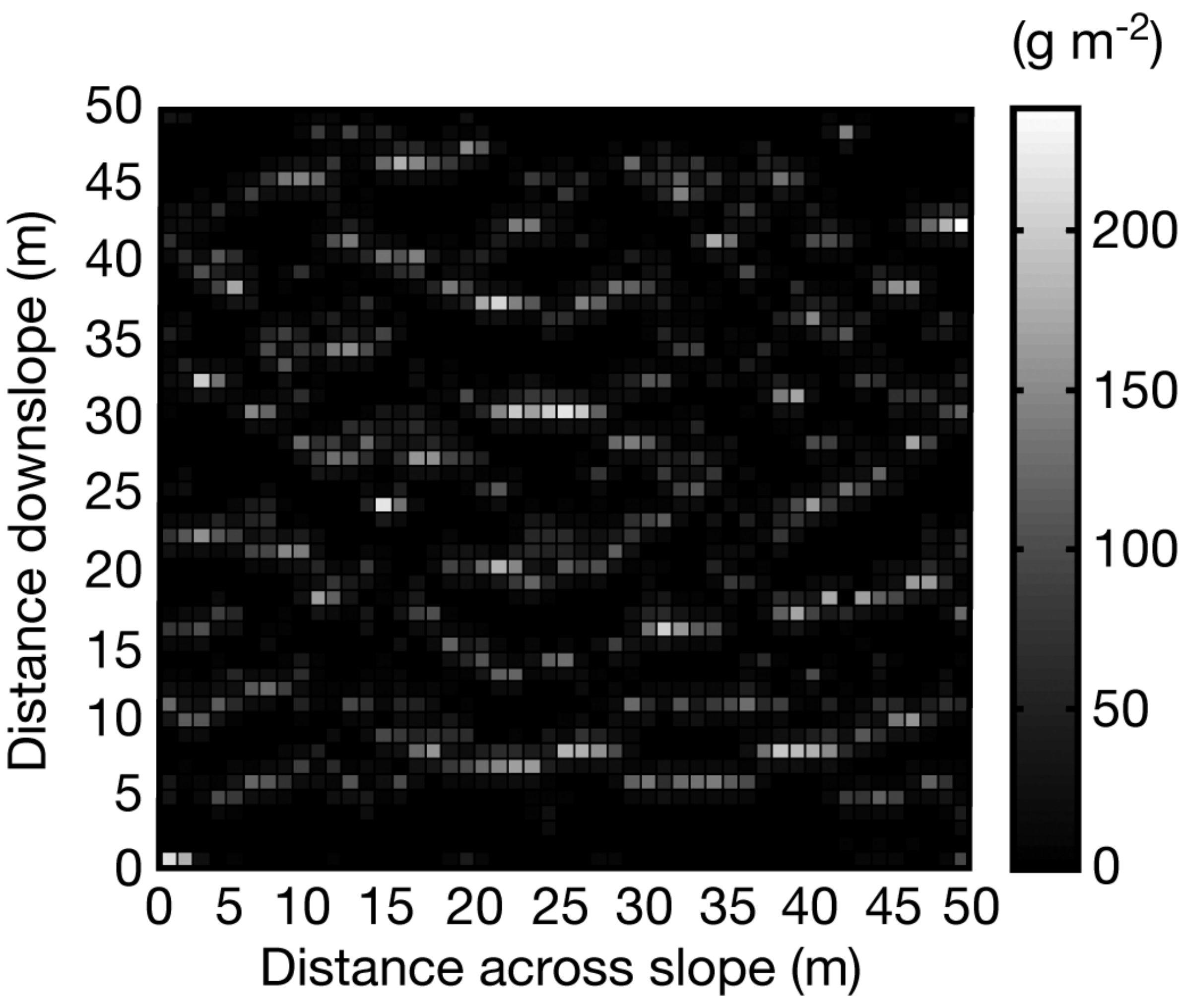

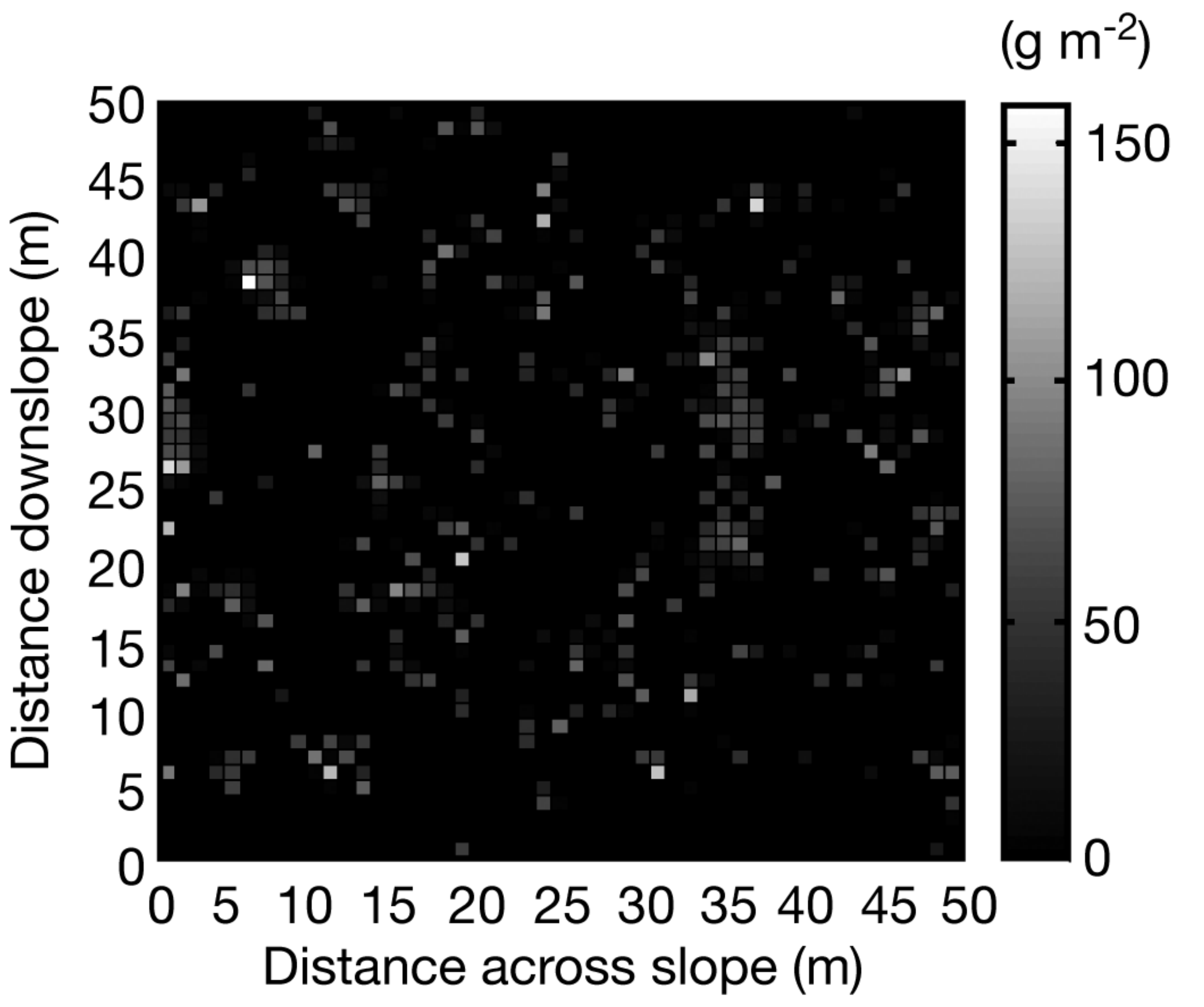

1955

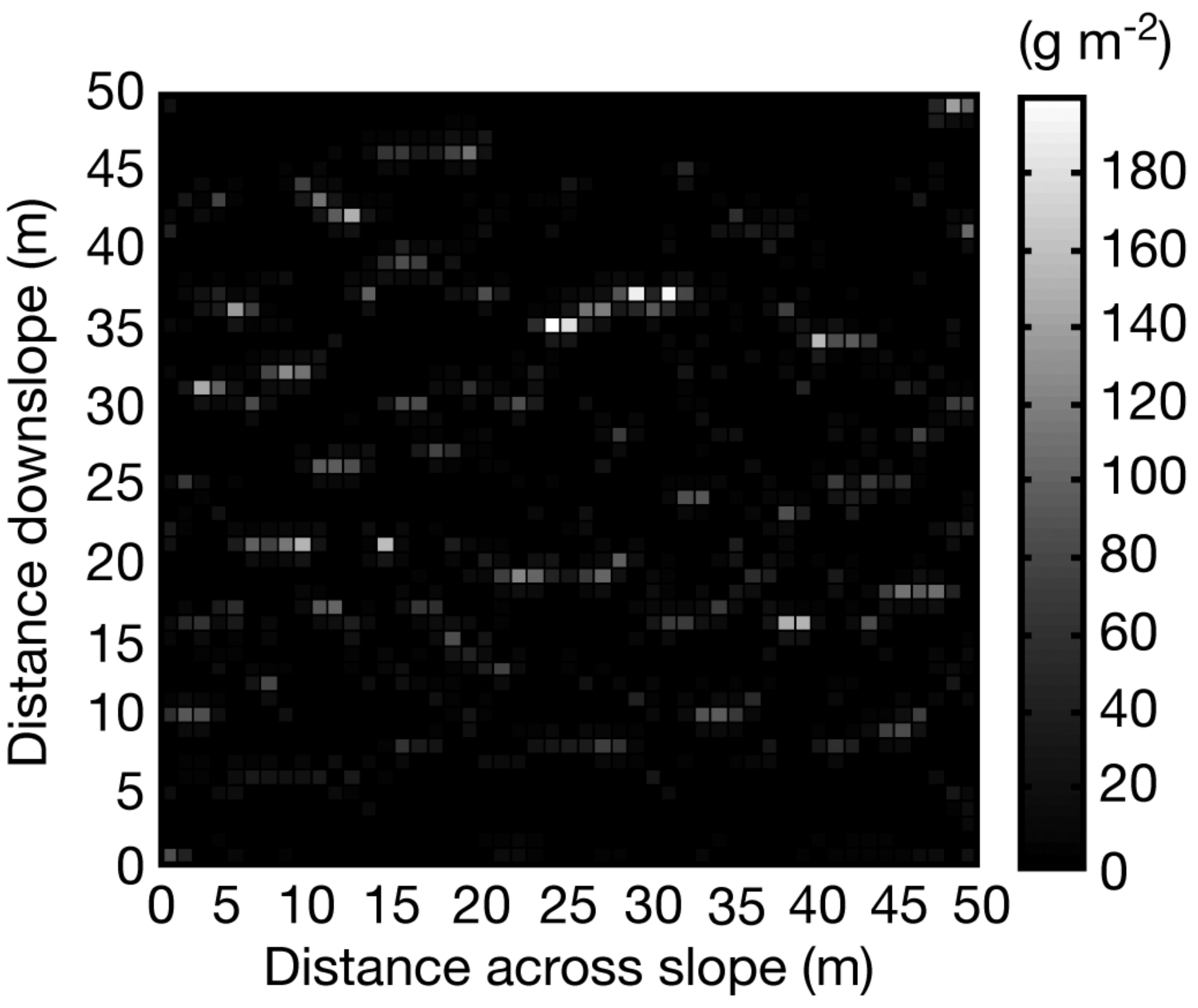

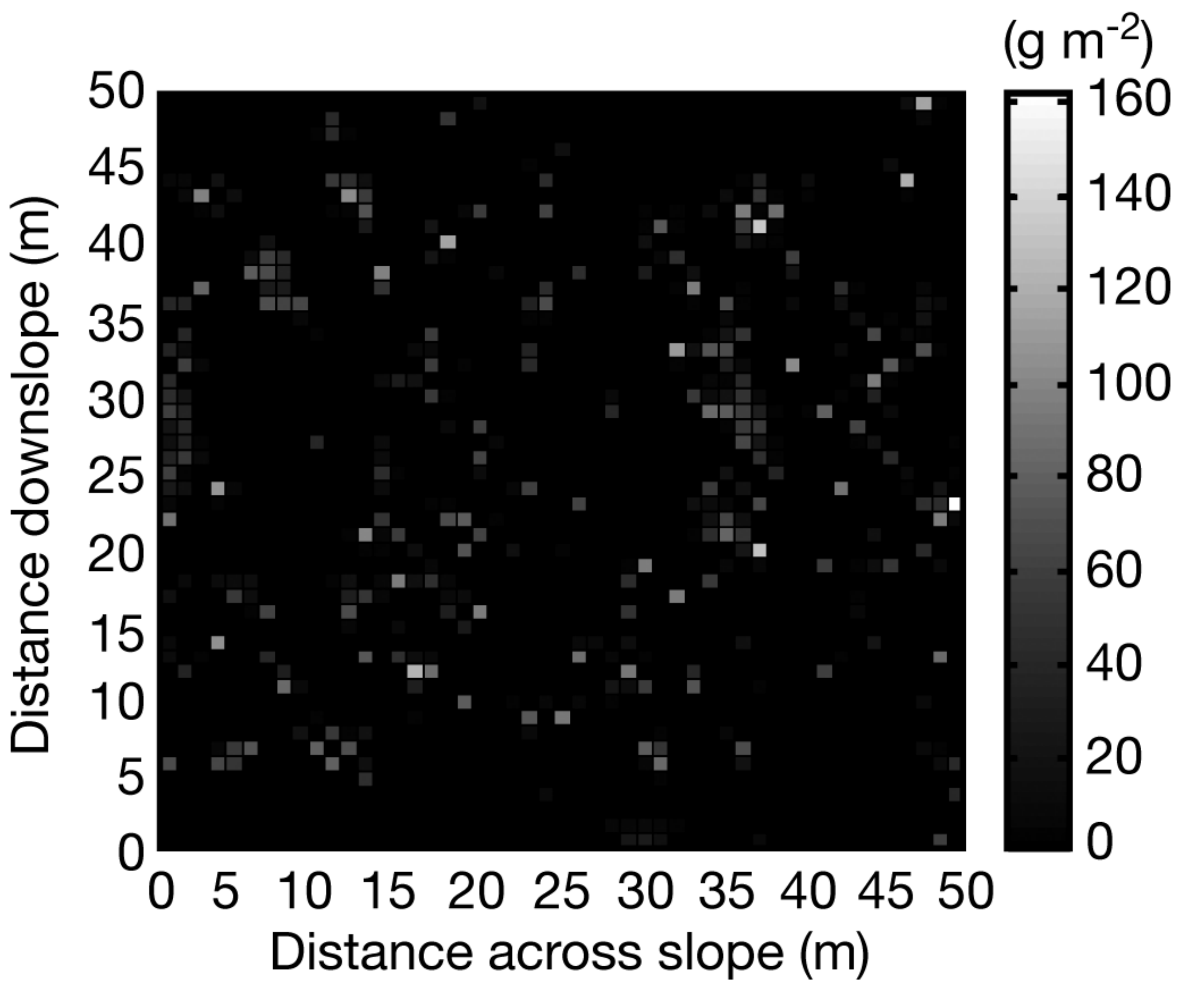

1965

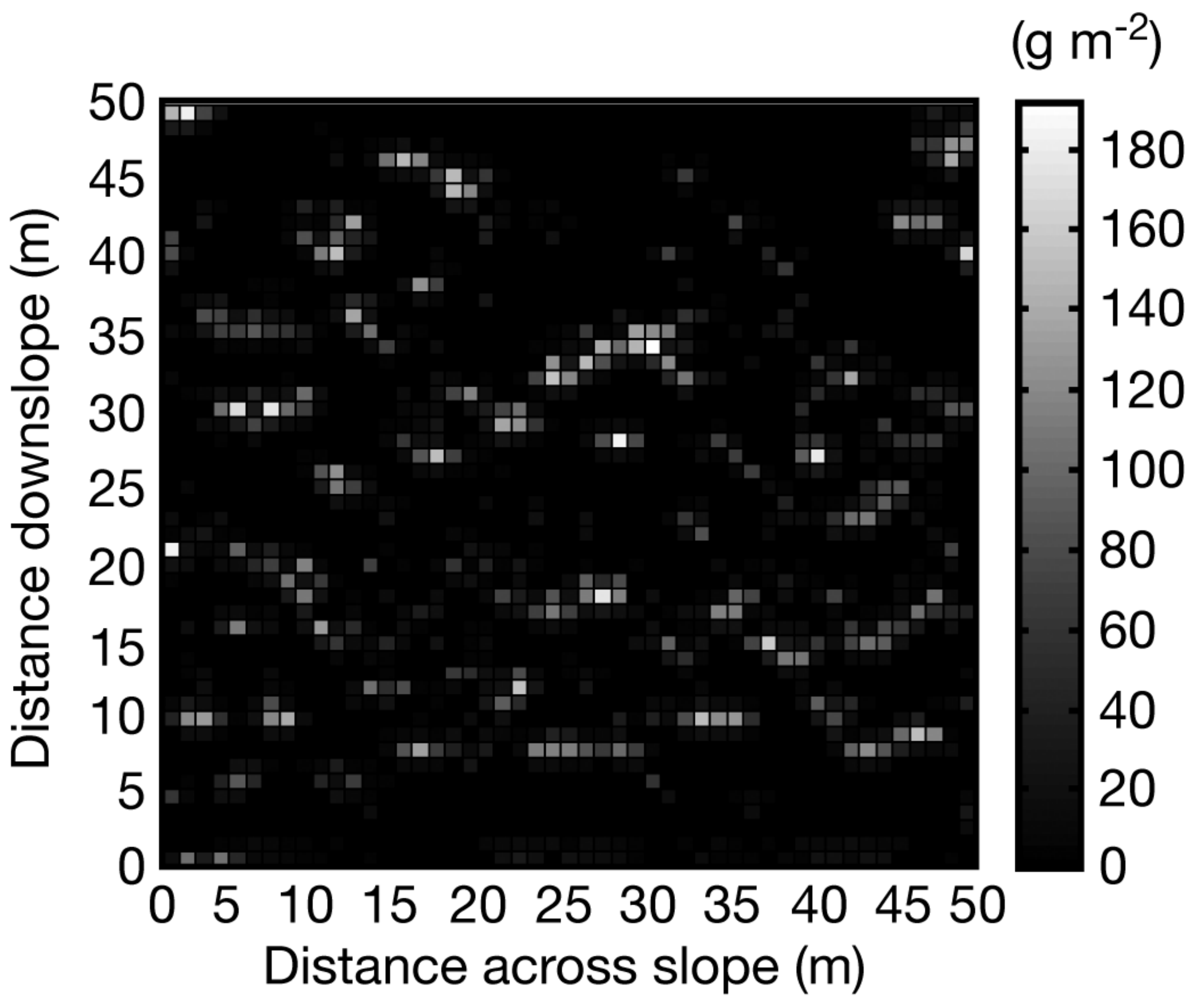

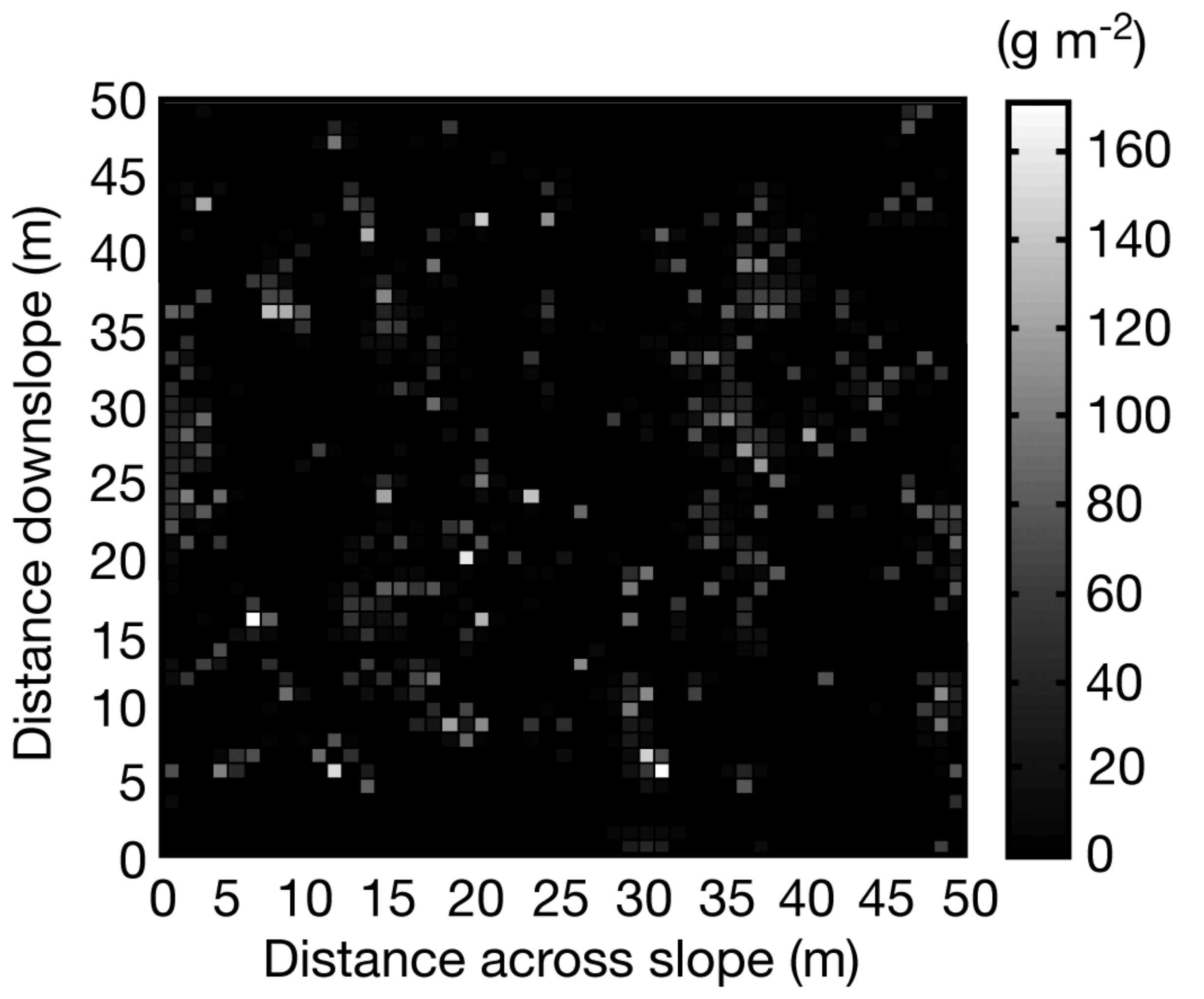

Year **map of grass biomass** **map of shrub biomass**

1975

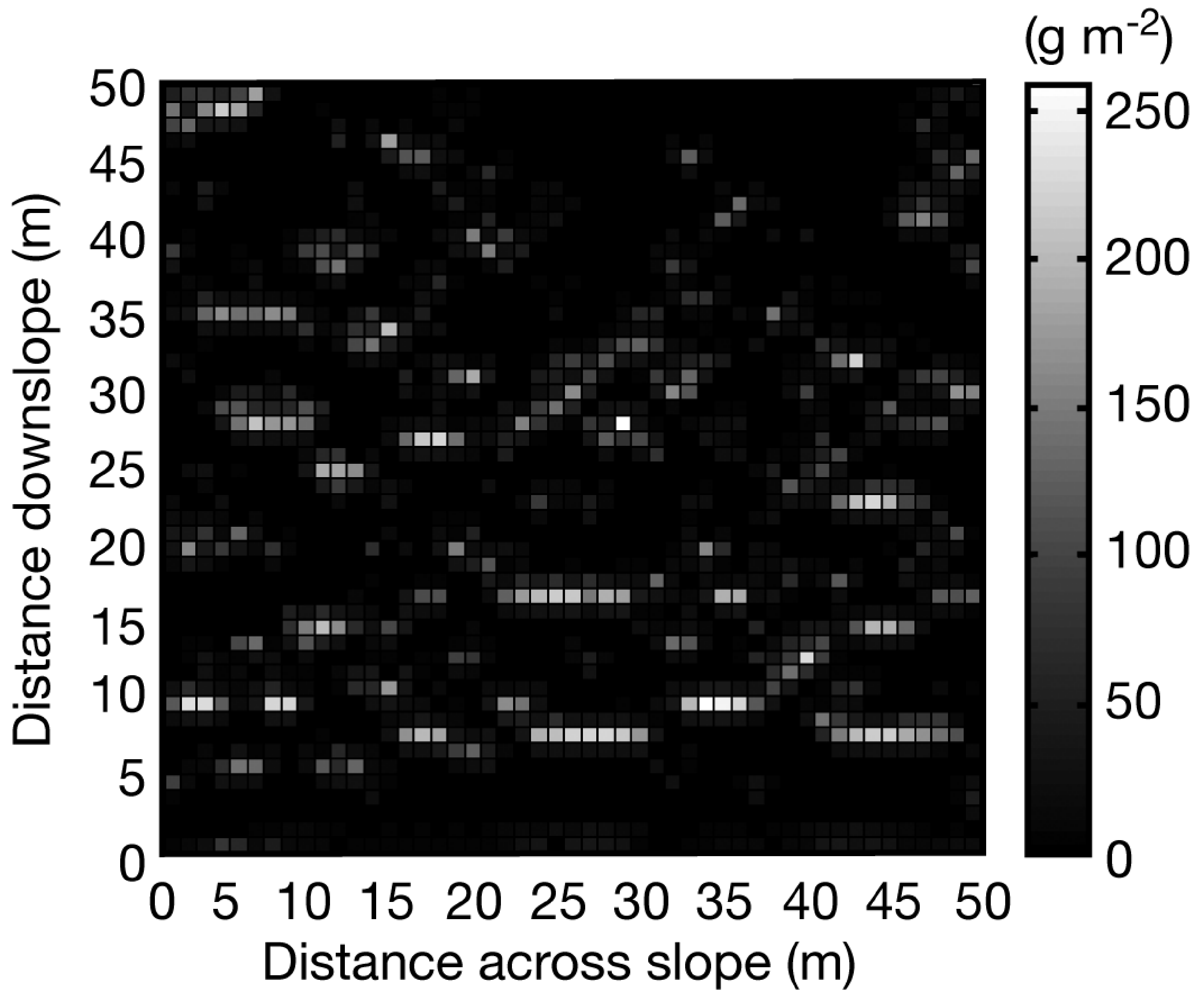

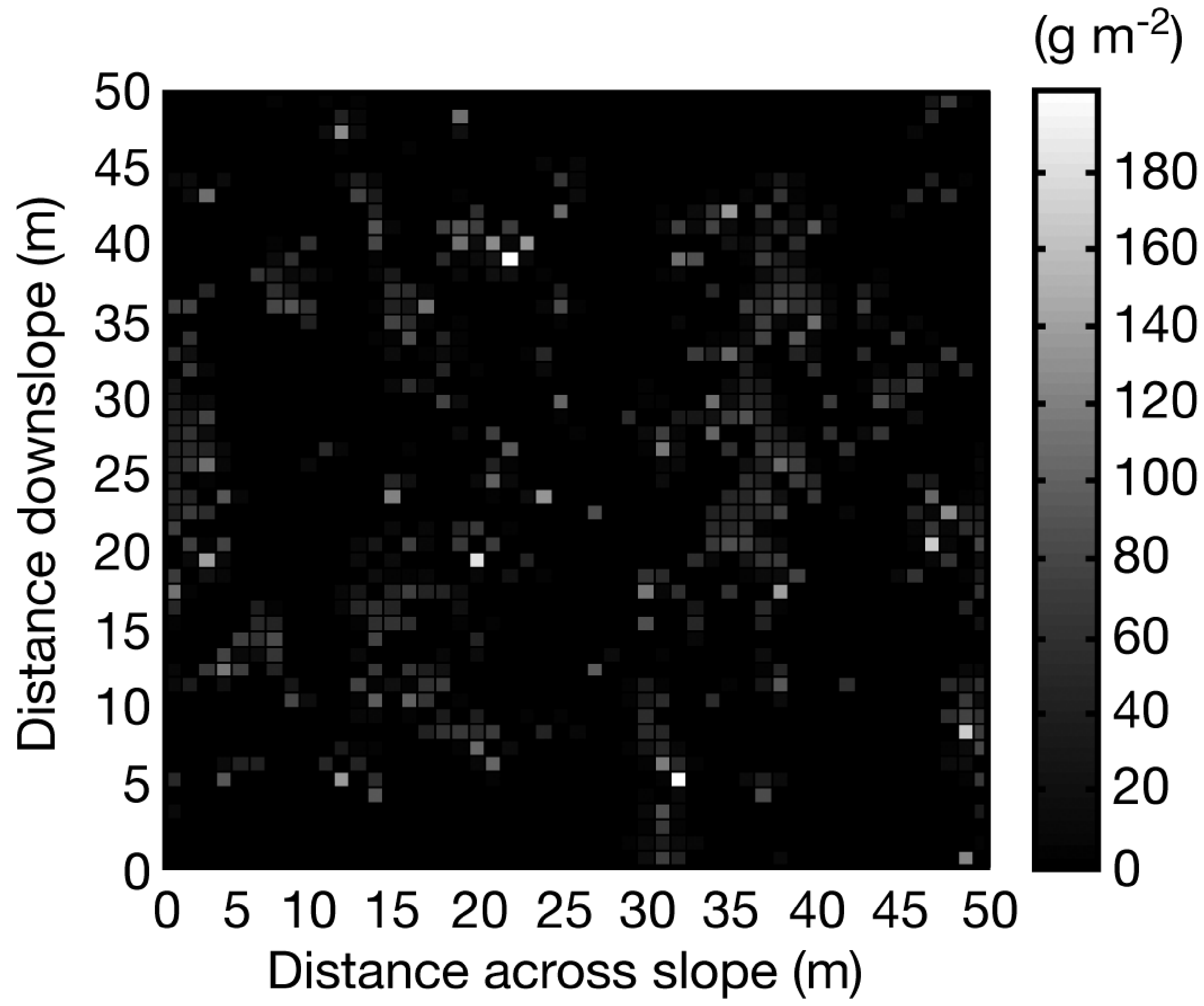

1985

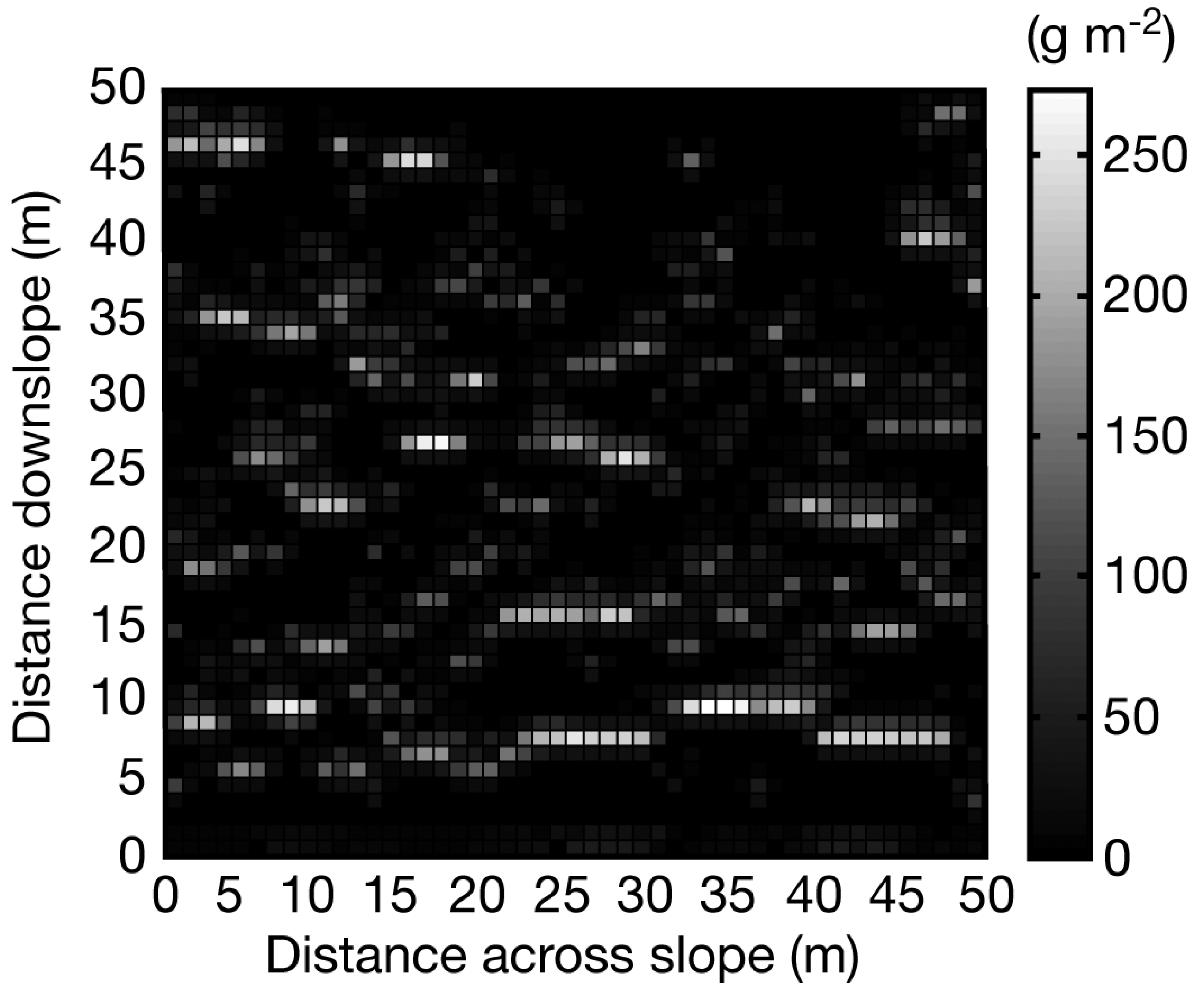

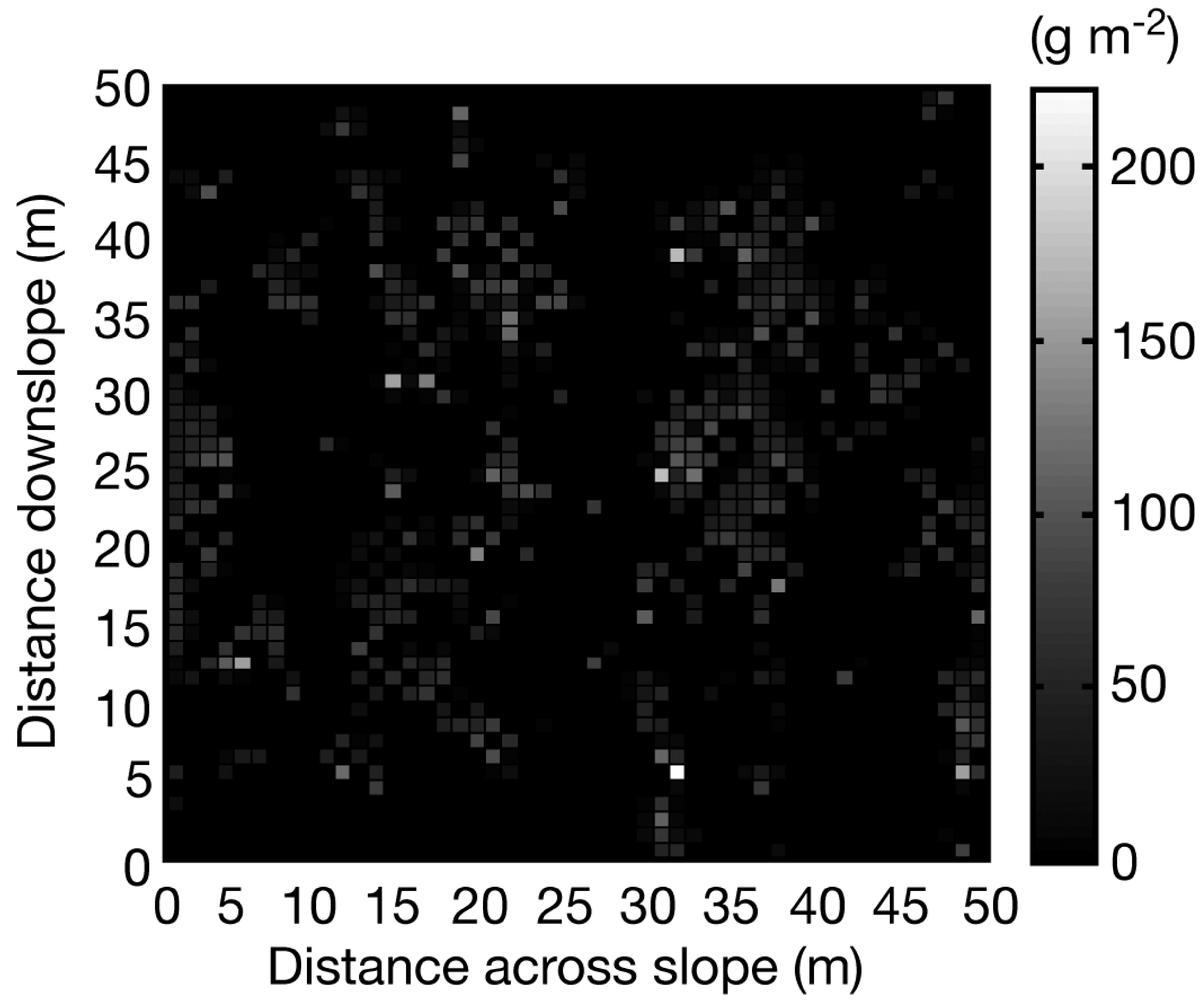

1995

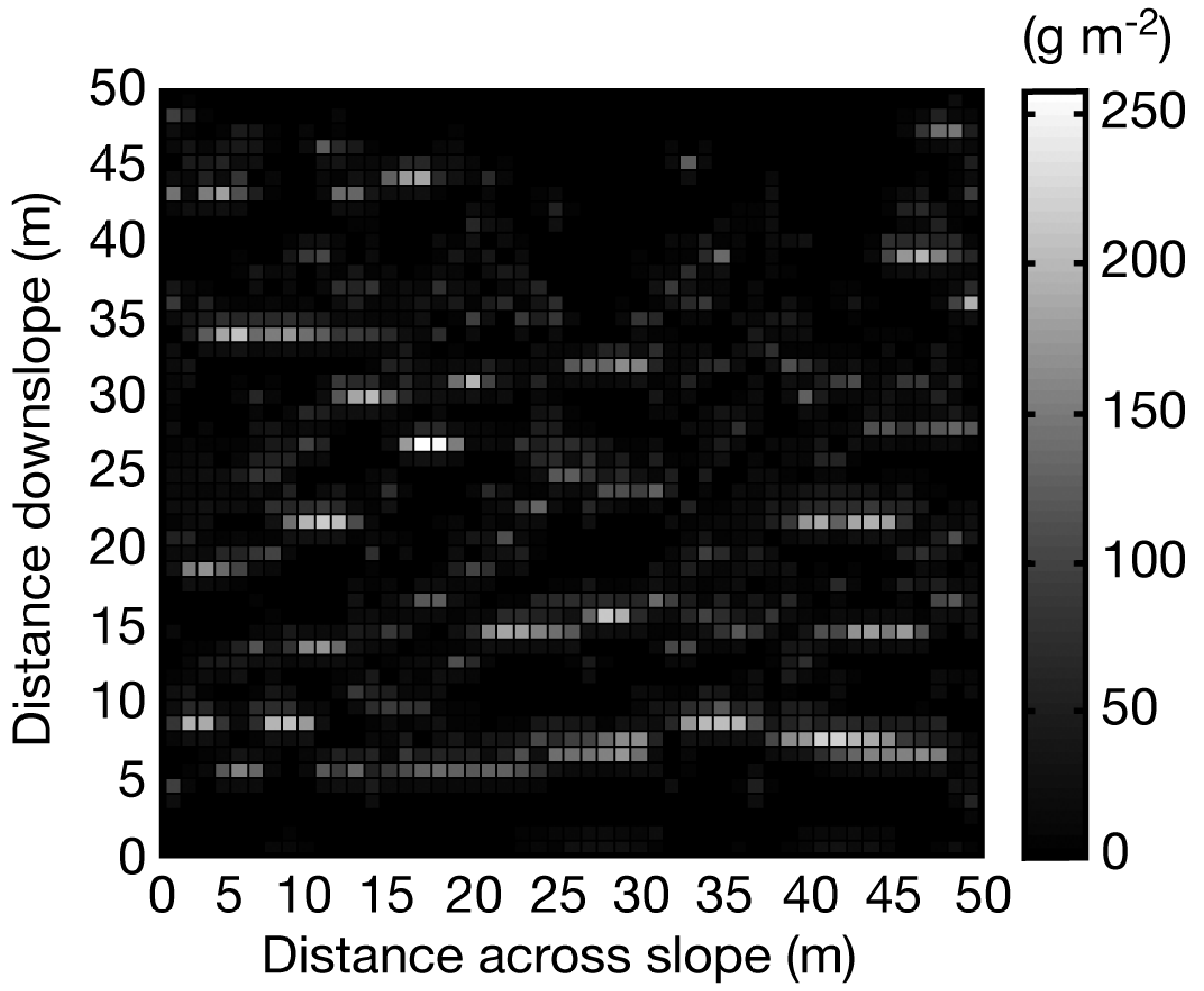

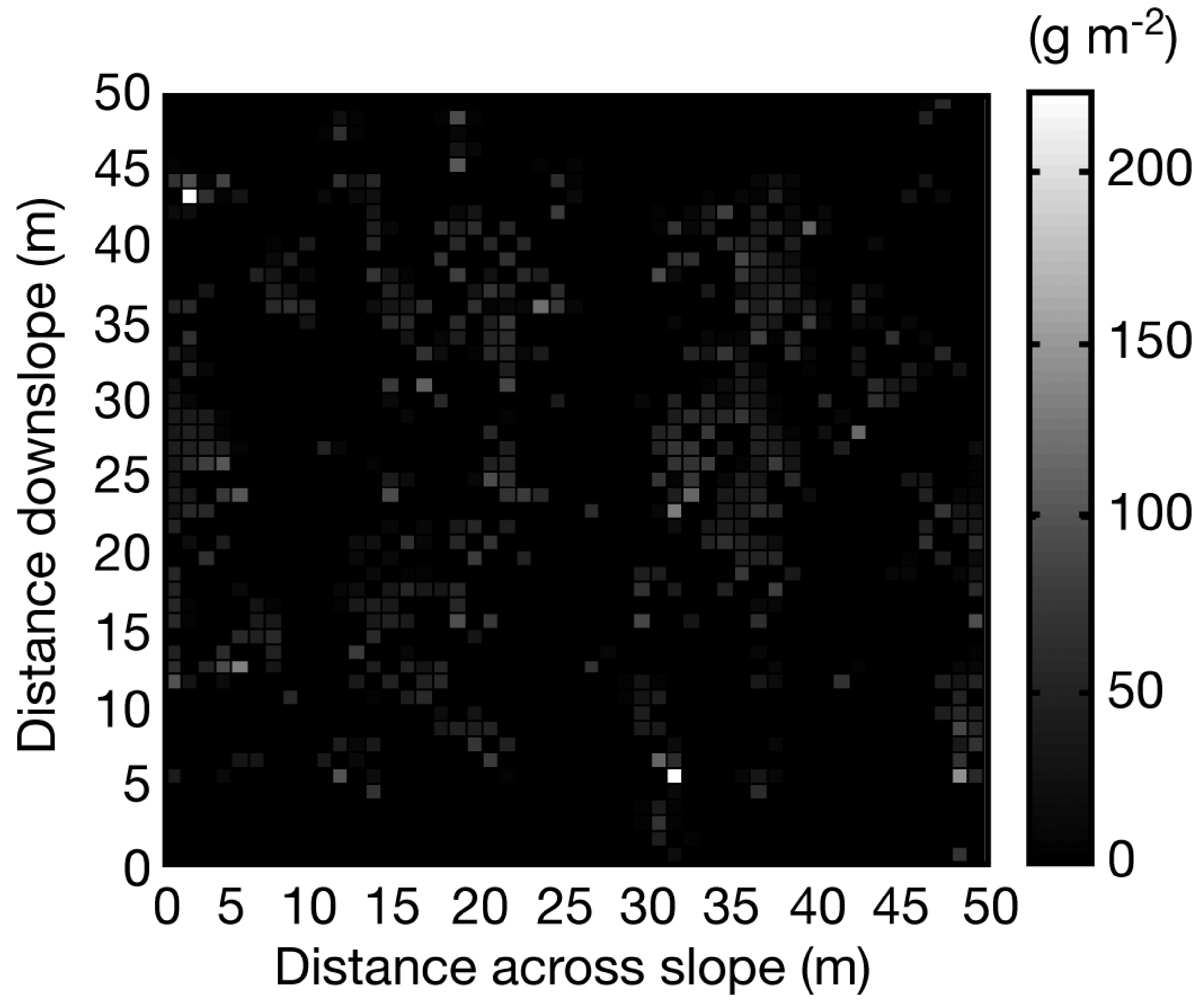

Year **Biomass of grass and shrub** **Resource density in each soil layer**

1925

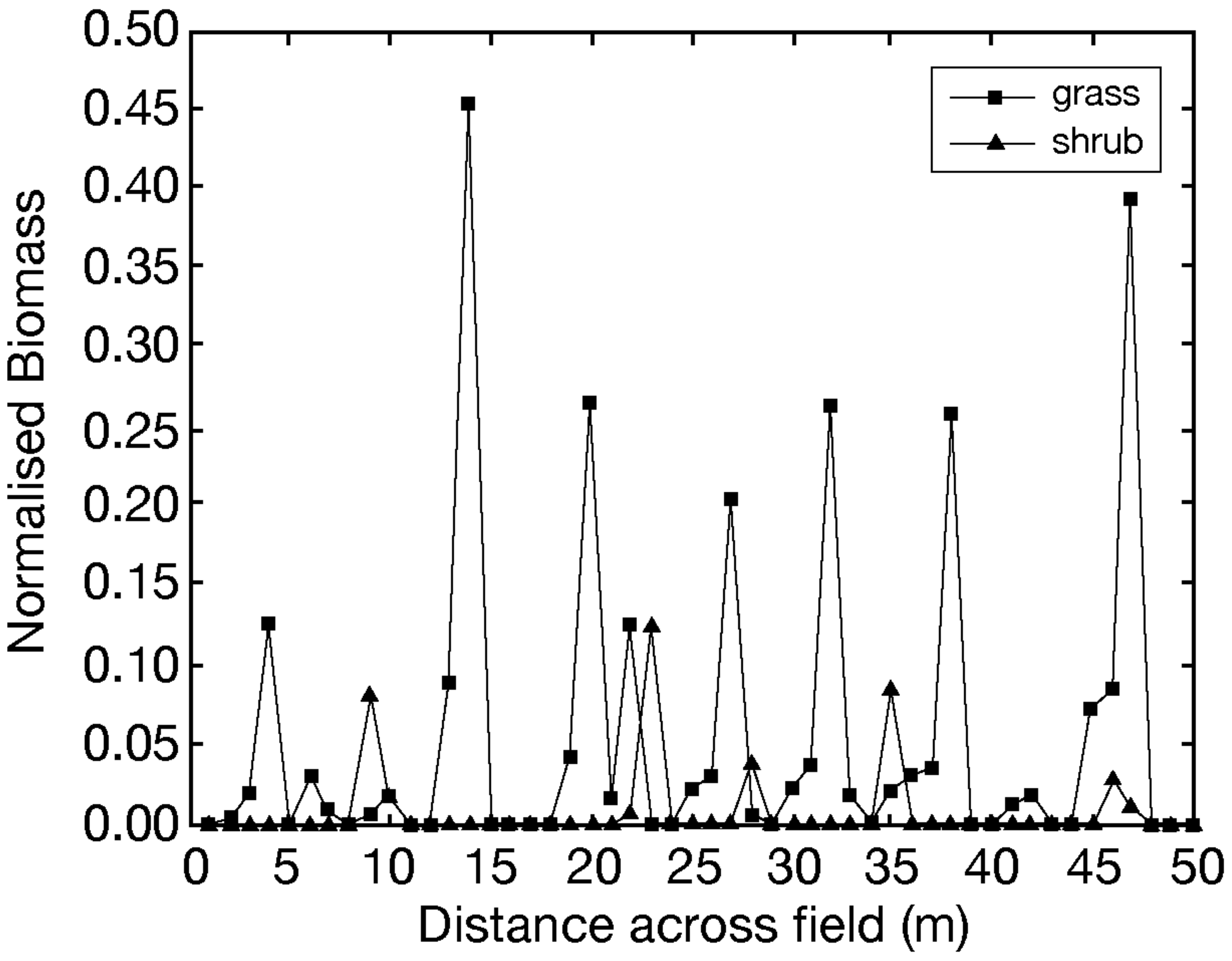

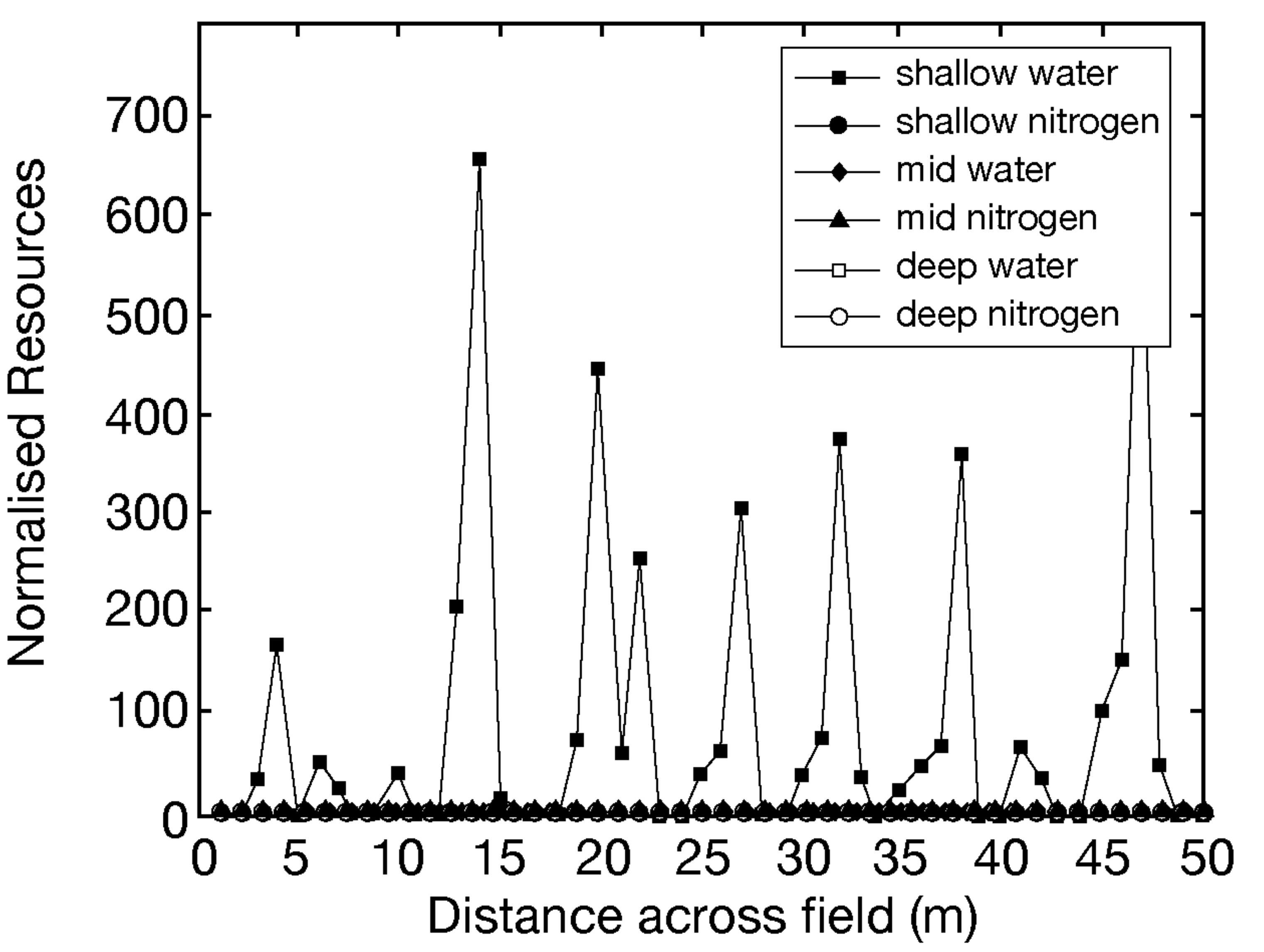

1935

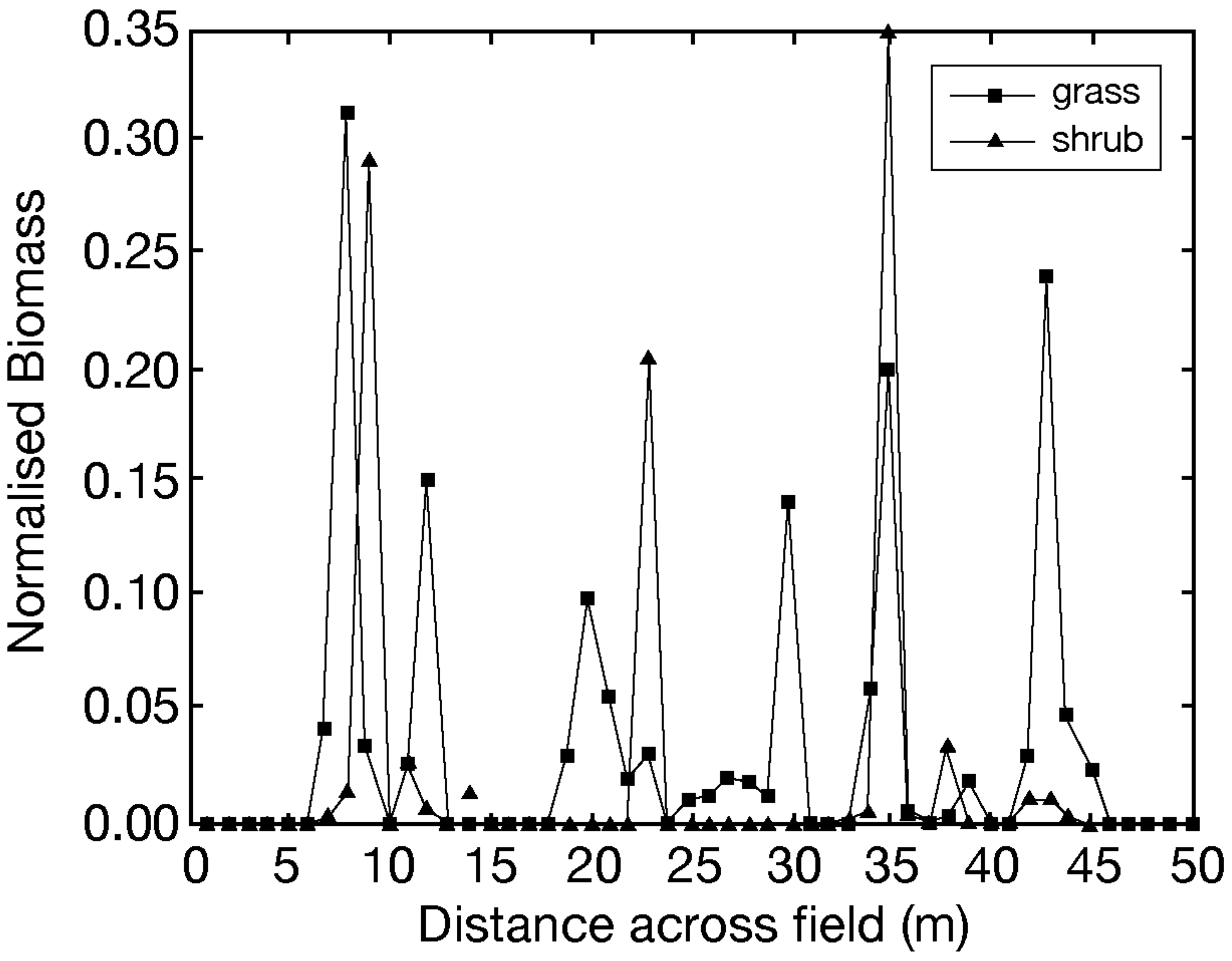

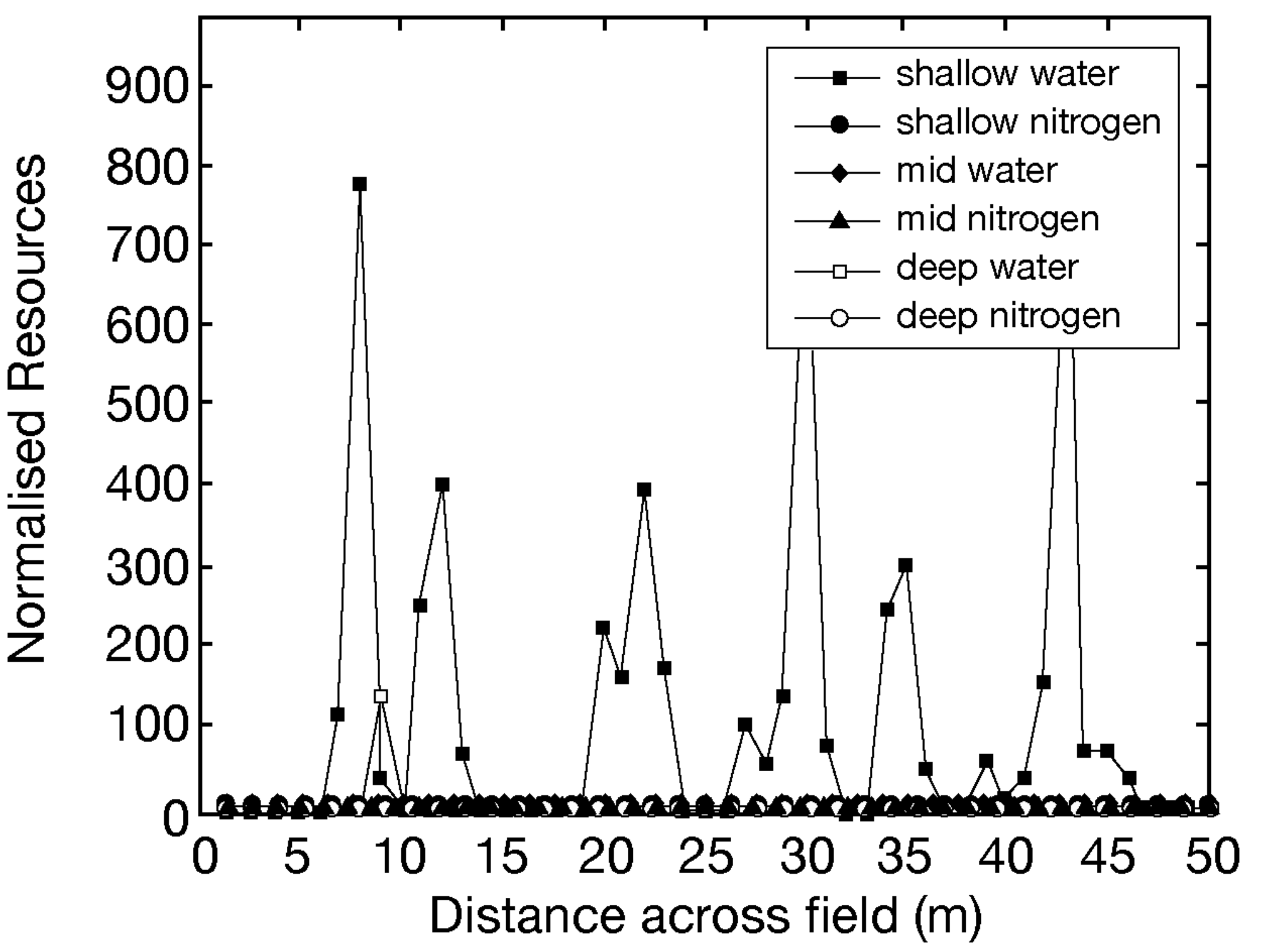

1945

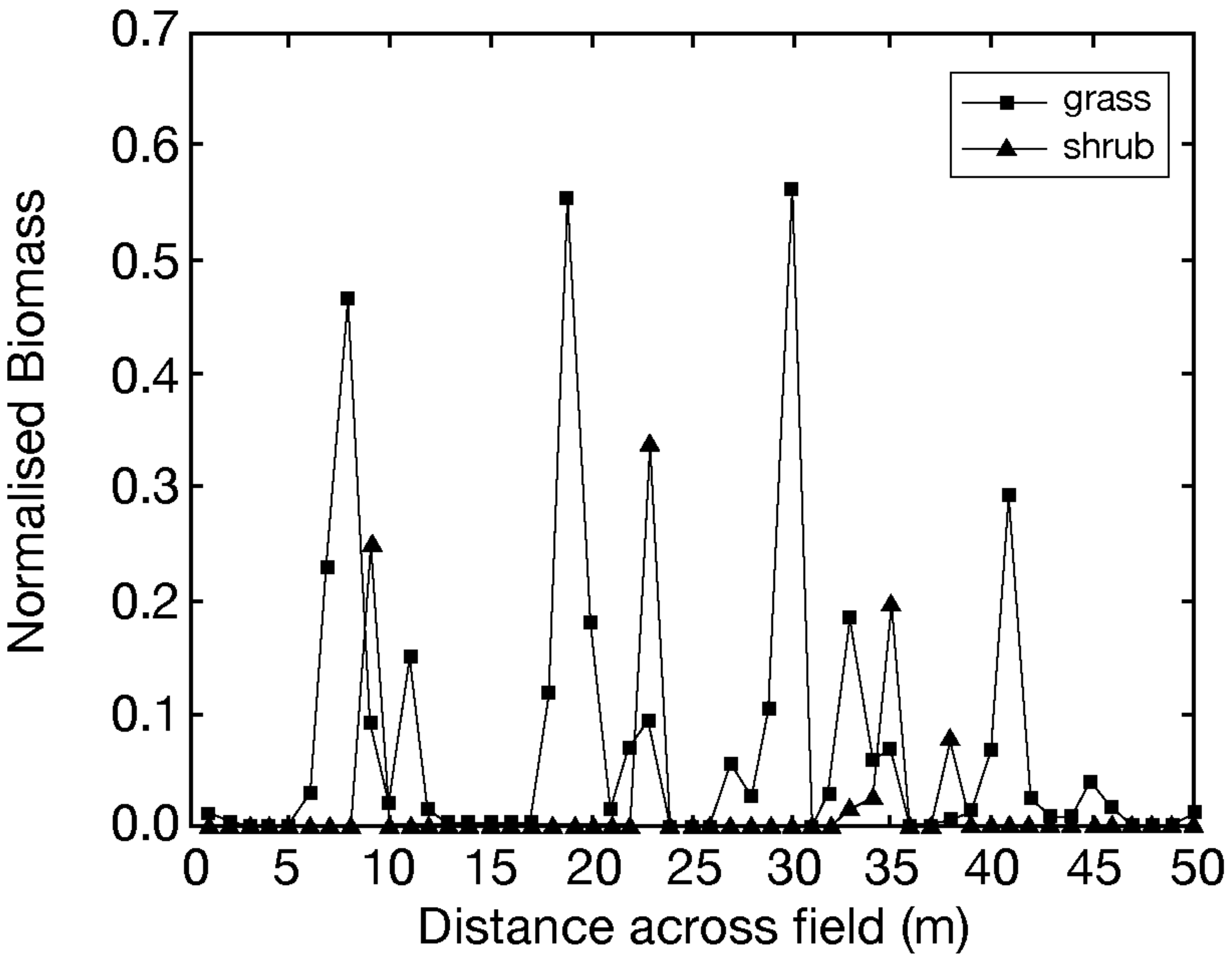

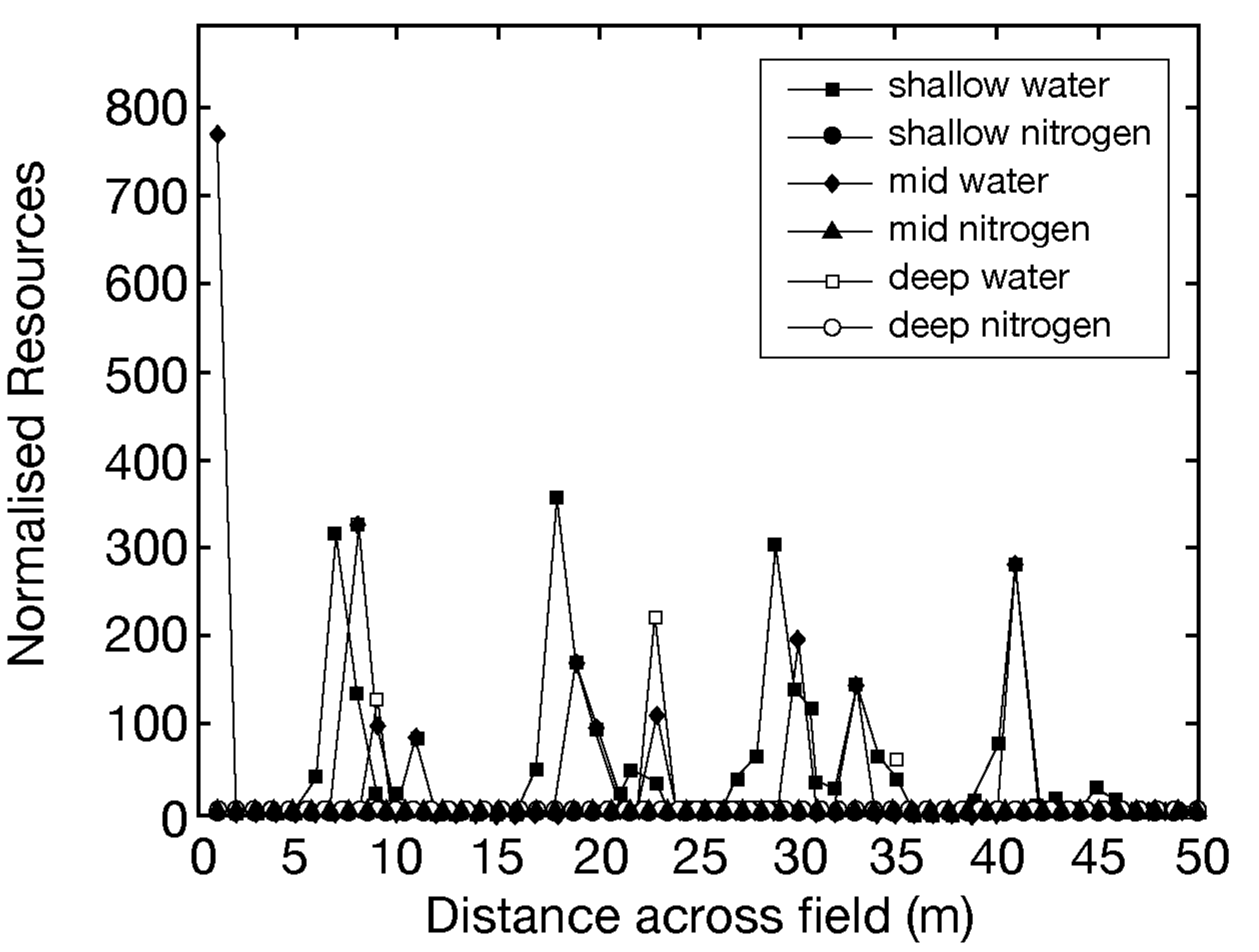

1955

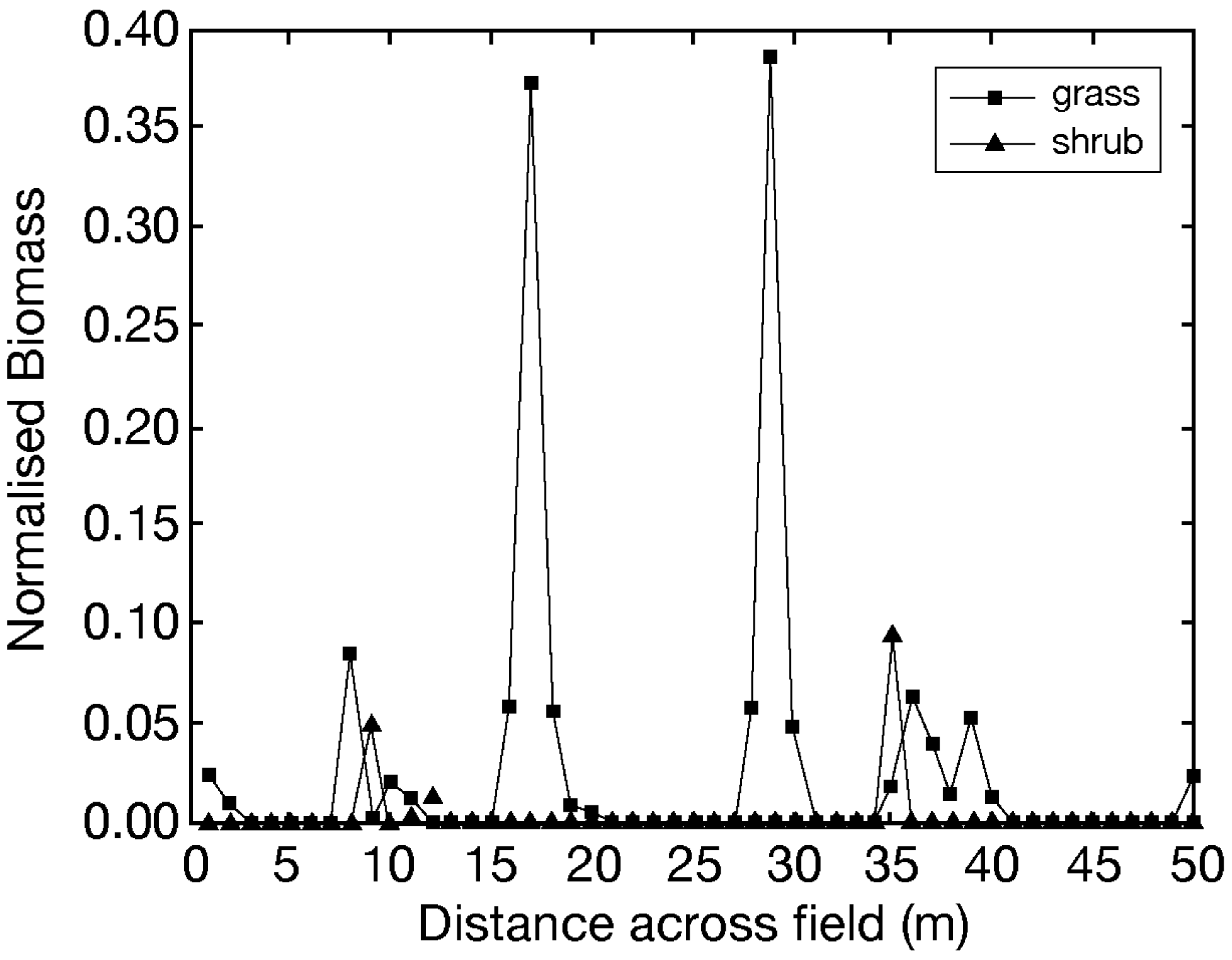

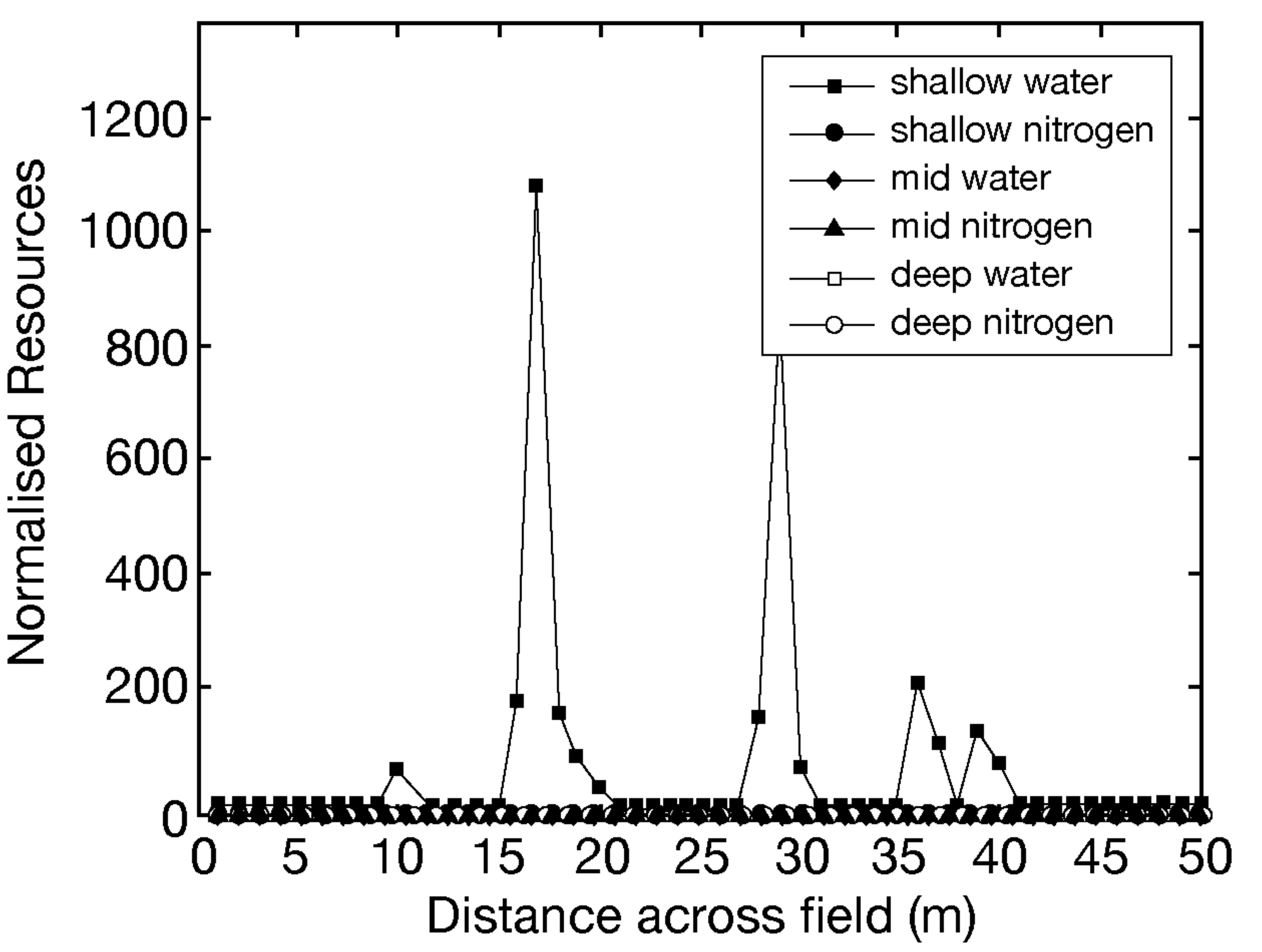

Year	Biomass of grass and shrub	Resource density in each soil layer

1965

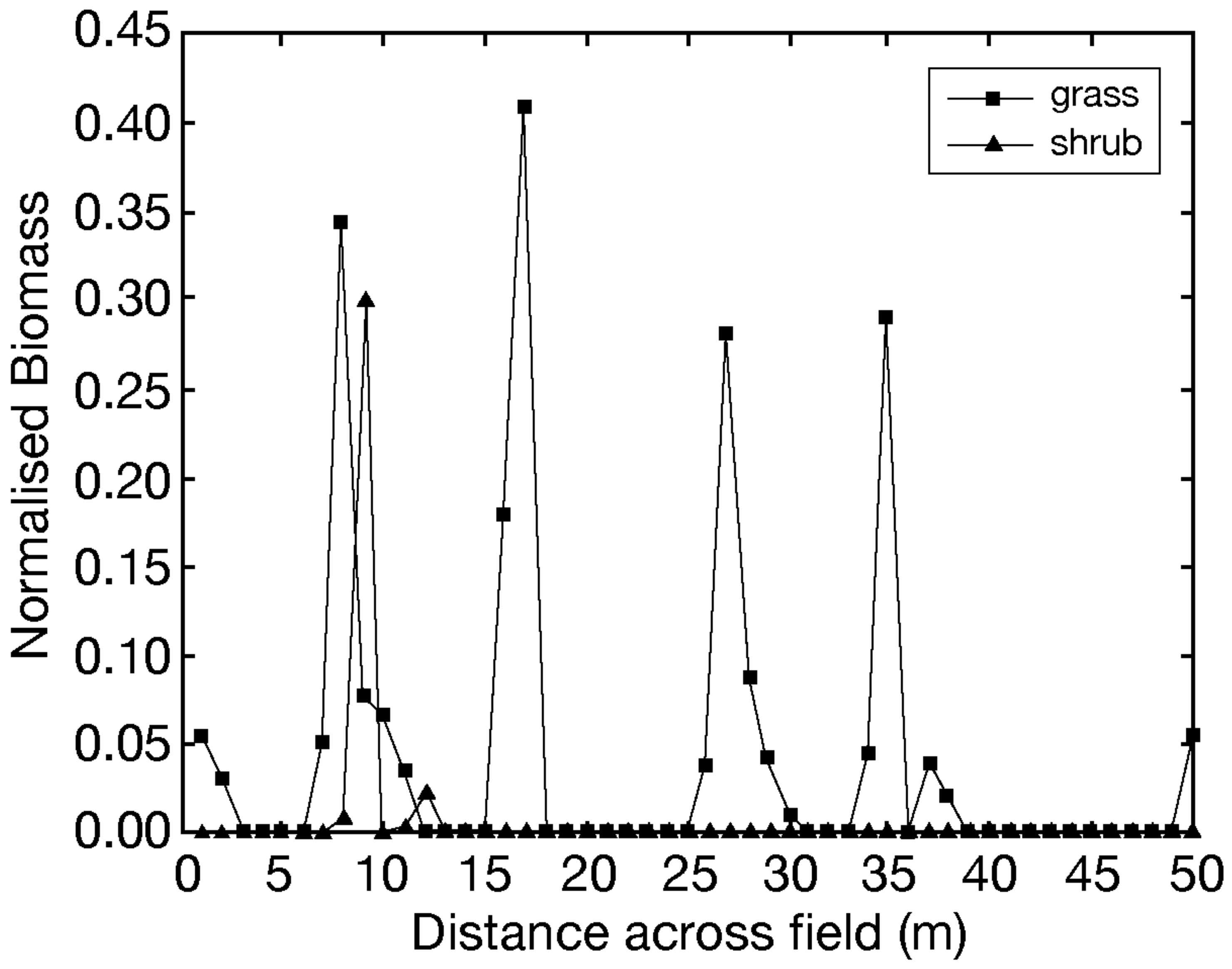

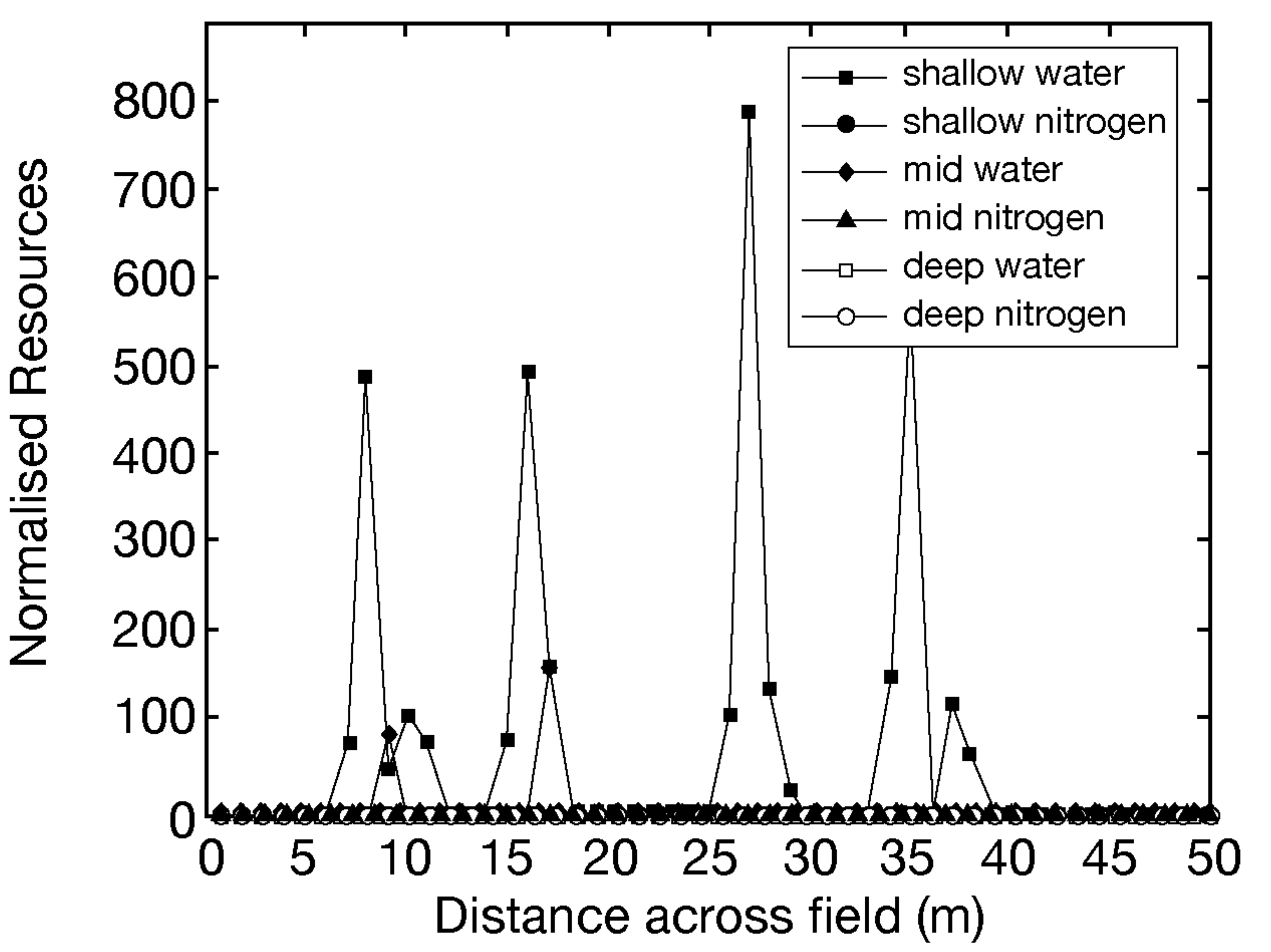

1975

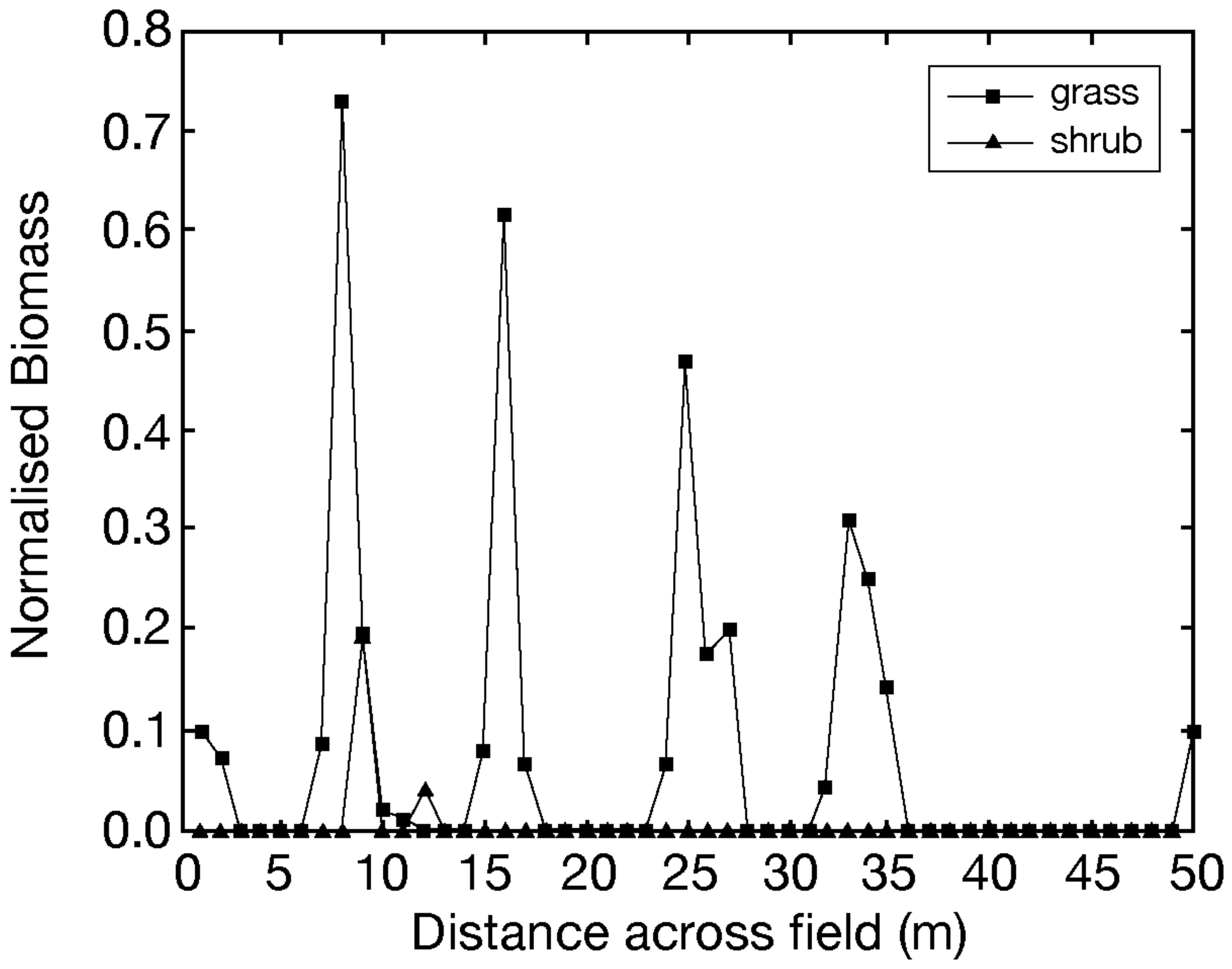

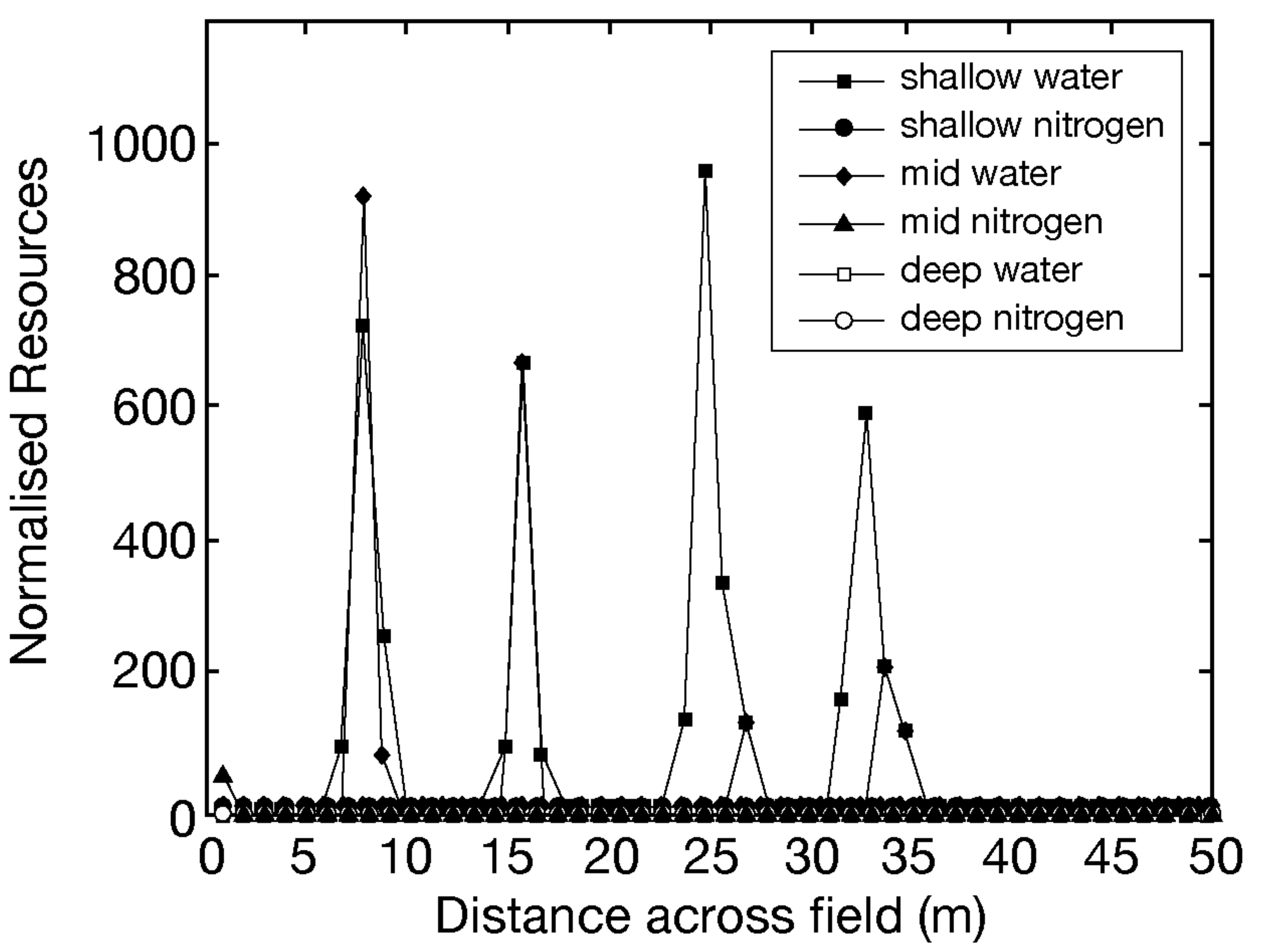

1985

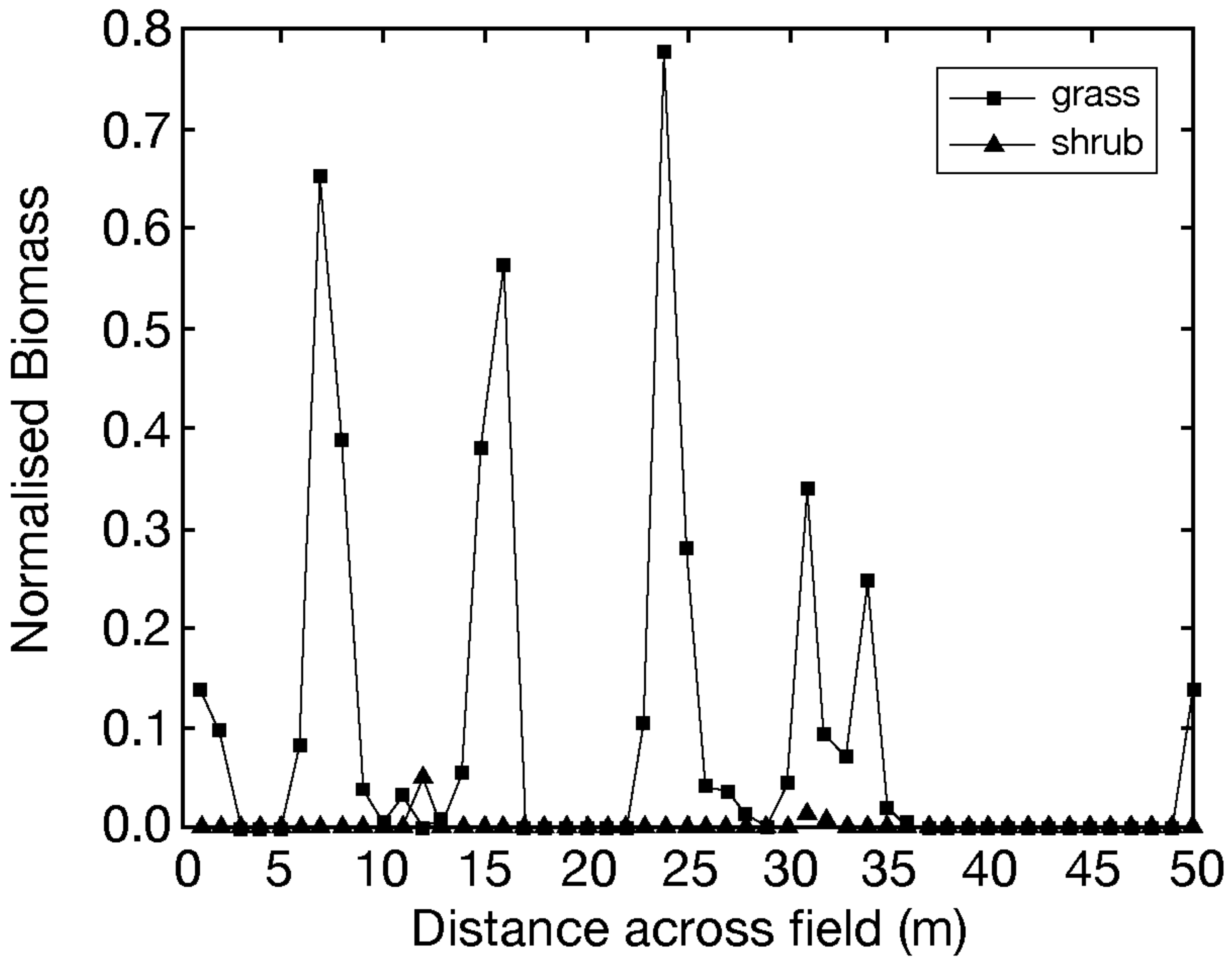

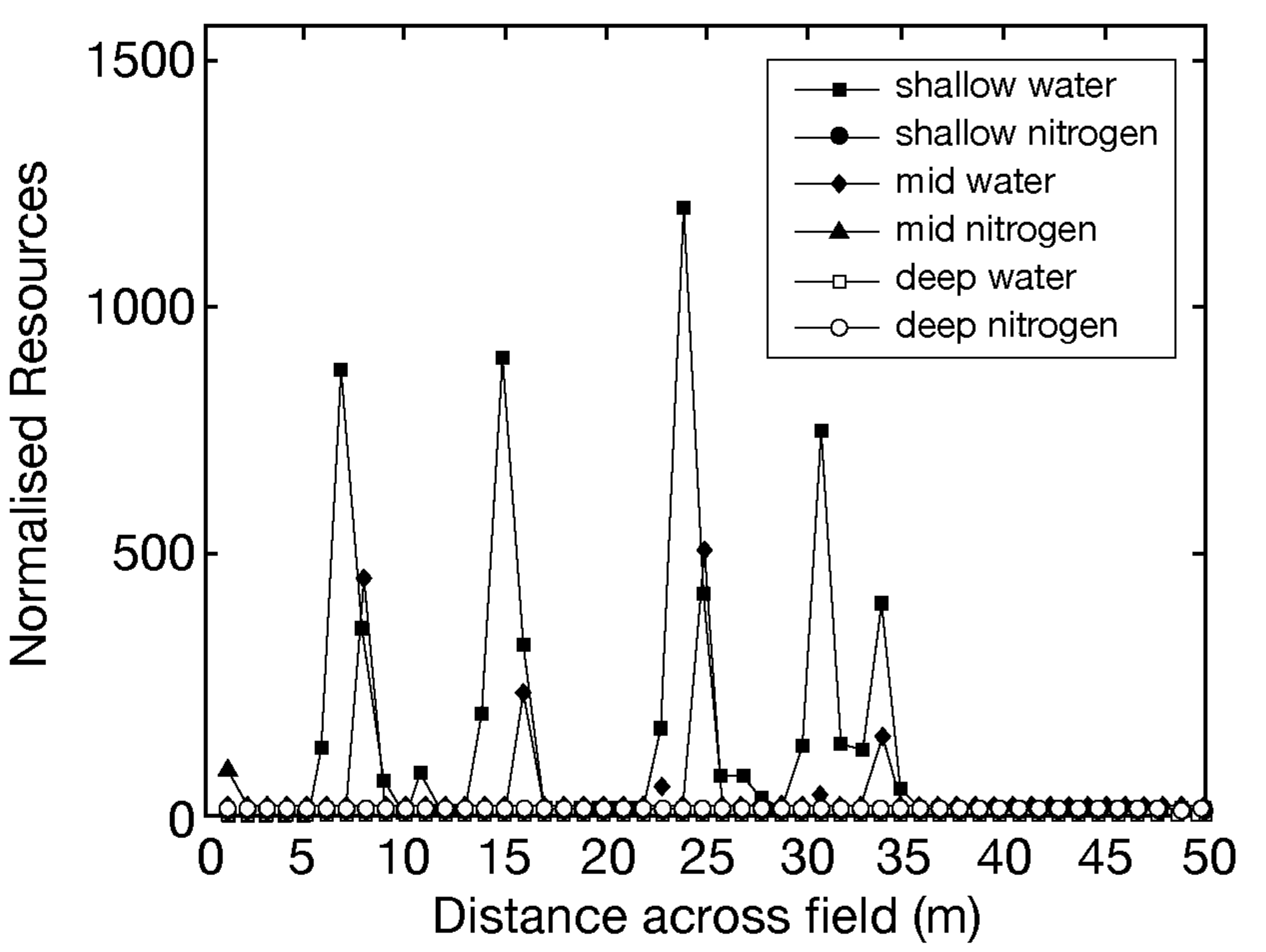

1995

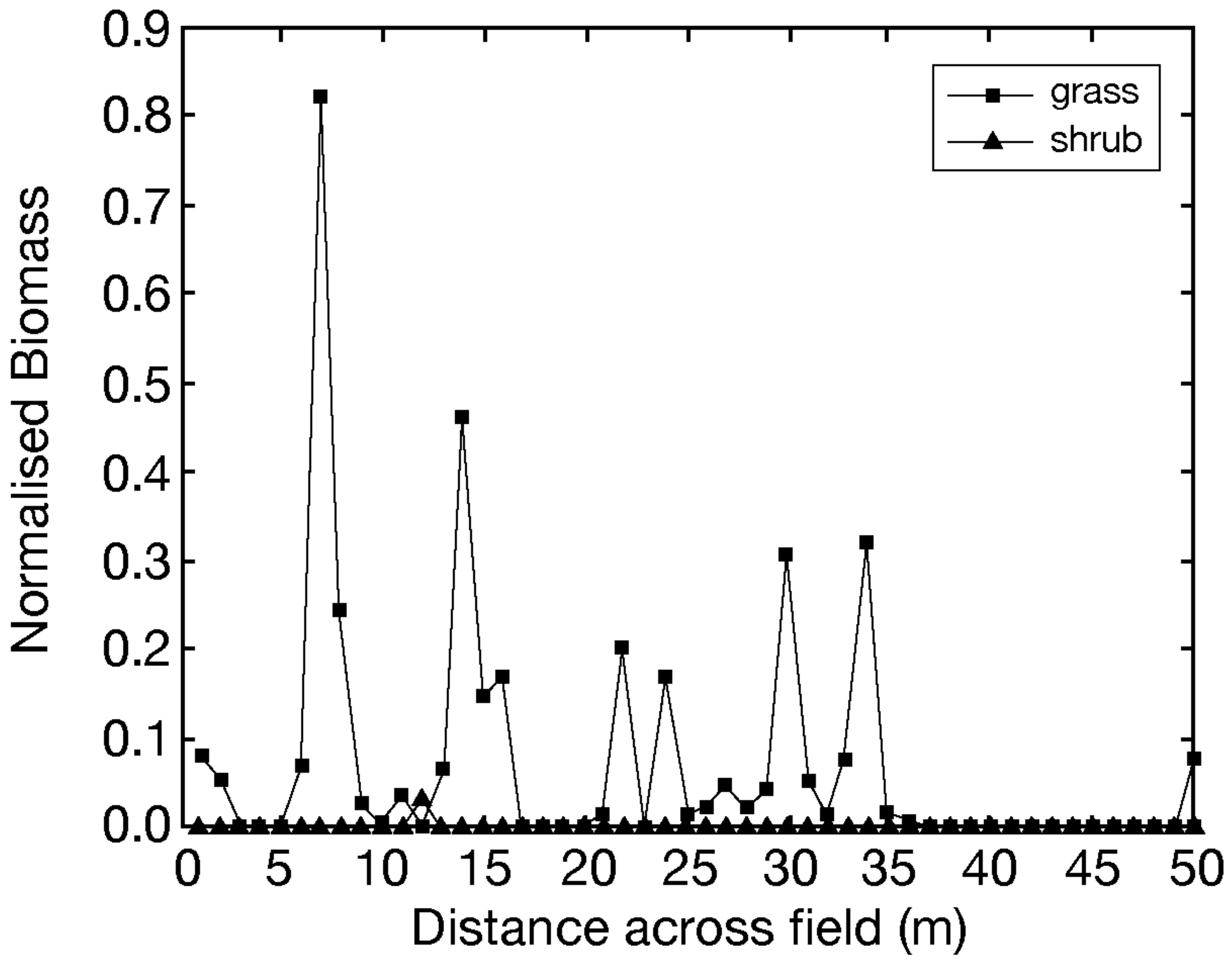

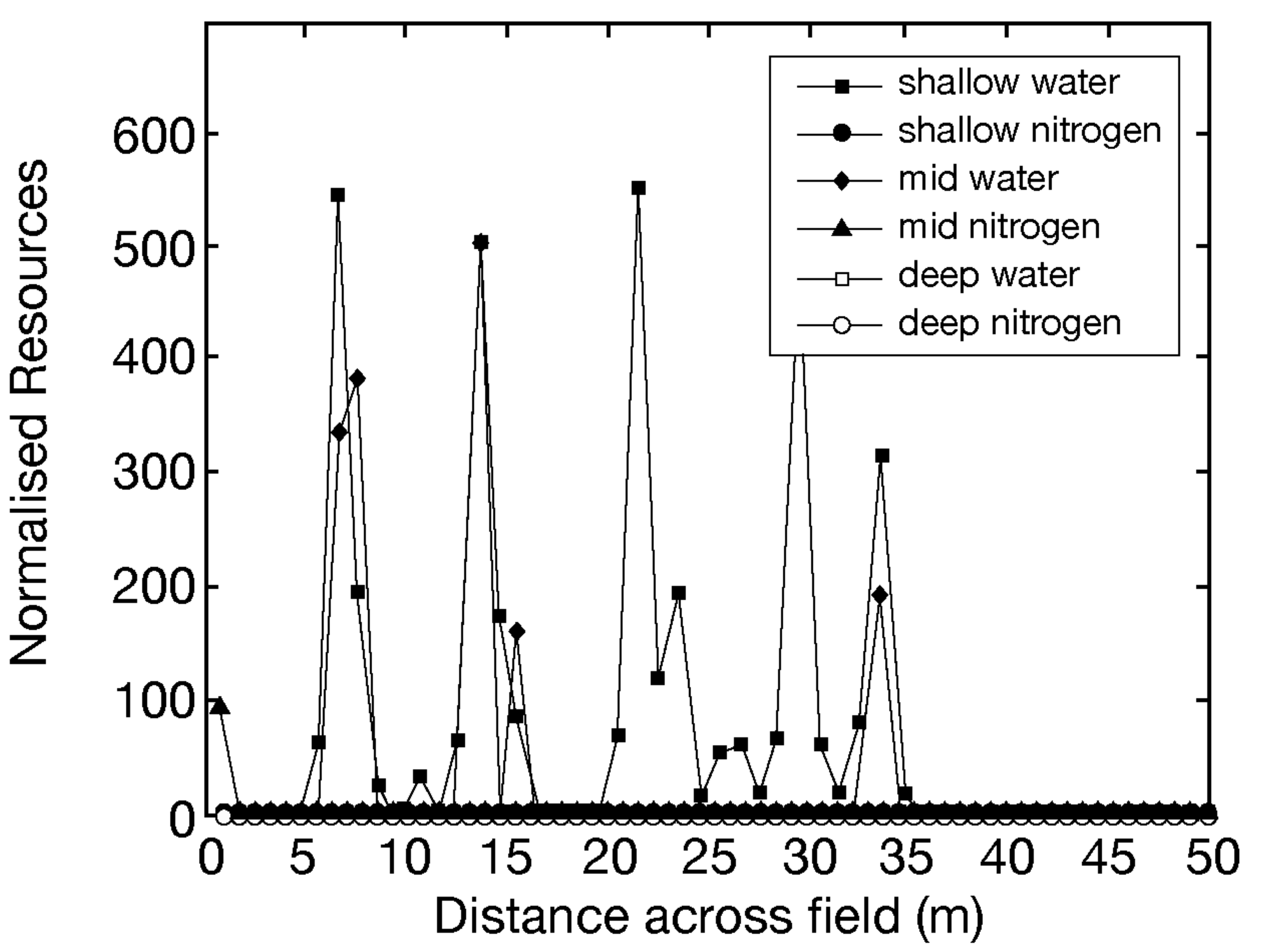

(a) Data illustrating grass biomass lost prior to the 1950s drought

Modelled grass response **Measured grass response**

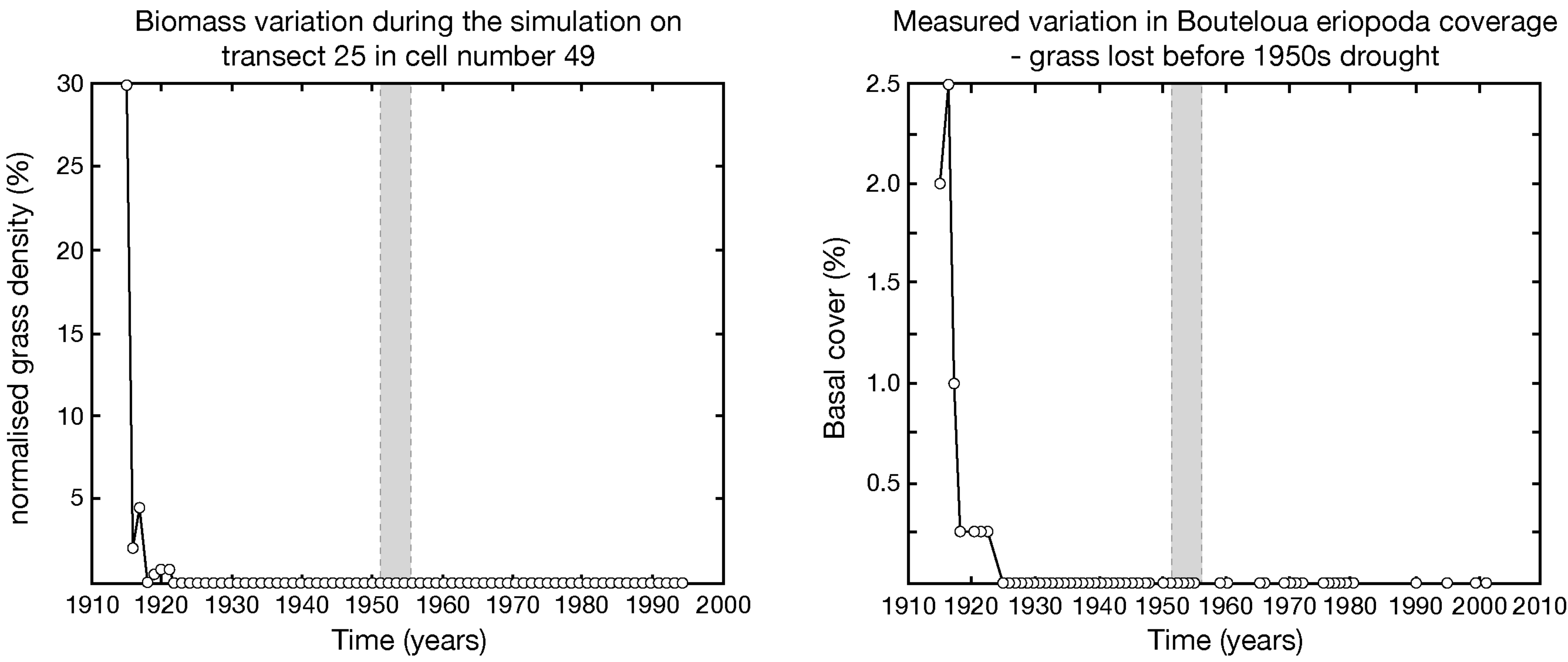

(b) Data illustrating grass biomass lost during the 1950s drought

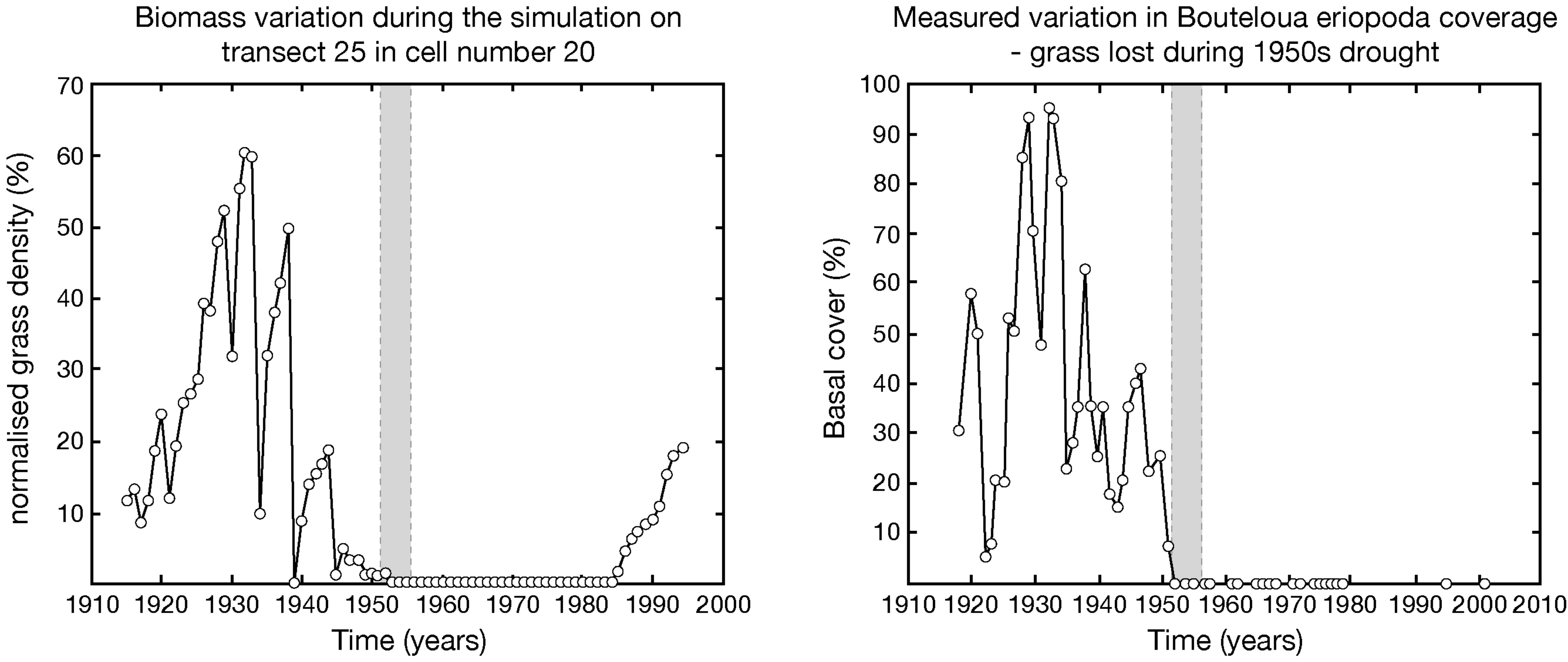

(c) Data illustrating grass biomass lost after the 1950s drought

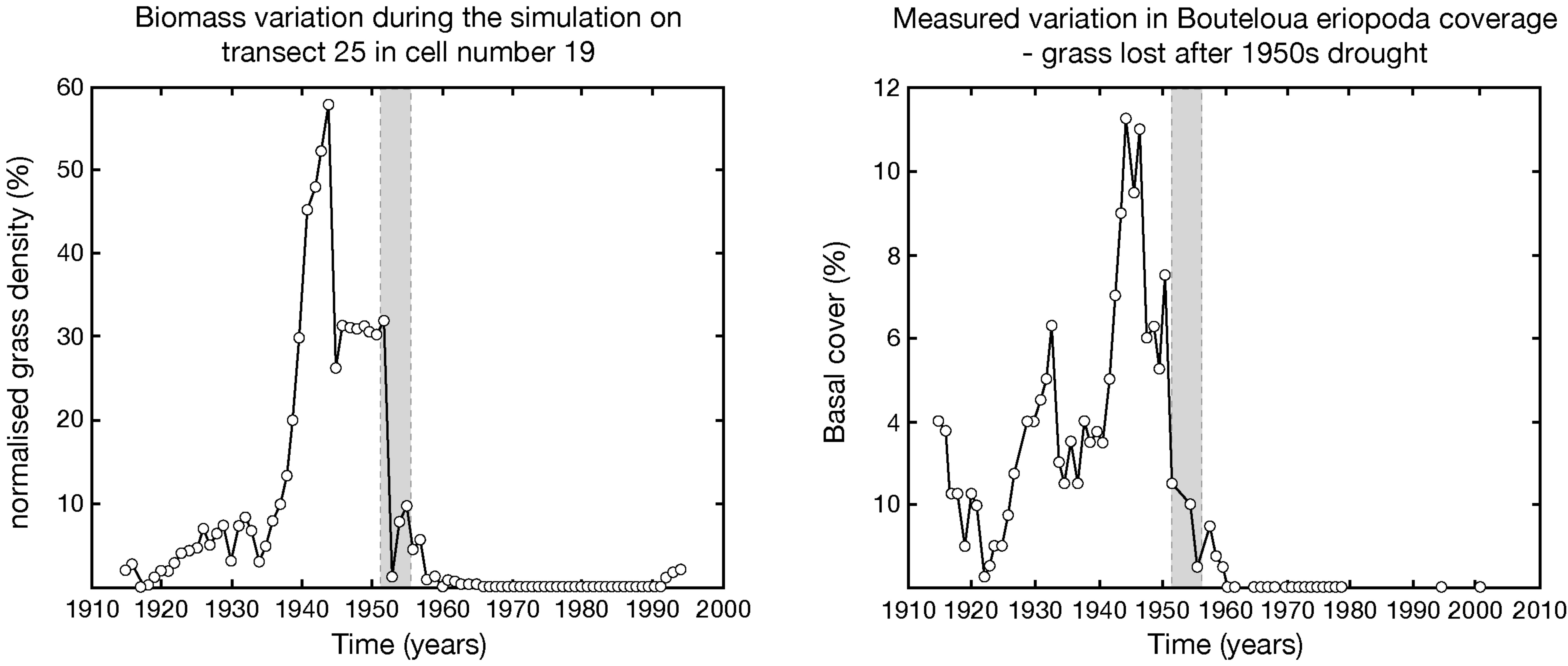

(d) Data illustrating grass biomass that persists after the 1950s drought